Scaling up catalytic microwave-assisted pyrolysis for energy production from biomass and plastic wastes

A DISSERTATION
SUBMITTED TO THE FACULTY OF THE
UNIVERSITY OF MINNESOTA

BY

Nan Zhou

IN PARTIAL FULFILLMENT OF THE REQUIREMENTS
FOR THE DEGREE OF
DOCTOR OF PHILOSOPHY

Advisor: Dr. Roger Ruan
April 2021

Acknowledgement

First and foremost, I am deeply grateful to my advisor and mentor, Professor Roger Ruan, for his guidance, support, encouragement, and patience throughout these years. I would also like to thank my current and past group members, including Shiyu Liu, Leilei Dai, Dr. Paul Chen, Dr. Min Min and many others, for their support and assistance for my research work. To my parents and grandparents, I am indebted for their unconditional support and love as always. Lastly, I owe a debt of gratitude to my wife for her sacrifice and patience through this journey.

Dedicated to my wife, Yun

Abstract

Our society currently faces the dual challenge of resource depletion and environmental pollution. Converting sustainable biomass and recycled plastic wastes into energy and fuel products provides an attractive solution to this challenge. Among the various conversion technologies, microwave assisted pyrolysis serves as a promising alternative to conventional pyrolysis technology due to several unique benefits inherent to its dielectric heating mechanism. Yet, scaled-up design and operation of this technology are still lacking. In order to improve feasibility and scalability of the microwave-assisted pyrolysis process, a novel system of continuous microwave-assisted pyrolysis (CMAP) featuring a mixing SiC ball bed was developed and first tested for fuel production from wood pellets. High quality syngas was produced from this process. Specifically, at temperature of 800^{o}C, producer gas with a high energy content of 18.0 MJ/ Nm^3 and a high syngas (H_2+CO) content of 67 vol.% was obtained at a gas yield of 72.2 wt.% or 0.80 Nm^3/kg d.a.f. wood pellets. Downstream condensation and physical adsorption lowered the tar concentration from 7.83 g/Nm^3 at the exit of pyrolysis reactor to below the detection limit at the end of the process. Energy balance analysis showed that a cold gas efficiency of 73.3% was achieved at 800^{o}C, which consumed 7.2 MJ electrical energy per kg of wood pellets. Further measures to improve the energy efficiency could potentially reduce the electricity consumption to 3.45 MJ/kg wood, enabling a net electricity production. Then, pyrolysis of different plastic wastes for fuel production was conducted in the CMAP system. Overall, plastic wastes, especially polyolefin base plastics, produced much higher heating value byproducts, and relatively simpler compositions, compared to biomass, thus making plastic wastes a more desirable

feedstock to produce high quality fuels, energy-efficiently. At 560^{o}C, the highest liquid product yield, 47.4%, was obtained for thermal pyrolysis of HDPE, together with 24.5% wax product. The PP with fillers, (i.e. the mineral, talc) acted as a catalyst and showed noticeable cracking activity. The application of catalysts in the CMAP process has shown a significant impact on product yields and composition. Under a temperature of 620^{o}C, incorporating ZSM-5 catalysts in a secondary catalyst bed, enabled the elimination of wax product and an increase of liquid yield to 48.9%, and the liquid products contained considerably higher contents of gasoline-range aromatics (45.0%) and isomerized aliphatic (24.6%) contents. However, ZSM-5 catalysts also showed a tendency of rapid deactivation, and loss of activity at a feedstock/catalyst ratio of 5. Energy balance analysis of the process showed that 5 MJ of electrical energy were required to process 1kg of HDPE with the CMAP system, giving a total energy efficiency as high as 89.6%Furthermore, 6.1 MJ of electrical energy could potentially be generated from the gas products alone, making the process energy self-sufficient. In order to address a series of issues facing the application of catalysts in scaled-up pyrolysis systems, a structured catalyst of SiC foam supporting ZSM-5, was developed and tested for *ex-situ* catalytic upgrading of biomass pyrolytic vapors. A hydrothermal synthesis method was used to synthesize the catalysts, which resulted in a thin layer of ZSM-5 crystals firmly attached to the structure of a macroporous SiC foam material. Results suggest that the structured catalyst was more active and stable, compared to the randomly packed bed of catalysts, and also had the advantages of reduced pressure drop and enhanced heat and mass transfer. Therefore, this structured catalyst may serve as a promising candidate for future catalysts applied in large scale pyrolysis operations.

Table of Contents

List of Tables

List of Figures

Chapter 1 Introduction

Fossil fuels, including petroleum, coal, and natural gas, accounted for 80% of global energy demand (13972 Mtoe) in 2019, and remained the dominant primary energy sources to propel global economic growth (IEA 2020). Among the various energy consumption sectors, transportation is the largest sector, responsible for 52% of oil demand worldwide in 2017. New technologies such as battery-electric cars are rapidly developing to reduce our dependence on conventional fuels. However, world oil demand is projected to keep rising before 2040, mainly due to the growing demand from other transportation vehicles e.g. trucks and aircrafts, as well as production of petrochemicals, from which a myriad of derivative products, such as plastics, are produced (IEA 2020). The share of petrochemicals in total oil demand is estimated to grow to 15% in 2040, driven by economics, and population growth, especially in emerging economies such as China and India.

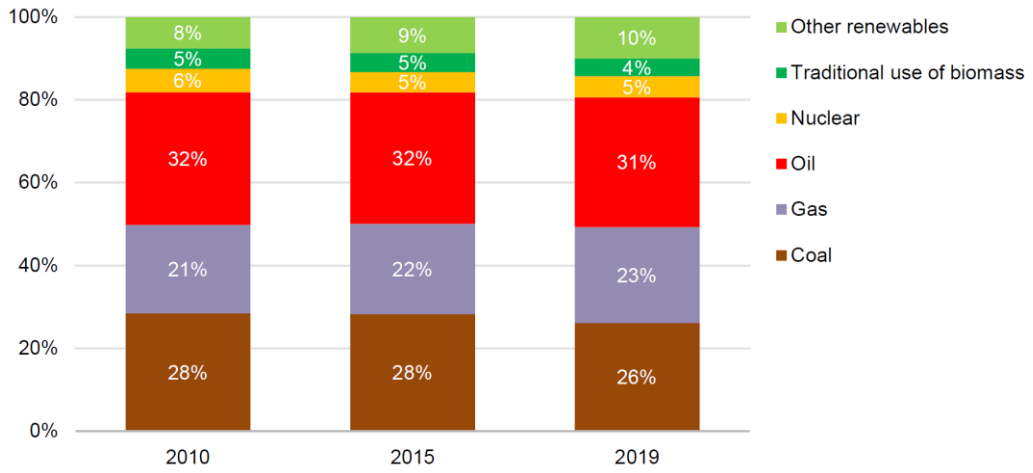

Figure 1 Share of total primary energy demand by fuel, 2010-19 (IEA 2020)

The heavy reliance on fossil fuels for transportation and chemicals, causes some of the greatest threats to humanity, such as global warming, air pollution, and energy insecurity (Hansen, Sato et al. 2016). As a result, transition to a cleaner, renewable, and sustainable production chain of fuels and chemicals is necessary and urgent. This calls for a combined effort, from various sectors such as new energy/fuel production technologies, innovative vehicle technologies, and energy conservation programs. Among the various alternative energy sources explored thus far, including wind, water, and solar radiation, biomass is unique because, as an abundant carbon-neutral material source, biomass can produce not only energy, e.g. heat and electricity, but also non-energy products, e.g. chemicals and materials. In this sense, biomass seems to be the only plausible alternative to fossil fuels. As a result, bio-refining has received increasing attention over the past few decades in R&D activities, as a crucial strategy to build a sustainable future by converting a broad range of biomass feedstocks into affordable biofuels, bio-power, and other bio-products (Cherubini 2010).

Another emerging source of both energy and materials, is plastic waste. Plastics have become an indispensable material of the modern economy, and they are used in an infinite range of products and applications due to their unrivalled functional properties and low cost. The drastic increase of plastic production over the past half-century has also brought global concerns including environmental pollution caused by plastic wastes. Nevertheless, the high energy content and abundant supply, make plastic wastes a great feedstock for energy production. In fact, many have suggested broadening the definitions of renewable energy to include energy from waste plastics. Waste plastics can be converted to electricity, synthesis gas (or syngas), fuels, and recycled feedstocks for new

plastics. Recovering this abundant energy also reduces waste sent to landfills and complements plastics recycling.

Among the various pathways to convert biomass and plastic wastes into energy products, thermochemical conversion approaches, including pyrolysis and gasification, have received considerable attention in research and development activities, considering their conversion efficiencies and flexibility with feedstocks. However, successful commercial scale-up applications of this technology are still lacking, due to significant technical challenges in terms of product yield and quality and process energy efficiency. Therefore, further advances in process development are still needed. Microwave assisted thermochemical processes serve as a promising alternative to technologies based on conventional heating, because microwave heating offers several unique benefits inherent to its dielectric heating mechanism. However, almost all related studies, so far, have been carried out in small lab-scale batch reactors, with a sample size typically less than 20 g. Therefore, it is necessary to scale up this technology and further investigate its feasibility for industrialization, at a much larger scale.

The overall objective of this dissertation is to improve the feasibility and scalability of the microwave-assisted pyrolysis process for energy production from biomass and plastic wastes. The specific objectives include:

1. Design, fabricate, and test a prototype system of continuous microwave-assisted pyrolysis and examine its feasibility for syngas production from **biomass feedstock.** The effect of processing temperature on product yields and composition will be studied and an energy balance of the process will be established to evaluate the energy efficiency of the process.

2. Modify the CMAP system and investigate its feasibility to produce fuels from **plastic wastes.** The effects of processing temperature, types of plastic composition, and catalysis on the product yields and composition, will be studied. An energy balance analysis will be conducted to evaluate the feasibility of this process.
3. **Develop a structured catalyst**, featuring high specific surface area and low pressure drop, which are desired but often overlooked properties for catalysts in scaled-up pyrolysis processes. The activity of this structured catalyst will be compared to those of other common configurations. The deactivation behavior and stability after regeneration will also be studied.

Chapter 2 Literature review

2.1. Overview of biomass as feedstock for biorefining

Biomass is a very broad concept embracing all organic material that stems from plants (or animals). Typical examples of biomass include agricultural and forestry residues and energy crops. More broadly speaking, organic wastes such as food wastes, wastewater sludge, and animal manure are also considered biomass since these waste materials initially come from plants. Originally derived from solar energy through photosynthesis, biomass energy has always been a major energy source in history, which contributed to 10% of the global primary energy supply in 2010 (Nakada, Saygin et al. 2014). This number is expected to increase as many countries and organizations have set their targets to increase the share of renewable energy in the energy sector. The International Renewable Energy Agency predicts that the biomass share in the global primary energy supply would double from the 2010 level by 2030, if a 36% renewable energy target were to be implemented globally (Nakada, Saygin et al. 2014). Among the 56 EJ biomass energy consumed worldwide back in 2010, 62% was used in the residential and commercial buildings sector, and another 15% in industry, mainly as a traditional low-grade fuel for direct heating purposes. Biofuel, mainly in the form of conventional bioethanol and biodiesel, made up 9% of the total bioenergy, while power generation from biomass, i.e. bio-power, only accounted for 8% (Nakada, Saygin et al. 2014). Over the past decade, a general trend has been observed, that traditional use of biomass, e.g. heating and cooking in rural areas commonly used in developing countries, has been gradually replaced by the modern use of biomass, e.g. biofuel and bio-power, which is cleaner and more efficient (STATISTICS 2018). For instance, in the United States, the

bioenergy market primarily comprises of conventional bioethanol (73%), biodiesel (11%), and bio-power (electricity) (12%) with negligible use for direct heating (Moriarty, Milbrandt et al. 2018).

It may be simple and straightforward to understand the benefits and potential exploitation of biomass as a source of energy and materials. But, to successfully achieve this goal requires a comprehensive strategy, to coordinate efforts from a variety of research fields, including plant genetics, biochemistry, biotechnology, biomass chemistry, separation technology, and process engineering, as well as industry and government collaborations. Biorefining is actually a complex strategy, and also a new manufacturing concept, that offers the opportunity to optimize the use of biomass for the sustainable production of biofuels, bio-power, and bioproducts (Ragauskas, Williams et al. 2006). Bio-refining is analogous to petroleum refining, where a complex of chemical processing units are used to separate/transform crude oil into a spectrum of products: gasoline, diesel fuel, jet fuel, naphtha, and other petrochemical materials such as plastics and BTX. In comparison, the **bio-refinery** concept embraces a wide range of processing technologies that could convert biomass into various products including both energy and non-energy products. There are various roadmaps and phases of bio-refining, considering the diversity of biomass composition and the conversion technologies available. For instance, different avenues of bio-refineries have been proposed, depending on the chemical compositions of various biomass feedstocks, including: triglycerides and lipids, sugars and carbohydrates, and lignocellulosic feedstocks (Maity 2015). In general, triglycerides and carbohydrate feedstocks are easier for conversion than lignocellulosic feedstock, and are therefore more developed commercially, due to their simpler and more uniform

compositions. Typical examples of these final products are biodiesel and bioethanol, produced through transesterification and yeast fermentation, respectively. In contrast, a lignocellulosic bio-refinery is more difficult and less developed commercially since its more complicated chemical composition and microstructure (e.g. the protective cell wall composed of lignin) create resistance to biological and chemical degradations.

2.1.1. Biochemical platform of lignocellulosic bio-refinery

Lignocellulosic feedstock, as the most abundant biomass resource available, can be processed through two general approaches: the biochemical approach and the thermochemical approach (Maity 2015). The biochemical approach of lignocellulosic biorefinery generally starts with pretreatment to disrupt the lignin and hemicellulose structures and enhance the accessibility of the carbohydrate portion for subsequent processing. The remaining cellulose and hemicellulose portion are then either biologically (i.e. through enzymatic fermentation) or chemically (i.e. through chemical processes such as acid hydrolysis) converted to monomer sugars, which are then fermented or chemically catalyzed into a range of products including advanced biofuels and intermediate chemicals (e.g. platform chemicals for further processing into various value-added bioproducts and commodity chemical products) (Choi, Song et al. 2015, Chandel, Garlapati et al. 2018, De Bhowmick, Sarmah et al. 2018). Typical examples of biofuels produced from this approach include both cellulosic ethanol via fermentation of sugars, and hydrocarbon transportation fuels produced from hydrodeoxygenation (HDO) of platform chemicals. Currently the cost of cellulosic ethanol (a second generation biofuel) doubles the cost of corn ethanol (conventional or first-generation biofuel) due to the expensive pretreatment steps, while the cost of the HDO process is also prohibitive

for production of hydrocarbon fuels from biomass (Regalbuto 2009, De, Saha et al. 2015). In order to produce high volume, low cost biofuels economically, which is a primary goal of a biorefinery, financial incentives must be provided for these low volume, high cost bioproducts. Recently, various strategies have been developed in the field of biochemical conversion, which have been described and critically reviewed by Sheldon (2014). Some examples include fermentation of carbohydrates to produce hydrocarbons, lower alcohols, diols, and carboxylic acids; also, acid catalyzed hydrolysis of hexoses to produce hydroxymethyl furfural (HMF), followed by subsequent conversion to important platform chemicals such as levulinic acid (LA), γ- valerolactone (GVL) and furan dicarboxylic acid (FDCA). However, with a few exceptions, such as conventional bio-product examples like paper and forest products, bio-products are generally still active subjects for research and development, and their commercial market is still emerging and immature. Therefore, continuous R&D efforts are still necessary to realize the economic goal of the bio-refinery (Moriarty, Milbrandt et al. 2018).

2.1.2. Thermochemical platform of lignocellulosic biorefinery

Compared to the biochemical approach, the thermochemical approach is less sensitive to feedstock composition variation, and therefore could expand the range of potential feedstocks while requiring less pretreatment steps (Tanger, Field et al. 2013, Li, Aston et al. 2016). Thermochemical conversion tends to have faster processing rates and better scalability, since many of the sub-processes use technologies related to those in the petroleum and petrochemical industries, that have been proven to have good economics on a large scale (Wright and Brown 2007). Therefore, thermochemical processing is closer to commercialization using lignocellulosic biomass, than the biochemical pathway.

Thermochemical processing pathways include gasification, pyrolysis, liquefaction, and combustion.

Hydrothermal liquefaction is still an emerging technology, which converts biomass into a liquid product called bio-crude under a hot, pressurized water environment. Typical hydrothermal processing conditions include temperatures in the range of 250–375^{o}C, and pressures of 4 to 22 MPa (40 to 220 Bar). The unique advantage of this process is that it dispenses the need of a drying step and therefore works best with wet waste and wet biomass such as algae (Gollakota, Kishore et al. 2018). The bio-crude is a highly viscous oil with a very complex profile of chemical compounds and relatively high nitrogen and oxygen contents, and therefore requires subsequent upgrading before it can used as a liquid fuel. This technology still faces a series of technical challenges to be market ready, mainly the high costs associated with the fabrication and operation of a continuous, highly pressurized system, as well as the upgrading process (Castello, Pedersen et al. 2018).

2.2.Biomass pyrolysis

Pyrolysis is the thermal decomposition of organic material (e.g. biomass) in the absence of oxygen. As a widely studied process, pyrolysis has shown the capability to produce a wide range of products including biochar, bio-oil and pyrolytic gas. Selective production of each product can be optimized by manipulating the process conditions (Kan, Strezov et al. 2016). The main target product, however, is usually bio-oil due to the strong interest in renewable transportation fuel. In this case, fast pyrolysis, i.e. a combination of high heating rate (10-200^{o}C/s) and short vapor residence time (<1s), is required to convert biomass into a liquid product called bio-oil at a high yield (e.g. 75%). The bio-oil can

then be upgraded to a usable liquid hydrocarbon transportation fuel. Growing attention from both academia and industry during the past few decades, has been focused primarily on three aspects of the biomass fast pyrolysis technology: reaction mechanism, reactor design, and bio-oil upgrading, with the goal being to produce a usable liquid product, cost-effectively.

2.2.1. Reaction mechanism

The complexity of biomass composition itself multiplied by the reactions involved during pyrolysis makes it very challenging to elucidate the pyrolysis mechanism. The most common approach to study the pyrolysis mechanism is by using thermogravimetric analysis data to build a macroscopic kinetic model, which can predict the formation rates of products (Wang, Dai et al. 2017, Zhou and Dunford 2017). Recent advances in analytical instrumentation methods (e.g. Py-GC-MS/FID, TG-MS, *in situ* spectroscopy, and isotopic labeling) have shed light on pyrolysis mechanisms, by providing more valuable information, such as quantitative evolutionary profiles of the reactants, intermediate products, and final products, during the pyrolysis process, which have been reviewed in detail by Wang, Dai et al. (2017). Yet the insight into pyrolysis reaction chemistry is still limited, and continued efforts are required in this field to provide more in-depth understanding of the reaction mechanisms, to guide the development of pyrolysis reactor design and catalysis systems.

2.2.2. Reactor design

At the heart of a fast pyrolysis process is the reactor. Currently one of the most developed fast pyrolysis reactor configurations is the fluidized-bed based pyrolysis system, since fluidized beds represent a well-established technology in the petrochemical industry, e.g. fluidized catalytic cracking (FCC) process. Pioneering work by the University of Waterloo back in 1980s and 1990s has laid the foundation for many fluidized bed pyrolysis studies, including several commercialization attempts with large-scale systems (Garcia-Nunez, Pelaez-Samaniego et al. 2017). Examples of fluidized bed pyrolysis systems include the bubbling fluidized bed, spouted fluidized bed, and circulating fluidized bed, done at various scales, from 20 kg/h to 8000 kg/h. In the past decade, several fluidized bed pyrolysis systems have been built for commercial applications (Bridgwater 2012, Radlein and Quignard 2013). While featuring high heating rates and bio-oil yields, fluidized bed pyrolysis also faces some inherent technical challenges, in order to become economically feasible. First, fluidized-bed reactors require excessive amounts of carrier gas in order to fluidize the materials, which is associated with significant energy consumption to move the carrier gas, as well as to heat the carrier gas to high temperatures. For instances, Park, Chang et al. (2016) reported the thermal efficiency of a fluidized bed drying system was less than 30% (heat required for drying/actual heat consumed) and similar results were reported by Liu and Ohara (2017). Second, biomass feedstock needs to be ground into fine particles of a narrow range of sizes, around 0.25mm, in order to ensure uniform fluidization and fast heating rates (Garcia-Nunez, Pelaez-Samaniego et al. 2017). In addition, the heat used in bubbling fluidized beds is typically generated from the combustion of pyrolysis gases and chars,

and then transferred to the sand through heating coils. The heat transfer rate in the coils is low due to the heating resistance inside the coils, and the limiting driving force, i.e. temperature difference between 800-600^{o}C inside the coils and around 500^{o}C for the sand; therefore, large heat exchange surfaces are required (Venderbosch and Prins 2010). The past decade has seen considerable R&D activities for innovating reactor configurations and in improving fluidized bed systems. For example, some of the new pyrolysis systems include ablative reactors, entrained flow reactors, auger reactors, and rotating cone reactors. However, due to the technical immaturity with these new reactors and a series of other technical issues with fluidized bed reactors, as well as a lack of confidence in economic prospects, and markets or legislative limitations, currently few pyrolysis commercial operations are running profitably (Bridgwater 2012, Radlein and Quignard 2013, Garcia-Nunez, Pelaez-Samaniego et al. 2017)

2.2.3. Bio-oil upgrading

Applications of pyrolysis bio-oil prior to upgrading are very limited because of several undesirable bio-oil properties, such as low heating value, high solids content, high viscosity, acidity, and chemical instability, most of which are associated with its high oxygen content (Czernik and Bridgwater 2004). Therefore, bio-oil upgrading, by removing oxygen content and improving quality, has become an active research focus. There are generally three actively studied approaches to bio-oil upgrading, including catalytic cracking, hydrotreating, and co-processing with fossil feedstocks in existing petrochemical processes.

- Co-processing

Co-processing bio-oil with petroleum feedstocks in existing refinery processes, such as fluid catalytic cracking (FCC), is being considered as a cost-effective way for biofuel upgrading and production, without the need for significant capital-intensive investments(Stefanidis, Kalogiannis et al. 2018). The technical feasibility of co-processing raw bio-oil with vacuum gasoil (VGO, an intermediate hydrocarbon product during petroleum refining) in the FCC unit has been demonstrated in a recent study, using a 200 kg/h demonstrate-scale unit (de Rezende Pinho, de Almeida et al. 2017). Up to 10% of bio-oil, having an oxygen content of approximately 50%, was directly fed into the FCC riser reactor. The oxygen present in the bio-oil was almost completely removed through catalytic cracking, as water, CO or CO_2, leaving only around 6600 ppm phenols in the produced fuel, at the 10% bio-oil blending ratio. However, additional tests conducted with the same bio-oil in two different experimental test series, showed that while a 9-month-old bio-oil did not cause operating problems in the FCC unit, a 21-month aged bio-oil did affect the operation of the unit by inducing a rapid increase of pressure drop across the reactor. This problem was associated with the chemical stability issue of raw bio-oil. The bio-oil renewable carbon conversion into liquid products (carbon efficiency) was reported to be approximately, only 30%. Due to these potential problems with the co-processing of raw bio-oil, several additional studies have proposed that further upgrading may be needed, before co-processing of raw bio-oil with petroleum. These studies have demonstrated that upgraded bio-oil (e.g. via CFP or hydrotreating) can be co-processed with less operational issues (Thegarid, Fogassy et al. 2014).

- Hydrotreating

Catalytic hydrotreating has been actively studied by researchers at the Pacific Northwest National Laboratory (Zacher, Olarte et al. 2014). Detailed description of a typical hydrotreating process has been reported by Wang, Elliott et al. (2016), wherein a two-stage catalytic reactor, containing Ru/C as the stage-I catalyst and CoMo/Al2O3 as the stage-II catalyst, were operated under the following conditions: 10.3 MPa, H_2 atmosphere, 400^{o}C. The first stage was for hydrogenation reactions, in order to stabilize the raw pyrolysis bio-oil; the second stage was for hydrodeoxygenation reactions, which directly determined the final yield of the upgraded oil. Results showed that the oxygen content was reduced to under 1%, while 90% of the carbon was kept in the upgraded oil. Griffin, Iisa et al. (2018) also reported similar results when hydrotreating CFP-oil using a less expensive catalyst, sulfide NiMo/Al_2O_3, in a 140 h time-on-stream experiment. 84 wt% of the hydrotreated product was found to have a boiling point in the gasoline and distillate range, and trace amounts of phenols were found to be the only oxygenated compound, indicating the high quality of the hydrotreated oil. However, the major limitation of the hydrotreating process is that the lifetime of the hydrotreating catalysts is still limited, which makes the overall process costly. Hydrotreating raw, fast-pyrolysis bio-oil is still a major challenge, due to fast catalyst deactivation, and therefore catalytic vapor upgrading before hydrotreating is almost a pre-requisite. Also, high pressures and reactor temperatures with flammable gases calls for special design and strict safety procedures.

- Catalytic cracking

Catalytic cracking receives the most attention among the three bio-oil upgrading approaches, and various catalyst materials and configurations have been explored (Rezaei, Shafaghat et al. 2014). In terms of catalyst materials, ZSM-5 as a microporous acidic zeolite catalyst, has received considerable attention because of its balanced performance featuring a high selectivity towards aromatics production and a moderate organic phase yield. These catalyst properties are related to its combination of moderate acidity, medium pore sizes, and moderate internal pore space, compared to other natural or synthetic zeolites (Carlson, Tompsett et al. 2009, Jae, Tompsett et al. 2011, Stefanidis, Kalogiannis et al. 2011). ZSM-5 has been used in many catalytic biomass pyrolysis studies of various scales, yet its performance is still far from perfect as it suffers from several drawbacks including low carbon efficiency (ca. 24% of CFP with ZSM-5) and rapid deactivation due to coking. For instance, Mukarakate, Zhang et al. (2014) monitored the real time deactivation behavior of ZSM-5 catalysts during upgrading of pine pyrolysis vapor. They found that, while fresh catalyst produced primarily aromatic hydrocarbons and olefins, with no detectable oxygen-containing species, after pyrolysis of roughly the same weight of biomass as catalyst weight (biomass to catalyst ratio, B/C=1), oxygenated products began to appear in the product stream. When the B/C ratio reached around 5, the oxygen content in the product was almost the same as that without catalysts, meaning catalytic effect had been completely lost at that point. Therefore, many recent studies have explored various other catalyst options, such as mesoporous acidic catalysts and metal oxide catalysts, which have been summarized in several reviews (Rezaei, Shafaghat et al. 2014, Kabir and Hameed 2017). For instance, researchers from

NREL have investigated a new catalyst, i.e. Pt/TiO_2, for catalytic cracking of biomass pyrolytic vapors. With this catalyst, oxygen in the biomass is generally removed as water instead of CO_2/CO as with ZSM-5, therefore the carbon yield is significantly improved (e.g. 45% vs. 24% of CFP with ZSM-5), and also the stability of the catalysts were improved due to lowered rates of coking. Yet, as a hydrodeoxygenation (HDO) catalyst, Pt/TiO_2 does require the addition of H_2 to the process, at near atmospheric pressure, which could be a safety concern (Griffin et al., 2018). Modifications of zeolite catalysts have also been explored by numerous recent studies. For example, surface treatment to obtain mesopores or macropores on zeolites surface structures has been investigated, in order to mitigate coking issues (Jia, Raad et al. 2017, Hertzog, Carré et al. 2018), and doping with metal species to improve catalyst performance has been studied (by Iliopoulou, Stefanidis et al. 2012, Widayatno, Guan et al. 2016).

The other important factor in catalytic biomass pyrolysis is the placement of catalysts in the process. In general, catalysts can be applied in the process either *in-situ*, i.e. where catalysts are in direct contact with biomass during pyrolysis, or *ex-situ*, i.e. where catalysts are placed in a separated catalyst bed downstream of the pyrolysis reactor for upgrading of the pyrolytic vapor. In this regard, most studies carried out in more industrially realistic systems, e.g. fluidized bed reactors, have been focused on the *in-situ* design, which is typical for a catalytic fast pyrolysis (CFP) process (Mullen, Boateng et al. 2011, Zhang, Carlson et al. 2012). In these systems, zeolite catalysts are usually spray-dried or extruded with binders, in order to form particles as fluidizing medium with suitable sizes for fluidization(Iisa, French et al. 2016). A critical issue with *in-situ* CFP is reported to be the rapid deactivation of catalysts due to coking. For instance, it has been

reported that the catalytic activity of HZSM-5 began to decrease due to coke formation after 40 min of operation at a weight hourly space velocity (WHSV) of 0.1(Carlson, Cheng et al. 2011); a pilot-scale in-situ CFP study that coke deposition, after only 5 min operation at 2.6 WHSV, accounted for as high as 25% of total input biomass(Mullen, Boateng et al. 2011). In order to address this issue, circulation fluidized bed reactors have been designed where the spent catalysts are circulated into a secondary reactor, called the regenerator, where they are burned before being transferred back into the fluidized bed pyrolyzer, thus, completing a continuous circulation that mimics a fluidized catalytic cracking (FCC) process in a petroleum refinery(Jae, Coolman et al. 2014, Paasikallio, Lindfors et al. 2014). However, the feasibility of this design is undermined by several issues, inherent in the *in-situ* process design, apart from its complexity. For instance, as demonstrated in several pilot scale studies, char cannot be separated out of the reactor, and has to be combusted together with the spent catalysts, which accumulates ash in the process, and may eventually lead to the irreversible deactivation of catalysts due to mineral deposition (Mullen and Boateng 2013, Paasikallio, Lindfors et al. 2014).

The alternative configuration is the *ex-situ* design. At the cost of additional heating of the catalyst bed, the *ex-situ* design requires less catalyst to achieve the same level of deoxygenation, and is less prone to coke formation and thus catalyst deactivation. Possible explanations for these advantages of *ex-situ* design include 1) sufficient contact between pyrolysis vapor and the catalyst, 2) independent control of the catalytic temperature, and 3) indirect contact between biomass/char and the catalyst (Gamliel, Du et al. 2015, Iisa, French et al. 2016, Hu, Xiao et al. 2017). However, most bench scale *ex-situ* CFP studies so far configure the catalytic fixed bed reactors by randomly packing

tens of grams of (or even less) catalyst powders (typically < 0.15 mm) or pellets (typically 1-2 mm) confined by a metal mesh or quartz wool. While it might work for small scale experiments and is easy to operate, a randomly packed bed would meet with severe limitations when scaled up into large operations, that might require kilograms of catalysts in one reactor. Therefore, special attention must be paid to the design of a catalytic reactor for scaled-up operations.

2.3.Biomass gasification

Producing liquid transportation fuel from biomass "pyrolysis", generally requires complicated and often prohibitive upgrading and downstream processes, as reviewed above. In comparison, syngas production from biomass "gasification" provides an alternative approach, to harness biomass energy that is self-sufficient in terms of energy consumption, and requires less processing steps, and therefore is currently more economically feasible (Sansaniwal, Pal et al. 2017). Gasification is a thermochemical conversion process where carbonaceous feedstock is partially oxidized, typically under temperatures over 600^{o}C, into a gas product with the help of a gasifying agent such as air, oxygen, CO_2, and/or steam. The raw product gas from gasification is a mixture of primarily CO, H_2, CO_2, CH_4, N_2, H_2O, and other organic (i.e. tars) and inorganic impurities (e.g., H_2S, NH_3, alkali metals). In addition, particulate matter may also be present in the raw syngas (a gas mixture of primarily CO and H_2) and may have to be removed in downstream processing. Syngas is a versatile fuel which can be used to produce various conventional end products such as H_2, heat, and electric power, and also liquid hydrocarbons through mature processes like adsorption, boiler combustion, gas engines or turbines, and Fischer-Tropsch processing; syngas can also serve as feedstock

to relatively novel processes, such as chemical synthesis and fermentation, to produce chemicals (Wang, Weller et al. 2008).

2.3.1. Gasification reactors

There are generally three types of biomass gasifiers that have been widely applied, i.e. fixed bed gasifiers, fluidized bed gasifiers, and entrained flow gasifiers (Sikarwar, Zhao et al. 2016, Situmorang, Zhao et al. 2020).

Fixed bed gasifiers are the oldest and simplest gasification systems, which can be divided into two groups, i.e. updraft (fuels entering from top and gas product exiting from the top) and downdraft (fuels entering from the top, and gas product exiting from bottom). Due to the different configurations in the relative movement of biomass and gasifying agents in the reactor, updraft gasifiers have higher thermal efficiency and lower pressure drop than downdraft gasifiers but suffer from higher tar content (e.g. 10-20 wt.%) in the produced gas.

The entrained flow gasifier, originating from the coal gasification industry, is designed to handle very fine particles, e.g. 75–100 μm at high temperatures ranging from 1400 to 1800^{o}C and high pressure of 20–70 bar. Due to small particle size and high temperature and pressure, the carbon conversion is almost 100%, and tar content is minimal (Briesemeister, Kremling et al. 2017). However, high investment and operating costs present serious barriers toward economic implementation of this technology (Sikarwar, Zhao et al. 2016).

The fluidized bed gasifier has enhanced mixing capability, heat transfer rate, and temperature distribution uniformity because of the turbulent fluidization mechanism. Fluidized bed gasifiers come in three basic types: bubbling fluidized bed, circulating

fluidized bed, and dual fluidized bed (DFB). With increasing carbon and energy efficiency from the bubbling fluidized bed to dual fluidized bed, the system complexity and scale also increase (Corella, Toledo et al. 2007). Currently, the DFB gasification process has gained global interest, with many systems established at various scales, including several commercial implementations, mainly in Europe (Benedikt, Schmid et al. 2018). Dual fluidized bed (DFB) gasifiers consist of two separate fluidized bed reactors, one being the gasifier and the other being the char combustor. Steam is used in the gasifier to obtain high quality gas product, while air is usually used in the combustor to allow combustion of chars, which provides the heat necessary to drive the steam gasification process. The heat is transferred from the combustor to the gasifier by the fluidized bed material, which is circulated between the beds (Karl and Pröll 2018). An example of such a system, also one of the largest biomass gasification systems to date, is the Swedish Gothenburg Biomass Gasification plant, built in 2015 with a biomethane production capacity of 20 MW. The cold gas efficiency and the overall plant efficiency are reported to be 71.7% and 57.7%, respectively (Alamia, Larsson et al. 2017). In order to improve the economic feasibility, Benedikt, Schmid et al. (2018) investigated the influence of several low cost feedstocks on a 100 kW DFB system. While not mentioned in these research articles, several review articles have pointed out a number of technical challenges in DFB systems, including low conversion of water/steam in the gasifier (Corella, Toledo et al. 2007), catalyst attrition, and reactor erosion due to the constant solid movement (Hanchate, Ramani et al. 2020), and process temperature control (Fuchs, Schmid et al. 2019).

2.3.2. Tar

Contrary to the common belief that biomass gasification is a well-established and commercialized technology, some technological and economic barriers still exist in its implementation at higher scale, which limits the commercial application of the technology. In terms of technological barriers, besides those associated with the reactors and process operations as mentioned above, perhaps the biggest technological challenge is the existence of various contaminants in the gas product, with tar being the most problematic issue (Asadullah 2014, Sikarwar, Zhao et al. 2016). Tar is a generic term referring to the dark-colored, viscous liquid byproduct which condenses at reduced temperatures during the gasification process. In terms of chemical composition, tar can be seen as a complex mixture of mainly condensable, single-ring to 5-ring aromatic compounds plus other oxygen-containing hydrocarbons and some polyaromatic hydrocarbons (PAHs)(Devi, Ptasinski et al. 2003). An example of tar composition and content in a typical fluidized bed gasifier, is shown in Table 1(Carpenter, Bain et al. 2010). In terms of abundance, benzene, toluene, and naphthalene are usually the top three compounds in tar (Brage, Yu et al. 2000).

Table 1 Average Tar Concentrations (g/Nm3) for different feedstocks under the following reaction conditions: steam/carbon=1, fluidized bed temperature 650°C, thermal cracker temperature 875°C (Carpenter, Bain et al. 2010).

	Corn stover	Vermont wood	Wheat straw	Switchgrass
Benzene	33.2	24.6	33.5	38.9
Toluene	10.8	7.0	9.9	10.4
Phenol	3.3	2.1	1.9	3.0
Cresols	0.2	0.2	0.2	0.2
Naphthalene	11.2	7.7	11.5	13.4
anthracene/phenanthrene	3.6	2.5	3.9	4.6
Other tar	22.5	14.9	23.3	25.7
Heavy tar	17.4	14.4	22.9	25.6
Total tar(>78)	69.1	48.8	73.4	82.9
Tar yield (g/kg of feed)	39.6	33.5	40.3	40.6
% of feed C in tar	12.5	9.7	10.7	12.7

Tar formation is undesirable mainly because of four problems it brings to the gasification process. **First**, most of the tar compounds are readily condensable, and thus cause fouling, efficiency loss, and unscheduled plant shutdowns by condensing on downstream pipelines, blocking gas coolers, and filter elements, which is a major issue in gasification plants. **Second**, certain tar species remain in syngas in the form of aerosols and makes it unacceptable for various end uses. Tar content in syngas varies depending on gasifier types, reaction conditions, and feedstock types, etc., but a generalization of crude tar content would be: updraft at 100 g/Nm^3, fluidized beds at 10 g/Nm^3, and downdraft at 1 g/ Nm^3 (Milne, Evans et al. 1998). In contrast, much lower tar contents are required by most applications: 50-500 mg/Nm^3, 100 mg/Nm^3, and 0.1 mg/Nm^3 for compressors, internal combustion engines, and methanol synthesis, respectively (Milne, Evans et al.

1998, Woolcock and Brown 2013). **Third**, tar formation represents a major carbon efficiency loss for the overall gasification process. Up to 10% of the total biomass high heating value (HHV) could be lost in the form of tar if left untreated. And **last but not least**, most of the compounds in tars, e.g. polycyclic aromatic hydrocarbons (PAHs), are toxic and pose a threat to the ecosystem, if directly discharged into the environment. These problems make tar formation the key technical barrier to large-scale implementation of gasification technology (Han and Kim 2008, Xu, Donald et al. 2010).

2.3.3. Tar removal

A large number of studies have been devoted to removing or converting tar from raw syngas, and the approaches applied generally fall into two categories: the **primary** approach and the **secondary** approach. In the primary approach, optimization of the gasifier design, proper selection of operating parameters, pretreatment of feedstock, and addition of bed catalysts are usually implemented to minimize the tar content produced and ideally eliminate the necessity of further downstream treatment (i.e. secondary approach) (Devi, Ptasinski et al. 2003). One primary approach, such as two-stage gasifiers, has shown to be capable of tar content reduction to 50mg/Nm^3 level, yet secondary methods must still be implemented in order to meet more stringent requirements (Torres, Pansare et al. 2007, Woolcock and Brown 2013)

For secondary tar removal, there are three main approaches existing to remove tars downstream of the gasifiers, namely, mechanical methods, thermal cracking, and catalytic cracking. In contrast to the other three approaches, which attempt to chemically convert the tar species into permanent gases by increasing the reaction rate of tar decomposition, mechanical methods remove tar from raw syngas by purely physical

separations. The most widely used process in current gasification plants is wet scrubbing, where water is generally used as a washing media to absorb the water-soluble fraction of tars and, also reduce the gas temperature to condense out the non-water-soluble portion of tars. Besides the clogging and fouling issue, a major problem intrinsic to wet scrubbers is the wastewater generation from the process. Special treatment of wastewater is required before final disposal, and this significantly adds to the operational costs, in many cases, to a prohibitive level (Milne, Evans et al. 1998). In addition, as with other mechanical methods, wet-scrubbing only removes tar from the raw product gas, while the energy stored in tar is also lost in the waste streams.

With regard to thermal cracking, typically temperatures between 1100^{o}C to 1300^{o}C are required to achieve fast and effective tar removal (Rabou, Zwart et al. 2009). Although thermal cracking is reported to achieve tar content down to 15mg/m^{3} at 1290^{o}C in 0.5 seconds, it suffers from significant cost increase and soot formation from polymerization of tar compounds, and therefore is rarely used in gasification plants (Lettner, Timmerer et al. 2007, Woolcock and Brown 2013).

Catalytic cracking, also referred to as hot-gas cleaning, is seen by many as the most promising method to remove tar from gasification syngas, because it can increase overall process efficiency by converting tars into syngas products, without incurring a heat penalty, and avoids thermal cracking, or wastewater generation involved in mechanical methods (Yung, Jablonski et al. 2009, Asadullah 2014). In contrast to thermal cracking which requires temperatures over 1000^{o}C to achieve sufficient tar removal, and steam reforming which requires over 900^{o}C, the application of catalysts can reduce the operating temperature typically below 800^{o}C by reducing the activation energy of steam

and dry reforming reactions, and could potentially avoid the need of additional heating of the gas stream as it exits the gasifier.

2.3.4. Power generation using biomass gasification syngas

Electricity production from the combustion of gasification syngas, is a potential application which has recently gained much interest, driven by legislation to reduce emissions, simplicity of the application, and technical advantages over conventional bio-power generation technology (Sikarwar, Zhao et al. 2016).

There is an ongoing global trend in pushing toward bio-power production. For instance, as the world's biggest energy consumer, China is aiming to increase the share of electricity production from renewable sources to at least 35% by 2030, and biomass power generation would account for 30 GW, or 15% of its total renewable energy (Zhang, Wang et al. 2017). Currently bio-power is predominantly produced by combustion technology which originates from traditional coal power generation technology. In these plants, biomass either as is (i.e. direct-fired) or mixed with other primary fuels, such as coal (i.e. co-firing) is burned directly in boilers to produce steam which then drives a turbine to generate electricity. Despite the large number of biopower plants established worldwide, many biomass power plants today rely on government subsidies to sustain economic operation, while many others without subsidies are mostly idled or financially failing (Moriarty, Milbrandt et al. 2018). The economic feasibility of the industry is faced with several bottlenecks. First, unlike wind power and solar power, biomass energy relies on collection and transportation of biomass feedstocks, and biomass logistics can be costly in many cases. The feedstock cost can be essentially zero where they are produced, since they are mostly, otherwise, unusable byproducts or

residue materials from agricultural or industrial processes. But these feedstock costs could increase to as high as 60% of the total biopower production cost, when the feedstock, such as agricultural crop residues, have to be collected and transported over long distances. This is especially true for conventional biopower plants which have to be built in relatively large sizes (10-25 MW) in order to be efficient, and therefore require significant amounts of feedstock material, collected with a long transportation distance (Moriarty, Milbrandt et al. 2018, He, Zhu et al. 2019). The other factor to consider is the biomass combustion technology itself. The main disadvantage of combustion technology is its low energy efficiency, which is reported to be approximately 20% for a typical direct-fired biomass power generation system (Bridgwater 1995). Another common issue with the technology is corrosion caused by depositions such as alkali chlorides produced in boilers burning biomass (Enestam, Bankiewicz et al. 2013).

Considering the factors mentioned above, investment in the biopower industry over the past few decades has moved towards small to medium scale (0.5-5 MW) biomass gasification power generation. The gasification-to-electricity route has a higher overall energy efficiency; the biomass is first converted to syngas, which can then fuel gas turbines or engines. Since gas turbines operate at a much higher temperature than steam turbines, e.g. 1500^{o}C vs. 600^{o}C, the energy efficiency of the gasification-electricity route is much higher than the conventional combustion route, e.g. 30-33% vs. approximately 20% (Ruiz, Juárez et al. 2013). The energy efficiency can be further increased by utilizing excess heat from the gas turbine in a steam cycle for producing additional electricity and heat, such as in an integrated-gasification-combined-cycle (IGCC) system. Other advantages of gasification include: less emission problems and less solid residue

left on the equipment. And last but not the least, gas product can be used in a greater variety of applications beyond electricity generation, such as H_2 production and synthesis of liquid fuels (Fischer-Tropsch) (Bridgwater 1995). In terms of the scale of gasification systems, instead of the large scale, i.e. >5MW, of industrial coal and petroleum coke gasification systems, the preferred scale for biomass gasification systems is small and modular. Small gasifiers, especially with capacities lower than 200 kW, can effectively handle locally produced biomass or municipal solid waste while avoiding high biomass collection and transportation costs (Situmorang, Zhao et al. 2020). The modular feature would enable the unit to be moved where the demand exists, such as in rural areas.

2.4.Microwave-assisted thermochemical conversion technology

For thermochemical conversion processes such as pyrolysis and gasification, temperature and heating rate are perhaps the most important parameters followed by other parameters such as residence time. The following table presents a basic idea of how various thermochemical processes, with different basic operating parameters, affect the final product distribution from typical biomass feedstock.

Table 2 - Heating characteristics of pyrolysis and gasification processes and their product yields

Process	Heating characteristics			Product Yield		
	Heating rate ($°Cs^{-1}$)	Temperature (°C)	Residence time (s)	Liquid (%)	Char (%)	Gas (%)
Slow pyrolysis	0.1-1	300-600	>450	30 (70% water)	35	35
Intermediate pyrolysis	10-200	450-600	10-300	50 (50% water)	20	30
Fast pyrolysis	>200	600-800	<2-5	75 (25% water)	12	13
Gasification	>200	>700	0.5-30	5	10	85

It is therefore easy to understand the need for uniform temperature distribution, fast heating rates, and controllable heat transfer in developing any thermochemical conversion reactor and process. However, since conventional heating methods always rely on heat transfer from the high-temperature heat source to the load at lower temperature, intense mixing is always required in order to meet special heating requirements. Therefore, as mentioned in Section 2.2.2 and 2.3.1, the fluidized bed reactor is the most adopted reactor design, mostly due to its excellent heating characteristics offered by the turbulent fluidization mechanism. However, as also pointed out in those sections earlier, the special need for fluidization also brings several challenges to the process, including: (1) difficulty in controlling uniform flow and residence time, (2) requirement of small particle size, (3) high ash content in the product, (4) dilution and heat loss due to carrier gas, and (5) complex structure and only economically viable in large scale operations. In contrast, microwave heating as an advanced heating method, provides an alternative to the conventional heating method, and offers many attractive features that open the door to novel reactor designs for thermochemical conversion processes.

2.4.1. Principle of Microwave Heating

Microwave is a form of electromagnetic radiation with wavelengths ranging from about one meter (frequency 300 MHz) to one millimeter (300 GHz). The most common frequency used in modern microwave application is 2450 ± 50 MHz, followed by 915 ± 13 MHz. Microwaves heat most materials on the principle of “dielectric” heating. In this process, microwave irradiation causes polar molecules and ions to constantly rotate as they try to align themselves with the high frequency alternating electromagnetic field,

generating friction among molecules and thus manifesting a temperature rise of the material (Grant and Halstead 1998, Haque 1999, Mishra and Sharma 2016).

The ability of a specific material to absorb microwave energy and convert it into heat depends on its dielectric and magnetic properties including: dielectric constant (ε′) and dielectric loss (ε ″). Experimental measurement of the dielectric properties for a specific material is very difficult, since they are a function of various factors including electric and magnetic field strengths, temperature, and time. Empirical equations shown below, are often used to explain the correlation of microwave power *P* absorbed by a given material, and the penetration depth (*d*) with its dielectric properties.

(1) $P = 2\pi f \varepsilon'' E^2$ [W/m^3]

(2) $d = \frac{c\sqrt{\varepsilon'}}{2\pi f \varepsilon''}$ [m]

Where:

f - microwave frequency (Hz),

ε''- dielectric loss

ε‘ - dielectric constant

E - electric field strength (v/m)

c – speed of light (3x10^{8}m/s)

Mishra and Sharma (2016) gave a comprehensive review of microwave interaction with various material types. Briefly, materials with low dielectric loss factors, such as quartz, Teflon, have a very large penetration depth and very little of the energy can be absorbed in the material, and therefore the material is considered transparent to microwave energy, i.e. an insulator. In contrast, materials with very high dielectric loss factors (e.g. metals) tend to reflect the microwave irradiation and have negligible penetration depth; therefore,

they are considered reflectors and generally do not absorb microwaves vary well, either. Between these two extremes are materials that have dielectric loss factors in the middle of the conductivity range, and these materials are considered microwave absorbents.

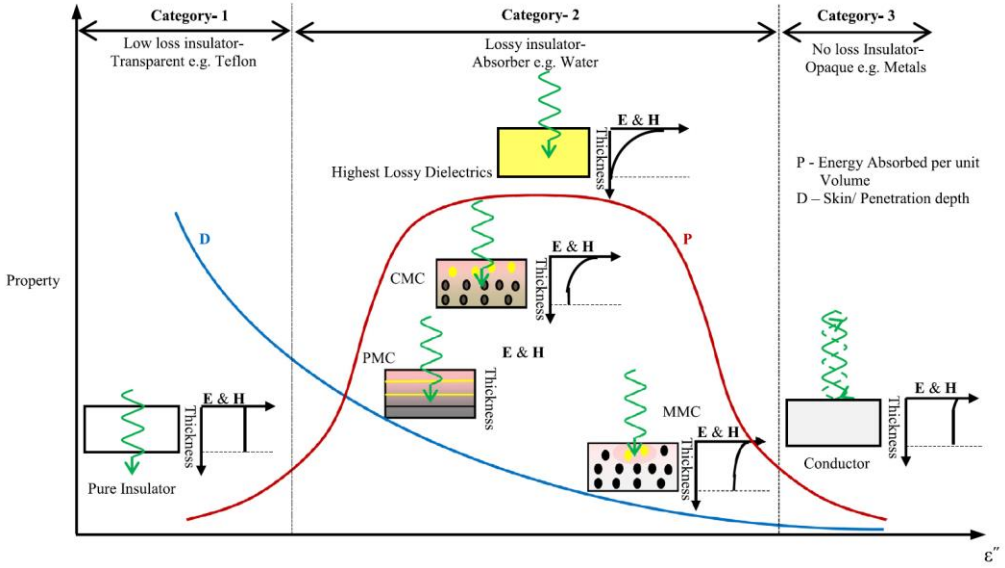

Figure 2 Microwave interaction with different types of materials (Mishra and Sharma 2016)

The ratio of the dielectric loss to dielectric constant, i.e. the loss tangent, tanδ= ε″/ε ′, is often used to describe the overall efficiency of a material to absorb microwave radiation. The following table shows the loss tangents of some common materials involved in the process.

Table 3 Dielectric loss tangents of different materials at a frequency of 2.45 GHz and room temperature (Zhang, Cui et al. 2020)

Material	$tan\ \delta = \varepsilon'' / \varepsilon'$
Coal	0.02–0.08
Water	0.12
Cellulose	0.035
Hemicellulose	0.062
Lignin	0.052
Polypropylene	0.0003–0.0004
Polystyrene	0.0002–0.0003
Polyethylene	0.0001–0.0002
Carbon foam	0.05–0.20
Charcoal	0.11–0.29
Carbon black	0.35–0.83
Activated carbon	0.22–2.95
Carbon nanotube	0.25–1.14
SiC	0.58–1.00

2.4.2. Microwave heating in thermochemical conversion processes

Owing to its inherent dielectric heating mechanism, microwave heating is associated with several unique advantages compared to conventional heating, and these advantages include selective heating (i.e. materials with different dielectric properties are heated by microwave irradiation to different degrees), volumetric heating (microwaves can penetrate uniformly throughout the volume of certain materials and thus deliver energy evenly) and rapid heating(microwave heating is an energy conversion process without heat transfer limitations). Therefore, it has been exploited extensively during the past few decades as an alternative heating approach in various applications such as chemical synthesis (Kappe 2004), food processing (Zhang, Tang et al. 2006), and more recently thermal processing of agricultural and industrial waste (Menéndez, Arenillas et al. 2010). Since organic solid waste materials including most biomass generally have low dielectric loss factors and therefore cannot be heated by microwave irradiation efficiently,

microwave absorbents are often added to the process to achieve fast and uniform microwave heating. For instance, the addition of SiC (silicon carbide) into a microwave heating process can significantly improve the heating rate, ranging from 4 to 40^{o}C/s (Kremsner and Kappe 2006, Zuo, Tian et al. 2011). Besides a high dielectric loss factor, a good microwave absorbent in the pyrolysis process also needs to have a high thermal conductivity and chemical inertness at elevated temperatures. Commonly used microwave absorbents in a pyrolysis process include carbon-based materials, e.g. graphite, char, and carbon black, (Menéndez, Arenillas et al. 2010), metal oxides(Li, Ma et al. 2013), and silicon carbide, which is considered as a superior option (Khaghanikavkani and Farid 2013, Zhou, Liu et al. 2018). Newly investigated materials also include graphene and activated carbons (Lam, Mahari et al. 2019, Jiang, Liu et al. 2020).

Many studies have compared thermochemical conversion processes using microwave heating with those using conventional heating, and results have suggested several advantages with microwave heating, including better energy efficiency, shorter processing time, easier heating control, and improved product quality (Huang, Chiueh et al. 2016, Zhang, Rajagopalan et al. 2017, Klinger, Westover et al. 2018, Parvez, Wu et al. 2019, Arpia, Chen et al. 2020). For instance, when it comes to the specific topic of producing syngas from pyrolysis of biomass, microwave heating has been demonstrated by several studies to be a superior method, as it can considerably improve syngas yield by promoting heterogeneous catalytic reactions, possibly through generating micro-plasmas and hot spots, when interacting with biochar (Domínguez, Fernández et al. 2008, Huang, Kuan et al. 2010, Beneroso, Bermúdez et al. 2013, Zhang, Dong et al. 2015). This

interaction between biochar and microwave irradiation also contributes to significant reduction in tar formation, which is deemed a critical technical obstacle in the biomass gasification process (Ruiz, Juárez et al. 2013). More details about the comparison between microwave heating and conventional heating for other types of biofuel production can be found in a recent review paper by Zhang, Cui et al. (2020). Currently most of the microwave-assisted pyrolysis or gasification processes reported in literature for bioenergy production are still batch processes with a sample size typically below 20g. In these lab-scale processes, the biomass feedstocks are either 1) premixed with the microwave absorbents and then heated from room temperature to pyrolysis temperature, or 2) dropped onto a bed of preheated microwave absorbents in a microwave reactor. Neither design is readily scalable to industrial operations due to their batch process nature. There are, however, a number of studies reporting scaled up reactors. For instance, Lin, Chen et al. (2012) developed a 10kW microwave heating system for pyrolysis of sewage sludge, yet the reactor was essentially a semi-batch design, since biochar product cannot be continuously discharged from the system. Payakkawan, Areejit et al. (2014) developed a continuous microwave assisted biomass carbonization system with a microwave output power of 8.5 kW and a processing rate of 350 kg/h of coconut shells. However the economic feasibility of this process is questionable, since no microwave absorber was used. Finally, Zhou, Liu et al. (2018) in our group developed a lab-scale continuous microwave assisted pyrolysis system with a capacity of 2g/min, yet this is more of a proof-of-concept study, and more work is needed to scale up the technology and further investigate its feasibility at a much larger scale.

2.5. Waste plastics as a source of energy production

Plastics have become an indispensable material of the modern economy used in an infinite range of products and applications, due to their unrivalled functional properties and low cost. The past half-century has witnessed a twenty-fold increase of plastic production, and this trend is expected to continue, with annual plastics production exceeding 500 million tons, and consuming nearly 40% of crude oil by 2050 (De Smet 2016, Sardon and Dove 2018, IEA 2019). However, the magnitude of plastic production also brings with it, global concerns related to problems including environmental pollution, unsustainable production, and poor recycling mechanisms of plastics, especially plastic packaging materials. For instance, over 80% of the 7 billion tons of plastics ever produced, end up in the environment as landfills or as waste e.g. marine litter; only 2% of new plastics are made from renewable resources; in addition, among the 78 million tons of plastic packaging produced annually, only 14% are recycled and merely 2% are recycled into the same or similar quality applications (De Smet 2016). Currently plastics are predominantly recycled through mechanical recycling, which typically involves collection, sorting, and washing before reprocessing into products. Yet, mechanical recycling is faced with several inherent challenges, including thermal-mechanical degradation, processing complex plastic mixtures (e.g. PVC and PET), and contaminants in recycled plastics, which often result in lower-value products of limited recyclability, and therefore are considered a down-cycling approach (Ragaert, Delva et al. 2017). This calls for exploration of alternative recycling approaches that could convert plastic wastes, an abundant resource, into more valuable products.

Pyrolysis of plastic wastes seems to be a promising chemical recycling method, as it is capable of decomposing plastic polymers to lower-molecular-weight products such as fuels and petrochemical feedstocks for energy and material recovery (Sharuddin, Abnisa et al. 2016). As an energy recovery process from plastics, pyrolysis is more favorable than incineration from an environmental point of view, since the latter requires advanced pollution control measures (e.g. high temperature (>850^{o}C) and long residence time (>2 s)) which are required to prevent emissions of toxic compounds such as dioxins(Shibamoto, Yasuhara et al. 2007, Yang, Sun et al. 2013). As a material recovery process, pyrolysis is very flexible in terms of handling contaminated plastics and heterogeneous plastic mixtures, including those that cannot be mechanically recycled (Ragaert, Delva et al. 2017). Compared to biomass, plastics have several advantages as feedstock for energy production from pyrolysis. First, since most common plastics such as PET, PE, PS, and PP contain only hydrogen and carbon in terms of elemental composition, the heating values of plastics are much higher than biomass, which often means a better energy balance for the pyrolysis process. More importantly, the product quality is also higher and easier to control due to its relatively simple composition and lack of the troublesome element, oxygen. However, plastics tend to melt to form a sticky and viscous liquid prior to thermal degradation, which causes many operational issues in the pyrolysis process, such as difficulty in mixing and fluidization (Arena and Mastellone 2000, Jing, Yan et al. 2014).

Successful implementation of plastic pyrolysis technology relies on several integral parts, including the choice of catalysts, pyrolysis reactor design, and process parameter optimization. Although the concept of plastic pyrolysis has been investigated for decades

and a considerable amount of data have been collected that help to elucidate the process from a fundamental level, most of the studies are conducted in small laboratory-scale rigs such as thermogravimetric analyzers, microreactors, and other batch laboratory reactors (Wong, Ngadi et al. 2015). Very limited consideration is given in these studies to scale up this process to an engineering scale unit operation, running in a continuous mode, which is a key step towards the real-world application of this technology. There are, however, several studies that have developed lab-scale continuous reactors for plastic pyrolysis, and these include horizontal screw reactors (Serrano, Aguado et al. 2001, Walendziewski 2005), conical spouted bed reactors (Elordi, Olazar et al. 2009, Alvarez, Lopez et al. 2017), and a stirred tank reactor (Auxilio, Choo et al. 2017), all of which have a throughput capacity below 10g/min. One exception is a two-step process recently developed by Kassargy, Awad et al. (2018), which consists of a horizontal screw reactor for melting and a vertical tube reactor for thermal degradation, and has a processing capacity of 3.1 kg/h. However, the details of this reactor design are rather limited for the evaluation of its scale-up potential. Overall, successful commercialization of this technology is still rare, since most of theses attempts still struggle with yield and quality issues of the products, and the reliability of the pyrolysis system (Arabiourrutia, Elordi et al. 2012, Wong, Ngadi et al. 2015, Alvarez, Lopez et al. 2017, Lopez, Artetxe et al. 2017).

2.6. Microwave-assisted pyrolysis of waste plastics for energy production

Microwave heating has been applied to the plastics pyrolysis process (i.e. microwave assisted pyrolysis, or MAP) for energy and chemical recovery as early as 2001 when

Ludlow-Palafox and Chase (2001) used a semi-batch reactor and carbon as a microwave absorbent to pyrolyze HDPE pellets and toothpaste packaging (i.e. aluminum/PE composite) laminates as an example of real-world plastic wastes. Results showed that this process could handle toothpaste packaging material quite well, while previous trials with conventional pyrolytic processing failed, indicating the potential advantage of microwave heating in treating mixed plastic wastes. Since then, the feasibility of this process has been actively investigated, and improved from several aspects, including types of waste plastics, microwave absorbents, and catalysts.

In terms of feedstock types, MAP of common plastics, including high-density polyethylene (HDPE), polypropylene (PP), and polystyrene (PS) have been investigated using char as a microwave absorbent (Undri, Frediani et al. 2014, Undri, Rosi et al. 2014). A general trend of HDPE>PP>PS in terms of resistance to thermal degradation, has been shown, in agreement to this same trend with conventional heating. Polyvinyl chloride (PVC) is a well-known, tricky component in mixed plastic wastes, because it tends to release HCl gas during thermal decomposition, and form chlorinated hydrocarbons when pyrolyzed, together with polyolefin-based plastics (Yu, Sun et al. 2016). In this case, MAP offers a unique advantage over conventional heating, because PVC has a higher dielectric loss factor than other plastics due to its polarity. Therefore, PVC could, first, be selectively heated by microwave irradiation (Moriwaki, Machida et al. 2006), which could potentially enable the timely separation of the dehydrochlorination reactions, before the thermal decomposition of other plastics (Kobayashi, Hori et al. 2019).

The use of a microwave absorbent is a critical component in the MAP process. Since many of the most common types of plastics, such as PTFE, PP, PE, and PS, have low dielectric loss factors, microwave absorbents are often added to this process in order to achieve the high temperatures necessary for pyrolysis reactions (Borges, Du et al. 2014). During a conventional heating process, the sticky nature and low thermal conductivity of melted plastics seriously limit the heat transfer process. In contrast, dispersed microwave absorbents can be heated directly by microwave irradiation at a very high rate, and act as a localized heating source to the surrounding feedstock, and therefore greatly improve the uniformity and rates of the heating process. By applying different types, amounts, and geometries of microwave absorbents, the heating rate and temperature distribution of the MAP process can be manipulated, and can ultimately affect the product profile and energy consumption (Khaghanikavkani and Farid 2013, Zhang, Rajagopalan et al. 2017, Mokhtar, Ethaib et al. 2018). For instance, Prathiba, Shruthi et al. (2018) compared polystyrene pyrolysis in both lab-scale fixed-bed MAP, and conventional electrical heating, and determined that the heating rate in the MAP process was eight times quicker than conventional heating. By increasing the ratio of the polystyrene (feedstock) to activated carbon (microwave absorbent) from 10:0.5 to 10:1 in the MAP process, the liquid oil yield increased from 77% to 93%. Also, the addition of microwave absorbents enabled the MAP process to consume less specific energy than that required by conventional pyrolysis with electrical heating, since a much shorter processing time was needed for the MAP process (Prathiba, Shruthi et al. 2018, Jing, Wen et al. 2020).

Catalyst is another important part of the MAP process, since catalysts can reduce the temperature and residence time required to break down volatile waxes (>C30) into liquid

fractions, and can also improve the selectivity to liquid products with desirable functional groups, or carbon number range. It is worthwhile, to first bring the concept of microwave-assisted heterogeneous catalysis into the discussion. Since the early 1990s, many studies have reported that microwave irradiation could significantly accelerate chemical reactions, compared to conventional heating. The proposed mechanisms for this "specific microwave effect" include localized hot spots, molecular agitation, radiation-induced bond rotation, and improved transport properties of molecules (Jacob, Chia et al. 1995). Later on, many of these hypothetical mechanisms have been debunked by studies which have shown no additional effect of microwave irradiation on chemical reactions other than dielectric heating, and further attributing the hypothetical non-thermal effect to temperature measurement inaccuracy (Shazman, Mizrahi et al. 2007). As more research efforts were evaluated, it became clear that any suspected acceleration of chemical reaction rates by microwave irradiation, originated from the fundamental dielectric heating process. However, this specific microwave effect does exist, because selective heating, which is inherent to the dielectric heating process, could achieve faster chemical reaction rates, by several times, as compared to conventional heating, given the same bulk medium temperature (Horikoshi and Serpone 2014, Dudley, Richert et al. 2015, Kokel, Schäfer et al. 2017). One recent piece of evidence is provided by Ramirez, Hueso et al. (2019) which was assisted with the help of advanced temperature measurement in the microwave field. In this case, microwave heating was shown to heat up the solid catalysts to temperatures higher than the reaction gas, thus boosting reaction selectivity and productivity of a heterogenous catalysis reaction (oxidative dehydrogenation of isobutane). This concept of microwave assisted heterogenous

catalysis has important implications to heterogenous reactions including pyrolysis of plastics, as it bears the potential of reduced energy costs and perhaps new reaction pathways. However, this concept has not been sufficiently explored in the case of MAP of waste plastics. Among the few studies published so far, which investigated the feasibility of incorporating catalysts into the MAP process, most of them were applied to ex-situ catalysis configurations in small-scale batches (i.e. catalyst packed in a secondary fixed bed, and heated by conventional electric heating method) and focused on conventional zeolite catalysts such as ZSM-5 and ZY (Zhang, Lei et al. 2015, Zhang and Lei 2016, Ding, Liu et al. 2019). Results showed gasoline range hydrocarbons, rich in aromatic compounds, that could be obtained through this process, at a yield generally over 50 wt.%. In order to fully utilize the advantage of microwave heating in the MAP of waste plastics, more fundamental research is needed to better understand the influence of microwave heating on catalyst materials, and to explore the various possibilities of combining microwave irradiation with catalysts. Interesting examples from this perspective include several recent studies, which explored materials that act as both microwave absorbent and catalyst, in the related processes (Lam, Liew et al. 2015, Song, Yan et al. 2018, Jing, Wen et al. 2020, Wang, Ke et al. 2020).

While the MAP technology is promising, with several advantages compared to conventional electrical heating, for chemical recycling of waste plastics, almost all of these studies are carried out in small lab-scale batch reactors with a sample size typically less than 20 g. Therefore more work is needed, in order to investigate this technological feasibility on a much larger scale.

Chapter 3 - Syngas production from biomass pyrolysis in a continuous microwave assisted pyrolysis system

3.1. Introduction

The heavy reliance on fossil resources for transportation fuels and chemicals poses some of the greatest threats to humanity such as global warming, air pollution, and energy insecurity, which calls for an urgent transition to a cleaner, sustainable, and renewable production chain of fuels and chemicals (Hansen, Sato et al. 2016). Biomass seems to be one of the most plausible alternatives to fossil fuel because, as an abundant carbon-neutral material source, it can be used to produce not only energy, e.g. heat and electricity, but also non-energy products, e.g. chemicals and materials (Cherubini 2010).

Among the various biomass conversion routes, thermochemical conversion, such as pyrolysis, is a very promising process to exploit the energy from biomass considering its efficiency of conversion and versatility with feedstocks (Sikarwar, Zhao et al. 2016). Conventionally, biomass pyrolysis studies are focused on producing high quality liquid product, e.g. bio-oil, which generally requires complicated and often prohibitive upgrading and downstream processes. And yet, maximizing syngas production from pyrolysis is much less explored even though syngas could serve as a versatile raw material to produce various products, including H_2, heat, electrical power, and liquid fuels (Mašek, Konno et al. 2008, Wang, Weller et al. 2008, Zhang, Dong et al. 2015). And compared with gasification, pyrolysis has the potential to produce a gas product of significantly higher syngas ($CO+H_2$) content and heating value because no gasifying agent is involved that dilutes the produced gas product(Zhang, Dong et al. 2015).

As covered in section 2.4.2, microwave heating has been demonstrated by several studies as a superior method over conventional heating for producing syngas from pyrolysis (Domínguez, Fernández et al. 2008, Huang, Kuan et al. 2010, Beneroso, Bermúdez et al. 2013). Microwave heating can considerably improve syngas yield by promoting heterogeneous catalytic reactions, possibly through generating microplasmas and hot spots when interacting with biochar (Zhang, Dong et al. 2015). And this interaction between biochar and microwave irradiation also contributes to significant reduction in tar formation, which is deemed a critical technical obstacle in the biomass gasification process. Other advantages of microwave heating over conventional heating include selective heating, volumetric heating, and rapid response, most of which are associated with its nature of dielectric heating (Asomaning, Haupt et al. 2018). Many recent studies have also demonstrated that microwave-assisted pyrolysis could achieve faster heating rates and better product quality, while using less energy than conventional electric resistance heating systems (Huang, Chiueh et al. 2016, Klinger, Westover et al. 2018, Parvez, Wu et al. 2019). Despite the potential technological advantages offered by the use of microwaves to drive pyrolysis processes for syngas production, few studies are available, at this point, that investigate the feasibility of this technology on experimental platforms, beyond conceptual designs and lab-scale batch reactors (Beneroso, Monti et al. 2017, Zhou, Liu et al. 2018).

In light of this knowledge gap in technology, scaling-up from lab results to industrial scale applications, a prototype continuous microwave-assisted pyrolysis (CMAP) system with a max throughput of ca. 10 kg/h has been developed in our lab. The system features a unique mixing silicon carbide ball bed reactor, which can operate reliably in a

continuous mode. In addition, it is designed to be portable and modular so that it can be readily scaled-up and deployed for on-farm production (Ruan, Chen et al. 2008). In this study, wood pellets were selected as the feedstock, considering that most U.S. bio-power is generated from woody biomass—including byproducts such as black liquor, and solids such as low-quality wood wastes (e.g., railroad ties and utility poles) and residues. In dedicated or cogeneration plants, such as pulp and paper mills or sawmills, wood pellets are a representative sample of woody biomass (Moriarty, Milbrandt et al. 2018). The design and overall performance of this prototype system is presented in this study. Its feasibility for syngas production from biomass feedstock was examined, in terms of the effect of processing temperature on product yields and composition. In addition, energy efficiency of the process, and measures to improve it, were assessed and discussed.

3.2.Materials and Methods

3.2.1. Feedstock and characterization

Premium grade wood pellets (approximately diameter 7.3mm* length10-25 mm) purchased from a local hardware store, were used as feedstock as is, for this pyrolysis process. Proximate analysis of the feed was determined following standard procedure ASTM E870. Elemental analysis (C, H, O, and N content) was determined using a CE440 Elemental Analyzer (Exeter Analytical, Inc. UK), and energy content, as higher heating value (HHV), was determined by an oxygen bomb calorimeter (Model 1341, Parr Instrument Company).

Table 4 Proximate analysis and elemental analysis (as-received basis) of the feedstock

Feedstock	HHV, MJ/kg	Proximate analysis, wt. %				Elemental analysis, wt. %			
		Moisture	Volatile Matter	Fixed Carbon	Ash	C	H	O	N
Wood pellets	20.6	7.24	76.15	16.30	0.31	50.31	7.82	41.77	0.10

3.2.2. Experimental apparatus and procedure

A continuous down-draft microwave-assisted pyrolysis system was designed and fabricated in-house as shown in Fig. 3. The system is equipped with six 1.5kW water-cooled magnetrons (Witol 2M463K-3), giving a total of 9 kW output microwave power and a processing capability of up to 10 kg biomass per hour. Major components of the system include material feeding system, microwave-assisted pyrolysis reactor, syngas cooling and cleaning system, cooling water system, and a PLC control system. The biomass feeding system consists of an airtight hopper and a screw feeder. Wood pellets are fed from the top, and into the reactor at a controlled rate. Pressure inside the reactor is also monitored from the top, via a water manometer. The core of the gasifier reactor is a cordierite ceramic tube with an outer diameter of 8" x height 16" x thickness 1", and an inner diameter of 6" (152.4 mm) which is loaded with 6 kg of silicon carbide balls of outer diameter 12mm as the microwave susceptors. Ceramic fiber thermal insulation materials are filled between the ceramic tube and the gasifier shell to minimize heat loss into the environment. The spatial arrangement of magnetrons has been properly designed to ensure heating uniformity (3 pairs of magnetrons at 120^{o} apart, one magnetron above its twin pair). During operation, magnetrons fixed to the outside of the stainless-steel reactor shell generate microwaves, which penetrate the ceramic tube and quickly heat up the SiC balls and the biomass feedstock inside the reactor. An important design

consideration for the system is the implementation of a mixing mechanism in the reactor. An auger shaft, driven by a motor of controllable speed, slowly stirs the SiC ball bed to serve three purposes: 1) improving heat transfer and temperature distribution homogeneity in the ball bed, 2) enabling grinding of the biomass pellets into tiny particles with the help of the SiC balls, and 3) allowing biomass and biochar to move downward through the ball bed, before dropping through 4mm-holes on the bottom perforated plate and then being collected in the char tank. A special oil seal on the reactor top, is designed to ensure gas-tightness while the mixing auger rotates. After separation from the solid biochar, the raw producer gas, under slight vacuum provided by a roots blower (installed after the condensers), passes through the cooling and cleaning system before exiting from the end pipe as syngas, for sampling, flaring, or direct utilization e.g. by a portable generator. The cleaning system consists of the following parts: a metal mesh filter, a water spray cooling system, two shell and tube condensers, and three cleaning tanks filled with zeolites. Cooling water is circulated within the system, including condensers and magnetrons, by an industrial water chiller to ensure stable operation of the system. The power and control signals of all electric parts are integrated in a PLC control panel, which allows easy control and monitoring of the system via an HMI display.

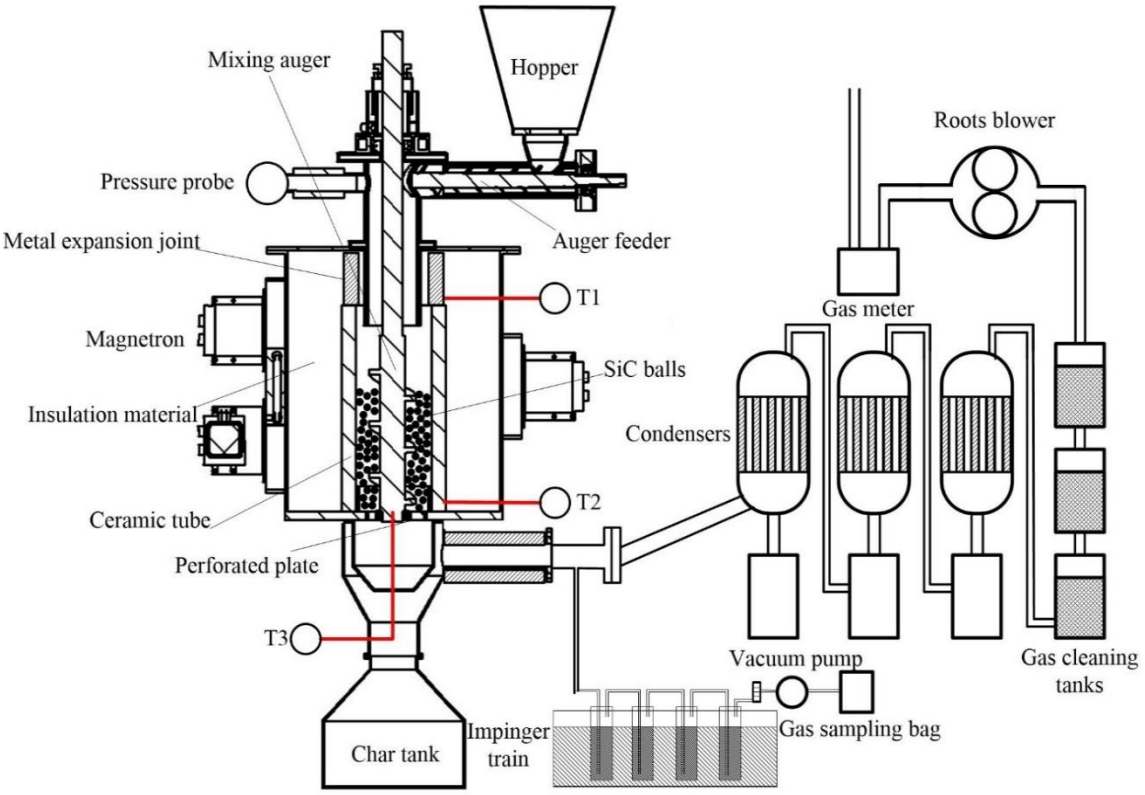

Figure 3 Schematic diagram of CMAP prototype system

Process temperature is monitored at three locations: top of the ceramic tube (T_1), external surface of the ceramic tube bottom (T_2), and bottom of the mixing shaft (T_3). Since directly measuring the temperature inside the ball bed is technically challenging during the operation of this system, the real-time ball bed temperature is estimated by the a calibration curve, $T_{ball\ bed} = 1.09*T_2 + 126^oC$, which was previously established by correlating T_2 with the ball bed temperature measured by an additional thermocouple inserted into the center of the ball bed during preliminary tests.

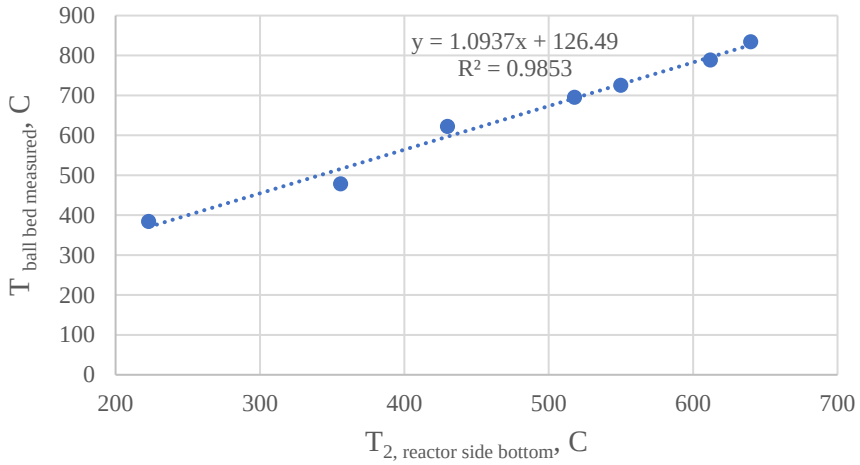

Figure 4 Correlation between T_2 and $T_{ball\ bed}$ obtained from preliminary tests

In a typical experiment, T_2 is used as the process temperature and maintained at set levels, e.g. 620ºC, by controlling on/off of the microwave power with the PLC control system. Pressure is maintained between 0.25'' to 0.5" H_2O vacuum by adjusting the frequency of the roots blower. 5 kg of wood pellets are loaded into the sealed hopper, and feeding rate is set to 2 kg/h to start the experiment, while the rotation speed of the mixing auger shaft is set at 8 RPM to match the processing rate. The pyrolysis reaction is deemed started once the producer gas can be ignited and burned steadily at the end pipe burner. The electrical energy consumption was calculated by recording the electrical power with a digital power meter (Omnimeter I v.3, EKM Metering Inc.).

3.2.3. Sampling and analysis

The total flow rate of the produced gas was recorded by a pulse output gas meter (EKM Metering Inc.) downstream of the roots blower. Tar concentration in the producer gas was measured by a modified method based on IEA International Energy Agency (IEA)

protocol (Simell, Ståhlberg et al. 2000). A side stream of 4 liters per minute of hot gas exiting the gasifier was routed into an impinger train by a vacuum pump, through a heated (350°C) and insulated tube, connected to the sampling port downstream of the gasifier. The impinger train, composed of four impingers, each containing around 50 ml of acetone, was placed in an ice water bath to collect the tars for further analysis. The sampling time was 15 min and the gas sampling volume was 60 L for each sample. The collected mixture of tar and acetone was analyzed by Karl-Fischer titration for water content determination and by GC-MS for tar composition evaluation. Then the acetone was removed by evaporation in a Rotavapor system (Buchi R-215) under 15" Hg vacuum pressure and 40°C water bath. Three tar samples were taken for each experiment. The final weight of the liquid product residue was determined as the amount of heavy tar, m_{tar}. Gas sampling bags were used to collect non-condensable gas products every 5 minutes for off-line analysis. Biochar was collected in the char tank system which is cooled by circulation water, and the weight was determined gravimetrically as m_{char}.

The percentage yield of each product is calculated as:

$$Y_g =$$

$$(\dot{V} + 4) \times 60 \times ([H_2] \times 2 + [CO] \times 28 + [CH_4] \times 16 + [CO_2] \times 44 + [C_2H_4] \times 28 + [C_2H_6] \times 30 + [C_3H_6] \times 42) \div 2462 \div \dot{m}_f$$

$$Y_{tar} = m_{tar} \times (\dot{V} + 4) \times 1000 \div 60 \div \dot{m}_f$$

$$Y_{water} = M\% \times m_{mixture} \times (\dot{V} + 4) \times 1000 \div 60 \div \dot{m}_f$$

$$Y_{char} = m_{char} \div t \div \dot{m}_f$$

$$Y_{unquantified} = 100 - Y_g - Y_{tar} - Y_{water} - Y_{char}$$

where, [gas component] is the average molar percentage of the component in multiple gas samples of the produced gas, $\dot{V}$ is the flow rate measured by the end gas meter in the unit of liter per minute, $\dot{m}_f$ is the feeding rate of the wood pellets, i.e. 2 kg/h, $M\%$ and $m_{mixture}$ are the moisture content and the weight of the liquid collected in the impinger train in the unit of g, respectively, ,and t is the elapsed time of an experimental run in the unit of hour.

The lower heating value (LHV, MJ/ Nm^3) of product gas is calculated by,

$$LHV = ([H_2] \times 108.0 + [CO] \times 126.4 + [CH_4] \times 358.2 + [C_2H_4] \times 590.4 + [C_2H_6] \times 637.8 + [C_3H_6] \times 870.0) \div 1000$$

The composition of non-condensable gas samples was determined by using a Varian Micro-GC (CP-4900) coupled with a thermal conductivity detector (TCD) and two analytical columns, namely Molecular Sieve 5A and the PoraPLOT Q. Standard gas mixtures were used to establish calibration curves for quantitative analysis of gases including H_2, CO, CO_2, CH_4 and C_2-C_4 alkanes and alkenes.

Tar composition was analyzed by using Agilent 7890-5975C GC/MS equipped with a 30 m × 0.32 mm HP-5 MS capillary column of 0.25 μm thickness. The oven temperature was programmed as follows: holding at 50°C for 2 min, then a heating ramp of 5°C /min to 280°C, and lastly holding for 5 min. The chromatographic peaks were identified by using National Institute of Standards and Technology (NIST) database. Relative abundance of each compound was semi-quantitatively determined as the area percentage

of the corresponding peak. Due the limited sample size of the collected heavy tar, the energy content (higher heating value) of each tar sample was estimated by first determining its elemental compositions on a CE440 Elemental Analyzer (Exeter Analytical, Inc. UK) and then calculating based on the following formula: HHV (kJ/kg)= $3.55C^2 - 232C - 2230H + 51.2C \times H + 131N + 20{,}600$ where C, H, N are mass% of carbon, hydrogen and nitrogen elements, respectively (Friedl, Padouvas et al. 2005).

The elemental composition of the biochar samples was determined by using an inductively coupled argon plasma optical emission spectrometer (ICP-OES, Thermo Scientific iCAP 7600 ICP-OES Duo) and a CE440 Elemental Analyzer (Exeter Analytical, Inc. UK).

At least ten syngas samples and three tar samples were taken during each experiment trial, and at least three replicate trials were conducted under a given temperature condition to obtain the data, with relative standard deviations (RSD) of less than 10%. The means and standard errors of data were used for analysis in this paper.

3.3.Results and discussion

The composition of non-condensable gas products and the tar, as well as the yields of gas, char, and solids to establish mass balances, were studied from four ball bed temperature levels: 630, 680, 740, and 800^{o}C. Both temperature and gas composition profiles were stable over the course of each experimental run, which lasted at least 1 hour for each run. Fig 5 and Fig. 6 show typical time course profiles of gas compositions and temperatures, respectively.

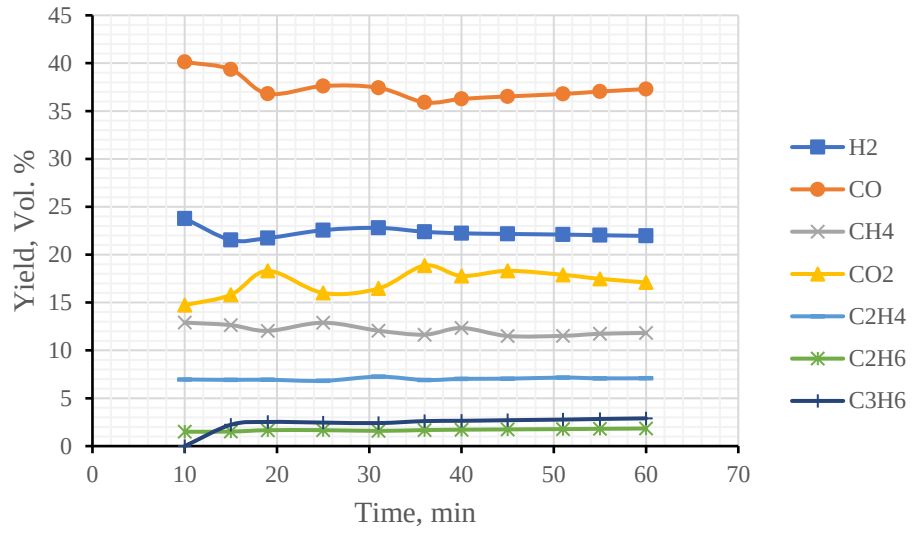

Figure 5 Evolution of gas composition profiles over the course of an experimental run at 740 ºC

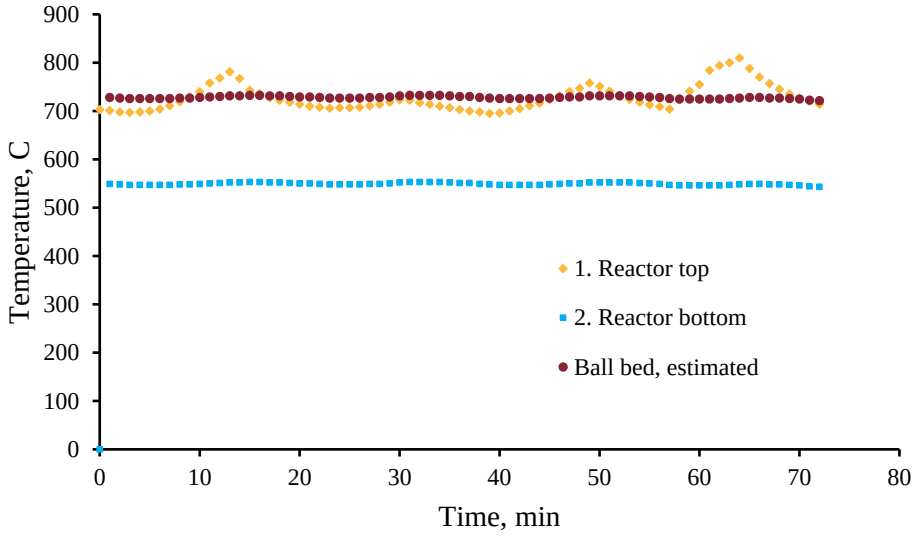

Figure 6 Temperature profile over the course of an experimental run at 740ºC

3.3.1. Gas product

Non-condensable gas composition under different reactor temperature conditions are presented in Fig. 7. The relative gas composition profile is generally in agreement with other wood pyrolysis results reported in literature, with CO and H_2 being the most

abundant species in terms of volumetric yield, followed by CH4, CO_2, and slight amount of C2-C3 hydrocarbons (Di Blasi, Signorelli et al. 1999, Dufour, Girods et al. 2009, Commandré, Lahmidi et al. 2011). As the reactor temperature increased from 630 to 800°C, the volumetric yields of H_2 and CO significantly increased while the other components remained relatively unchanged, indicating that gas quality increased with temperature. In addition, the total gas yields also increased, from 0.42 to 0.80 Nm^3/kg d.a.f. wood pellets, mainly due to the increasing yields of H_2 and CO.

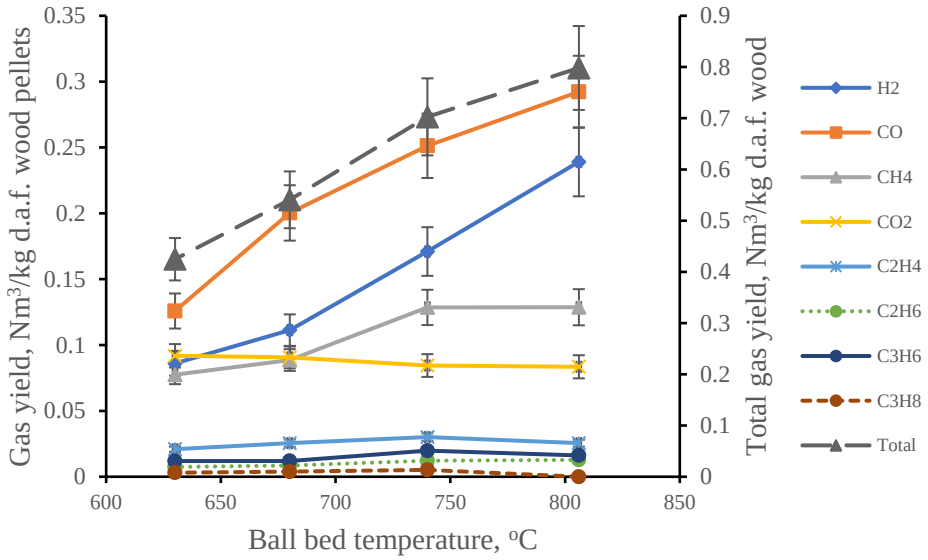

Figure 7 Gas product compositions and yields at different process temperatures

Three typical thermochemical process designs have been reported in literature for syngas production from wood, i.e. pyrolysis, gasification, and a two-stage gasification process. When compared to conventional pyrolysis processes, either using a batch-mode tube furnace or a continuous-mode fluidized bed reactor, two major distinctions were observed. While the highest total gas yield, i.e. 0.80 Nm^3/kg, is comparable to those from other wood pyrolysis studies, the producer gas in this study features a very high energy

content, i.e. 18.0-19.8 MJ/ Nm^3 LHV in contrast to 5-12 MJ/ Nm^3 reported in other studies (Di Blasi, Signorelli et al. 1999, Morf, Hasler et al. 2002, Dufour, Girods et al. 2009, Commandré, Lahmidi et al. 2011). This is partially because no carrier gases, e.g. N_2, are involved in the process, which would otherwise dilute the gas product. Another factor that may have played a role, is the use of microwave irradiation as the heating mechanism, which will be discussed later in section 3.3.3. The other difference is that our process required lower temperatures to produce similar gas yields, compared to those of conventional pyrolysis. For instance, in a wood pyrolysis study using a conventional electric heating furnace, Dufour, Girods et al. (2009) reported the gas yields at 900^{o}C and 1000^{o}C to be 0.68 and 0.75 Nm^3/kg d.a.f. wood, respectively, while in our process similar gas yields (0.70 and 0.80 Nm^3/kg d.a.f. wood) were obtained at 740 and 800^{o}C. This trend would be more pronounced if compared with other relevant studies (Di Blasi, Signorelli et al. 1999, Morf, Hasler et al. 2002). In fact, the general conclusion that microwave assisted pyrolysis produces higher gas yields, and also higher syngas contents than those from conventional heating pyrolysis, has also been confirmed by several studies directly comparing these two processes in independent experiments (Dominguez, Menéndez et al. 2007, Parvez, Wu et al. 2019). In addition, when compared with the gasification process, CMAP obtained similar volumetric gas yields, but again the gas quality was much higher in terms of syngas ($CO+H_2$) content and heating value (typically 5 MJ/ Nm^3 LHV vs. our results of ~18 MJ/ Nm^3), partly because the gasification agent diluted the producer gas from the common gasification processes (Kim, Yang et al. 2013, Guo, Dong et al. 2014, Cheah, Jablonski et al. 2016). The other interesting process to compare, is the two-stage gasification process, where a primary pyrolysis step is followed

by a secondary catalytic process, to further crack the primary products (Xiao, Meng et al. 2011, Efika, Wu et al. 2012, Xie, Kong et al. 2012). As the data in Table 5 demonstrate, this process could obtain a much higher gas yield and also gas quality, e.g. 2.0 Nm^3/kg d.a.f. wood, 68% $CO+H_2$ and a tar content of 60 mg/Nm^3, due to water-gas shift reactions. It does, however, rely on the addition of steam and catalysts, as well as a high processing temperature in the pyrolysis stage, e.g. 700°C, all of which could undermine the energy efficiency of this process.

Table 5 Comparison of syngas production performance with previous studies

Reactor type	Process conditions	Gas yield	H_2+CO, vol %	Tar yield	Ref.
CMAP system	800°C; 2kg/h feeding rate	72.2 wt.%; 0.80 Nm^3/kg d.a.f. wood	67%	2.7 wt.%; 7.83 g/Nm^3	This study
TFP	1000°C; batch mode	65 wt.%; 0.75 Nm^3/kg d.a.f. wood	76%	3.0 wt.%	(Dufour, Girods et al. 2009)
FBP	900°C; 0.36 kg/h	58.1 wt.%	48%	6.9 wt.%	(Fuentes-Cano, Salinero et al. 2018)
FBG	750-800°C; 55 kg/h; ER=0.19	0.81 Nm^3/kg d.a.f. wood	33%	Not available	(Kim, Yang et al. 2013)
A two-stage reactor (SKP+CP)	500°C + 760°C; 0.24 kg/h; Ni based catalysts	54 wt.%	73%	24.9 wt. %	(Efika, Wu et al. 2012)
A two-stage reactor (FBP + CR)	700°C + 650°C; 0.12 kg/h; Steam/carbon ratio=3; Ni based catalysts	2 Nm^3/kg d.a.f. wood	68%	60 mg/Nm^3	(Xiao, Meng et al. 2011)

Note: TFP, tubular furnace pyrolyzer; FBP, fluidized bed pyrolyzer; FBG, fluidized bed gasifier; SKP, screw kiln pyrolyzer; CR, catalytic reformer; All references can be found in the mansucript.

3.3.2. Tars

The evolution of tar composition and heavy tar yield with reactor temperature is illustrated in Fig 8. Over 40 major peaks were identified in each chromatograph, and the tar compounds were classified into four categories according to the functional groups: single-ring aromatics, i.e. benzene and its derivatives, single ring phenolics, i.e. phenol and its derivatives, polycyclic aromatic hydrocarbons (PAH), and others (mainly oxygenated derivatives of PAH). With the increase of reactor temperature, relative abundance, i.e. peak area ratio, of phenolics gradually decreased, while that of PAH increased, especially at higher temperatures. This trend is in agreement with the tar evolution mechanism reported in literature: phenolic compounds as typical secondary tar components are important precursors for the formation of the tertiary tars, i.e. PAHs (Morf, Hasler et al. 2002, Palma 2013). Meanwhile, the yield of gravimetrically measured heavy tar monotonously (monotonously? – why not use "predictably") dropped from 10.1 to 2.7 wt.% as the temperature increased, reflecting the thermal destruction of tar compounds. The corresponding tar concentration for 2.7 wt.% heavy tar yield was 7.83 g/Nm^3. In contrast, tar yields of 3.0% and 6.9% have been reported for conventional pyrolysis processes operating at 1000^{o}C and 900^{o}C, respectively (Dufour, Girods et al. 2009, Fuentes-Cano, Salinero et al. 2018). From the perspective of a pyrolysis process, the tar yield of the CMAP system is very low. However, the tar concentration still requires significant reduction for the syngas to be used as a more valuable feedstock, beyond direct combustion. For instance, acceptable tar content levels for compressors, internal combustion engines, and methanol synthesis are 50-500 mg/Nm^3, 100 mg/Nm^3,

and 0.1 mg/Nm^3, respectively (Woolcock and Brown 2013). In addition, single ring aromatics, e.g. benzene and toluene, and PAH, e.g. naphthalene and phenanthrene, remain as the predominant tar compositions even at 800^{o}C, reflecting the thermal stability of these compounds, and therefore the need for secondary tar removal processes. Note that these tar samples were taken before the producer gas entered the condensers and cleaning tanks. Additional tar samples were also taken at the end of the discharge pipe, but the heavy tar yields were below the detection limit of the sampling protocol, so a quantitative result is not available. However, this does show that the downstream system can effectively remove tars through condensation and physical adsorption at the current scale.

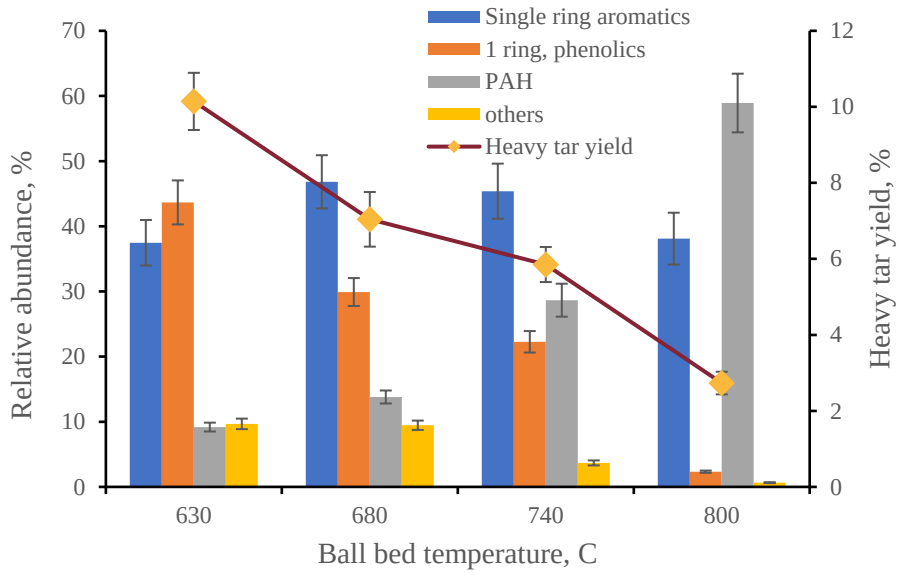

Figure 8 Heavy tar compositions and yields at different process temperatures

3.3.3. Mass balance

Mass balance as a function of reactor ball bed temperature was established by individually quantifying the yields of non-condensable gases, water, heavy tar, and char

under each experimental condition, and the data are illustrated in Fig. 9. The total quantified fractions add up to ca. 95 wt.% for all conditions. One of the probable factors that account for the unquantified fractions is the gravimetric method used to quantify tar contents, which is also reported in previous studies (Dufour, Girods et al. 2009, Commandré, Lahmidi et al. 2011). The acetone evaporation step in the protocol could have also evaporated light tar components and thus lead to underestimation of tar yields.

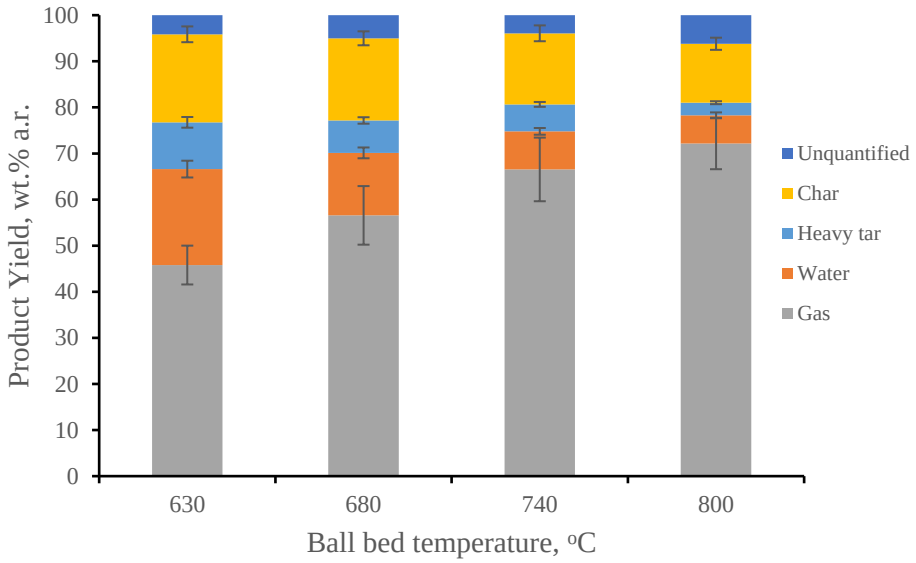

Figure 9 Product distribution at different process temperature

In general, the yields of gas increased predictably with temperature, while those of water, heavy tar, and char declined with temperature. The yield of water at 630°C was 20.8 %, significantly higher than the moisture content of the wood feedstock, i.e. 7.24%. This was due to the formation of water from the pyrolysis reactions. Water yield decreased as reactor temperature increased because high temperature favored several steam-consuming reactions including $C + H_2O \rightarrow CO + H_2$ and $CO + H_2O \rightarrow CO_2 + H_2$. The first reaction might also have contributed to the decrease of char yields from 19.1% at 630 °C to 12.8%

at 800ºC (Morf, Hasler et al. 2002). At the temperature of 800ºC, the gas yield reached 72.2 wt.%, very close to the volatile matter content of the wood, i.e. 76.15%, indicating the pyrolytic gas production potential was almost fully utilized.

As discussed earlier, microwave assisted pyrolysis tends to promote the production of syngas and reduce tar production in comparison to pyrolysis with conventional heating (Dominguez, Menéndez et al. 2007, Parvez, Wu et al. 2019). The mechanism behind this pattern has been revealed by recent studies to be associated with heterogenous reactions between primary tar and biochar enhanced by microwave irradiation (Beneroso, Bermúdez et al. 2016). Table 3.3 presents the elemental composition of biochar samples produced at the process condition of 800ºC from CHN elemental analysis and ICP-OES analysis. Only those metal species with a content of higher than 100 ppm were included in the table. On one hand, the produced biochar consists of 83 wt.% of carbon, which might contribute to the hot spot effect since carbonaceous species prove to be good microwave absorbers (Ellison, McKeown et al. 2017). On the other hand, the total metal amount in the biochar was around 4.2 wt.%, and major species include Ca, K and Mg, which had been reported by many previous studies to be active in converting primary tar compounds to permanent gases (Zhang, Chen et al. 2016). Therefore, due to the combination of carbon and catalytically-active metal oxides, biochar serves as both a microwave susceptor for heating the biomass, and also as a catalyst for cracking reactions of primary tars in the microwave-assisted pyrolysis process. This speculation is supported by several other studies. Luo, Bao et al. (2018) showed that biochar, as a catalyst under microwave irradiation, could achieve a tar removal efficiency of 94% at merely 600ºC, which was a much lower temperature than conventional catalytic tar cracking

temperature, e.g. 800°C. This was attributed to the existence of alkali and alkaline earth metals (AAEMs) in biochar and also the hot spot effect of biochar under microwave irradiation. Similar results were also reported by Chen, Li et al. (2018). The CMAP system takes advantage of this mechanism by allowing sufficient interaction between primary tar and biochar, which is ground into small particles and slowly moves downward through the ball bed.

Table 6 Elemental analysis of the biochar

Sample	HHV, MJ/kg	CHN analysis, wt.%			ICP analysis, mg/g					
		C	H	N	Al	Ca	Fe	K	Mg	Na
Biochar	34.3	83.45	4.64	0.52	1.22	18.20	2.41	14.89	4.67	0.41

3.3.4. Energy cost

Although a comprehensive energy balance for the process is not available due to the difficulty in completing the mass balance, relevant data available are presented in Fig.10 to help assess the energy efficiency of the process. The energy flow data were obtained by normalizing the results from the experimental condition at 800°C reactor temperature, to 1kg wood pellet input. Electrical power input was recorded by a power meter, while wood input energy and product output energy were accounted for, at their lower heating values (LHV). The energy content in the output gas and input wood pellets were 13.7 MJ and 18.7 MJ (per 1 kg of wood pellets), respectively, and therefore the cold gas efficiency on a LHV basis (i.e. energy content in the gas divided by that in the wood feedstock) was 73.3%, which was higher than those reported in most biomass gasification studies, e.g. 40-65% (Sheth and Babu 2009, van der Meijden, Veringa et al. 2010, Guo, Dong et al. 2014). This is mostly due to the fact that, in a typical gasification process, part of the feedstock energy content is used to supply the heat needed for gasification reactions. In

contrast, reaction heat in this pyrolysis process (CMAP) is provided by an external energy source, i.e. microwave irradiation. This means the higher gasification efficiency along with higher gas quality of this process does come with an extra energy cost. In this process, 4.6MJ, or 1.3 kWh, magnetron input energy was needed to process 1 kg of wood pellets at 800°C. Another 2.6 MJ, or 0.7 kWh of electrical power were consumed by other parts in the system, including a water chiller and several electric motors for moving parts. Therefore, a total of 7.2 MJ, or 2 kWh of electrical energy were required to produce syngas of 13.7 MJ, char of 4.4 MJ and tar of 1.0 MJ.

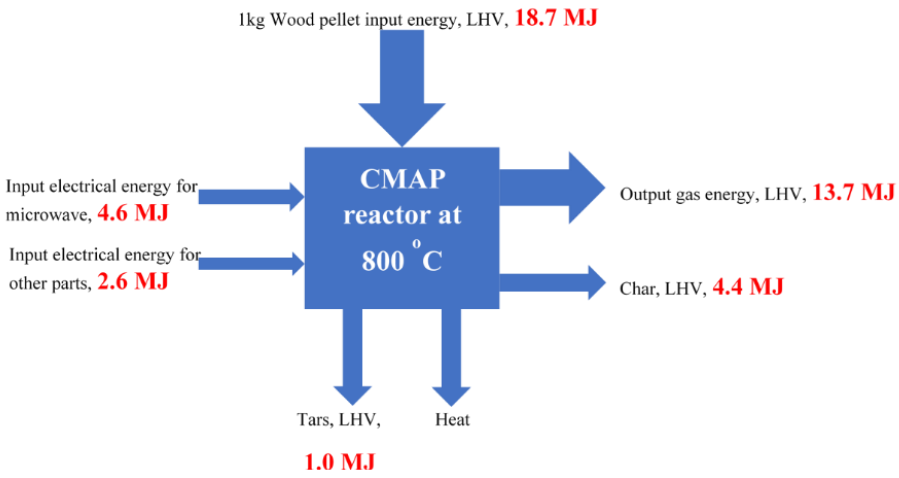

Figure 10 Energy flow of the CMAP system at the ball bed temperature of 800°C

Direct and fair comparison with other pyrolysis studies in terms of energy consumption is difficult due to limited data availability and different process conditions reported in literature. For instance, Daugaard and Brown (2003) determined that the specific heat needed to process 1 kg dry pine wood particles in a fluidized bed fast pyrolysis reactor with a temperature near 500°C was 1.6 ± 0.3 MJ. Zhao, Zhang et al. (2011) reported the energy consumption of a batch-mode microwave pyrolysis process to be 0.65 kWh/kg of

wheat straw. The process temperatures in these studies were significantly lower, and therefore energy consumption as well as the gas yields (less than 30 wt.%) were considerably lower than in our process. In contrast, in another study, of which the reaction conditions are comparable to ours, Beneroso, Bermúdez et al. (2016) proposed a microwave-induced two-step pyrolysis process for syngas production from bio-waste, where tar from the first pyrolysis step is further cracked at 800^{o}C in the second step to produce syngas; based on their estimation for a scaled-up version of the process, 4.2 kWh electrical energy is needed to produce 1 m^3 of syngas with an energy content of 3.75 kW h/m^3 (thus an energy loss, rather than an energy gain). In this regard, the specific energy consumption in our process is much lower, which could be attributed to the application of silicon carbide, a strong microwave absorber, in contrast to biochar, as in their process. Nevertheless, considering a typical conversion rate of 40% from thermal energy (a low-grade energy) to electricity (a high grade energy), the energy efficiency of this process does need further improvement in order to promote its economical feasibility, and this could be achieved through the following aspects:

a. Improving microwave heating efficiency

While microwave heating allows non-contact, selective, faster, and more volumetric heating than conventional heating, its energy efficiency is of particular concern, especially in this process. The overall energy efficiency of microwave heating can be considered as the product of two factors, the microwave generation efficiency (i.e. from electricity to microwave irradiation) and the microwave absorption efficiency (i.e. from microwave irradiation to effective heat). Microwave generation efficiency depends on factors including the quality, age, and working temperature of the magnetron(s)

(Atuonwu and Tassou 2018). Measurement based on IEC 60705 standards showed a generation efficiency of 55% at room temperature and full power with new magnetron models used in this study, which was in agreement with results reported in literature(Wang, Zhao et al. 2015). The efficiency could decline over time under our process conditions because of continuous operation, and high process temperature. On the other hand, microwave absorption efficiency is more complicated because it depends on the degree of impedance matching between the microwave source and the load, and it varies at different temperatures, making the experimental measurement for a given process very challenging. In our system, silicon carbide, an excellent microwave absorbing material, effective at a wide range of temperatures (Yang, Yuan et al. 2013), is applied in a sufficient amount, relative to the microwave power, so that the effect of load volume can be neglected. Therefore the microwave absorption efficiency could be roughly estimated to be 0.9 (Wang, Zhao et al. 2015). In this regard, the overall microwave heating efficiency in this process is estimated to be 0.5 under the best scenario. This means less than half of the electrical energy is converted into effective heat for the pyrolysis reaction, while the rest is mostly dissipated as heat in the magnetrons, which in turn is added to the cooling load of the chilled water. This leaves significant room for improvement. One option is to switch to 2450MHz magnetrons of higher quality, or to 915 MHz magnetrons, which reportedly have microwave generation efficiencies as high as 88%. Another interesting option is to apply solid-state microwave heating, which is still an evolving technology, but has the potential to surpass the performance of magnetrons in terms of energy efficiency (Atuonwu and Tassou 2018).

b. Minimizing heat loss

Based on the energy expenditure data presented in Fig. 5 (?), heat loss could be as high as 6.8 MJ/kg wood in the process, which takes up 26.2% of the total energy input into the process. The heat loss is mainly composed of three fractions, including: (a) magnetron heat dissipation (at least 2.3 MJ/kg as discusses earlier), (b) reactor heat dissipation from high temperature reactor core to the surroundings, and (c) sensible heat lost during cooling of the syngas and char. Besides increasing microwave heating efficiency as discussed earlier, heat loss can be mitigated by several other strategies including enhancing thermal insulation of the system, and recovering the waste heat for utilization. For instance, the sensible heat of the high temperature producer gas exiting the reactor could be recovered by heat exchangers to produce hot air, water, or steam depending on the specific needs (Pavlas, Stehlík et al. 2010); or thermoelectric devices could be attached to hot surfaces to convert waste heat into electricity (Ma, Lin et al. 2015). In addition, the energy load associated with the cooling water circulator can be reduced by using a closed-loop water circulation system using natural cooling.

c. Lowering the operating temperatures

Despite the fact that microwave assisted pyrolysis requires lower temperature to achieve a given gas yield, compared with pyrolysis using conventional heating, an even lower processing temperature is highly desirable, since higher temperature often means lower energy efficiency due to both greater energy input and heat loss. This can be achieved by application of catalysts, and nickel based catalysts are well known for promoting gas production under pyrolysis or gasification conditions (He, Xiao et al. 2010, Zhang, Dong

et al. 2015). However, more research is still needed to, cost-effectively, incorporate catalysis into the process (Zhou, Liu et al. 2018).

In order to quantitatively show the potential of reducing energy consumption in the CMAP system, a preliminary analysis was conducted on the basis of the following assumptions: 1) Current 2450MHz magnetrons could be replaced with 915 MHz magnetrons with a 88% microwave generation efficiency; 2) A closed-loop water circulation system using natural cooling could replace the current cooling water circulator, so the specific energy consumption of current water chiller, 1.7 MJ/kg, can be eliminated; 3) the exhaust heat from the producer gas could be recycled, to heat the feedstock from room temperature to 200^{o}C, which requires around 0.21 MJ heat per kg of wood pellets; 4) The enthalpy to pyrolyze pine wood at 500^{o}C in a fast-pyrolysis condition is 1.6 MJ/kg of wood (Daugaard and Brown 2003), and the pyrolysis enthalpy changes linearly with temperature. Based on the assumptions above, the total electricity consumption of this process could be reduced to

$$\frac{1.6\text{MJ}}{\text{kg}} \times \frac{(800-200)}{(500-25)} \div (0.88 * 0.9) + \frac{(2.6-1.7)MJ}{kg} = 3.45\ MJ/kg$$

In this case, if the produced gas is used to power an electrical generator, assuming a 35% conversion efficiency, the system could be self-sustained and even deliver a net electricity production of 1.35 MJ/kg.

3.3.5. Discussion on the unique advantages of the CMAP system

As reviewed in Section 3.1 as well as in Section 2.4.2, microwave-assisted pyrolysis processes in general have the following advantages over conventional heating-based pyrolysis: better energy efficiency, shorter processing time, easier heating control, and

improved product quality (Huang, Chiueh et al. 2016, Zhang, Rajagopalan et al. 2017, Klinger, Westover et al. 2018, Parvez, Wu et al. 2019, Arpia, Chen et al. 2020).

In addition to these advantages that are common in microwave-assisted pyrolysis in general, the specific reactor design of this system has brought about several additional benefits. First, as the key part of this system, the SiC ball mixing reactor design simultaneously allows 1) continuous operation, 2) grinding of large biomass pellets, 3) controllable gas residence time (by adjusting the amount of balls and ball sizes, etc.), and 4) homogenous heat transfer and temperature distribution. Moreover, the CMAP system provides the opportunity of primary tar species to sufficiently interact with biochar, which is an effective microwave susceptor for heating, and a catalyst for cracking reactions due to its combination of carbon and catalytically active metal oxides e.g. alkali and alkaline earth metals (AAEMs), and therefore could promote the production of syngas while minimizing tar yields. Furthermore, this system uses minor vacuum instead of a carrier gas such as N_2 to maintain the necessary atmosphere for pyrolysis. This not only avoids the dilution of the producer gas, but also eliminates the energy consumption that would otherwise be required to heat up the carrier gas to high temperatures. In addition, Mahari, Chong et al. (2018) compared pyrolysis processes under a vacuum environment to a nitrogen atmosphere, and found that the former process achieved a faster heating rate and a shorter process time.

To estimate the energy savings associated with using vacuum, the following conditions were assumed:

1. In a typical lab-scale fluidized bed fast pyrolysis system, about 70 L/min (@20 ^{o}C, or 4.87kg/h) of N_2 is needed to process 2.2 kg/h biomass (Boateng, Daugaard et al. 2007).
2. A typical fast pyrolysis process temperature is 500^{o}C, meaning the carrier gas temperature is raised by 475 ^{o}C
3. The average specific heat of nitrogen gas between 25^{o}C to 500^{o}C is 1.062 kJ/kg, /^{o}K;

Therefore, to process 1 kg of biomass in a typical fluidized bed fast pyrolysis process, the energy required to heat up the carrier gas is

4.87kg/h * (1.062 kJ/kg, K)*475K/ (2.2 kg/h) =1.12MJ/kg

, which is almost 70% of the reaction enthalpy to pyrolyze pine wood at 500^{o}C in a fast-pyrolysis condition (1.6 MJ/kg wood).

3.4.Summary

This work presents the design of a continuous microwave assisted pyrolysis (CMAP) system and the test results of its overall performance for syngas production from biomass. This prototype system is featured with a silicon carbide ball reactor bed and a mixing mechanism, which allows for rapid and uniform heating, and continuous operation for the process. Experimental results showed that higher processing temperatures promote the production of gas products, especially CO and H_2, and lower the yields of tar, water, and char. Specifically, at the temperature of 800^{o}C, a gas yield of 72.2 wt. % or 0.80 Nm^3/kg d.a.f. wood pellets, was obtained. The producer gas product was characterized by a high energy content of 18.0 MJ/ Nm3 with a high syngas (H2+CO) content of 67 vol%. The tar concentration of was 7.83 g/Nm3 for the producer gas exiting the reactor, but

downstream condensation and physical adsorption could further lower the tar concentration below the detection limit. The high gas yields and quality in this process, compared to pyrolysis with conventional heating, at similar temperature levels, could be attributed to two factors: 1) the heterogenous reactions between primary tar and biochar enhanced by microwave irradiation, and 2) the absence of carrier gas such as N_2 in the process that would otherwise dilute the producer gas. In terms of energy efficiency, a cold gas efficiency of 73.3% was achieved at 800^{o}C, which comes at the cost of 7.2 MJ or 2 kWh of electrical energy per kg of wood pellets. Further measures to increase the energy efficiency of the process were proposed, including: improving microwave heating efficiency, minimizing heat losses, and possibly lowering the operating temperatures. Potentially, the electrical consumption could be reduced to 3.45 MJ/kg wood, enabling a net electricity production from the process.

Chapter 4 Catalytic fast pyrolysis of plastic wastes in a continuous microwave assisted pyrolysis system for fuel production

4.1. Introduction

As reviewed in Section 2.5, plastic wastes, on one hand, is considered an enormous environmental issue, but on the other, could also be seen as a great source for energy and material production. Compared to biomass, plastics have several advantages as feedstock for energy production, including relatively simpler and more uniform chemical composition, higher heating value, and absence of troublesome element such as oxygen. In addition, fillers are often added into virgin resins during plastic manufacturing in order to achieve the desired chemical or mechanical properties of the final plastic products such as enhanced hardness and strength. Common fillers are often minerals such as calcium carbonate, kaolin, talc, mica, etc. (Xanthos 2010). These fillers could act as *in-situ* catalysts during the pyrolysis process.

Pyrolysis of plastic wastes seems to be a promising chemical recycling method to complement or even replace the current mechanical recycling approach because it is capable of converting plastic wastes into higher value products such as fuel and chemicals for energy and material recovery. Successful implementation of plastic pyrolysis technology relies on several integral parts, such as: choice of catalysts, pyrolysis reactor design, and process parameter optimization. In terms of pyrolysis reactor design, most of the studies are conducted in small laboratory-scale rigs such as thermogravimetric analyzers, microreactors, and other batch laboratory reactors (Wong,

Ngadi et al. 2015), with limited consideration given to scale-up. There are, however, a number of research studies, and even industrial operations, with scaled up systems. But overall, successful commercialization of this technology is still rare, as most of these attempts still struggle with yield and quality issues of the resulting products, and the reliability of the pyrolysis system (Arabiourrutia, Elordi et al. 2012, Wong, Ngadi et al. 2015, Alvarez, Lopez et al. 2017, Lopez, Artetxe et al. 2017). For instance, most plastics tend to melt below 200ºC to form a sticky and viscous liquid prior, to thermal degradation starting at about 300–330°C; this causes many operational issues in the pyrolysis process, such as difficulty in mixing and fluidization (Arena and Mastellone 2000, Jing, Yan et al. 2014).

In this regard, microwave assisted pyrolysis (MAP) serves as a promising alternative, as compared to other pyrolysis technologies, based on conventional heating, because microwave heating offers several benefits to the plastic waste pyrolysis process. First, microwave heating with its selective heating feature, could enable the MAP process to treat plastic mixtures that would otherwise cause problems in a conventional pyrolysis system. For instance, Polyvinyl chloride (PVC) is a well-known tricky component in mixed plastic wastes, due to its tendency to release HCl gases during thermal decomposition, and to form chlorinated hydrocarbons when pyrolyzed together with polyolefin-based plastics (Yu, Sun et al. 2016). However, microwave irradiation could selectively heat PVC first, because of its higher dielectric loss factors than other plastics (Moriwaki, Machida et al. 2006); this could potentially enable the separation of the dehydrochlorination reactions of PVC from the thermal decomposition of other plastics (Kobayashi, Hori et al. 2019). Second, with the help of dispersed microwave absorbents,

the MAP process could save energy by achieving faster heating rates than in a conventional heating process. Dispersed microwave absorbents, which are heated directly by microwave irradiation at a very high rate, act as a localized heating source to the surrounding feedstock, and therefore greatly improve the uniformity and rates of the heating process. In contrast, the sticky nature and low thermal conductivity of melted plastics often seriously limit the heat transfer in a conventional heating process.

However, with the potential advantages offered by the MAP technology for chemical recycling of waste plastics, almost all related studies so far have been carried out in small lab-scale batch reactors, with a sample size typically less than 20 g. Therefore, it is necessary to conduct further testing, to investigate the feasibility of MAP technology at a much larger scale.

In this chapter, the feasibility of catalytic pyrolysis of plastic waste for energy recovery was investigated in a continuous microwave-assisted pyrolysis (CMAP) system recently developed in our lab. Since PE, PP, and PET account for most of the plastic wastes and PET is widely recycled with mechanical processes, PE and PP were selected as feedstock for this study. The effect of different processing temperatures, different plastic compositions, and application of catalysts, on product yields and composition, were studied. In addition, an energy balance of the process was analyzed and discussed.

4.2.Materials and Methods

4.2.1. Feedstock and characterization

Most of the experiments were carried out by using HDPE chips with a dimension of ca. 2mm*3mm*1mm. These chips were produced by shredding real world post-consumer plastic wastes from industrial packaging and molding processes (kindly provided by

Resynergi Inc., Rohnert Park, CA). Other materials tested include recycled PP chips (also provided by Resynergi Inc.) and PP pellets of ca. 3mm diameter (purchased from HQC Inc., Oswego, IL). Proximate analysis of the feed was determined following standard procedure ASTM E870. Elemental analysis (C, H, O, and N content) was determined using a CE440 Elemental Analyzer (Exeter Analytical, Inc. UK); energy content, as the higher heating value (HHV), was determined by an oxygen bomb calorimeter (Model 1341, Parr Instrument Company). The catalyst used in this study was ZSM-5 pellets (dimension Φ2×2-10 mm, Si/Al molar ratio=19, specific surface area, ⩾250 m^2/g, pore volume ⩾0.25 cm^3/g) purchased from ACS Material (Pasadena, CA). Catalysts were reactivated by calcination at 550°C in air for 5 hours before each experiment.

Table 7 Proximate analysis and elemental analysis results (as-received basis) of the feedstock

Feedstock	**HHV, MJ/kg**	**Proximate analysis, wt. %**				**Elemental analysis, wt. %**		
		Moisture	Volatile Matter	Fixed Carbon	Ash	C	H	N
HDPE chips	45.8	0	99	0.1	0.9	85.1	13.3	0
PP chips	46.7	0.1	99.2	0.6	0.1	84.2	13.3	0
PP pellets	29	0.1	64.7	1.1	34.1	53.5	8.9	0

4.2.2. Experiment apparatus and procedure

A recently developed continuous down-draft microwave-assisted pyrolysis system was used in this study. Fig. 11 shows the schematic diagram of the experimental setup; details of the system design can be found in our previous publication (Zhou, Zhou et al. 2020). This system has a total microwave output power of 9 kW and a processing

capability of up to 10 kg of plastic per hour. Feedstock stored in an airtight hopper is fed into the top of the reactor at a controlled rate via an auger feeder. Inside the main reactor, 6 kg of 12mm silicon carbide balls are contained in a cordierite ceramic cylinder which is continuously mixed by an auger shaft and heated by microwave irradiation, allowing continuous processing of the plastic feedstock. After separation from ash, the primary pyrolytic vapor goes through a catalytic packed bed which is externally heated at a controlled temperature for catalytic upgrading. A side stream of the hot vapor is sampled right after the catalytic packed bed reactor, by a series of glass condensers for off-line composition analysis, while the main pyrolysis vapor stream goes through a stainless-steel condenser system, where condensable products and non-condensable gases are separated and collected. Special attention has been paid to the airtightness of the system by incorporating components such as an oil seal, metal expansion joint, and graphite sealing. Pressure inside the reactor is monitored by a water manometer, and is maintained around 0.25'' H_2O of vacuum by adjusting the frequency of the roots blower. Since directly measuring the temperature inside the ball bed is technically challenging during the operation of this system, a calibration curve was established experimentally, and is used to estimate the ball bed temperature T_b based on the T_2 measurement. Electrical energy consumption is monitored by a digital power meter (Omnimeter I v.3, EKM Metering Inc.).

In a typical experiment, T_b is used as the process temperature and maintained at set levels, e.g. 620^{o}C, by controlling the "on/off" setting of the microwave power with a PLC control system. Unless otherwise stated, the feeding rate is set to 2 kg/h; 200 g of ZSM-5

catalyst pellets are used in each experiment, giving a weight hourly space velocity (WHSV) of 10 h^{-1}, and the catalytic reactor temperature is maintained at 400°C.

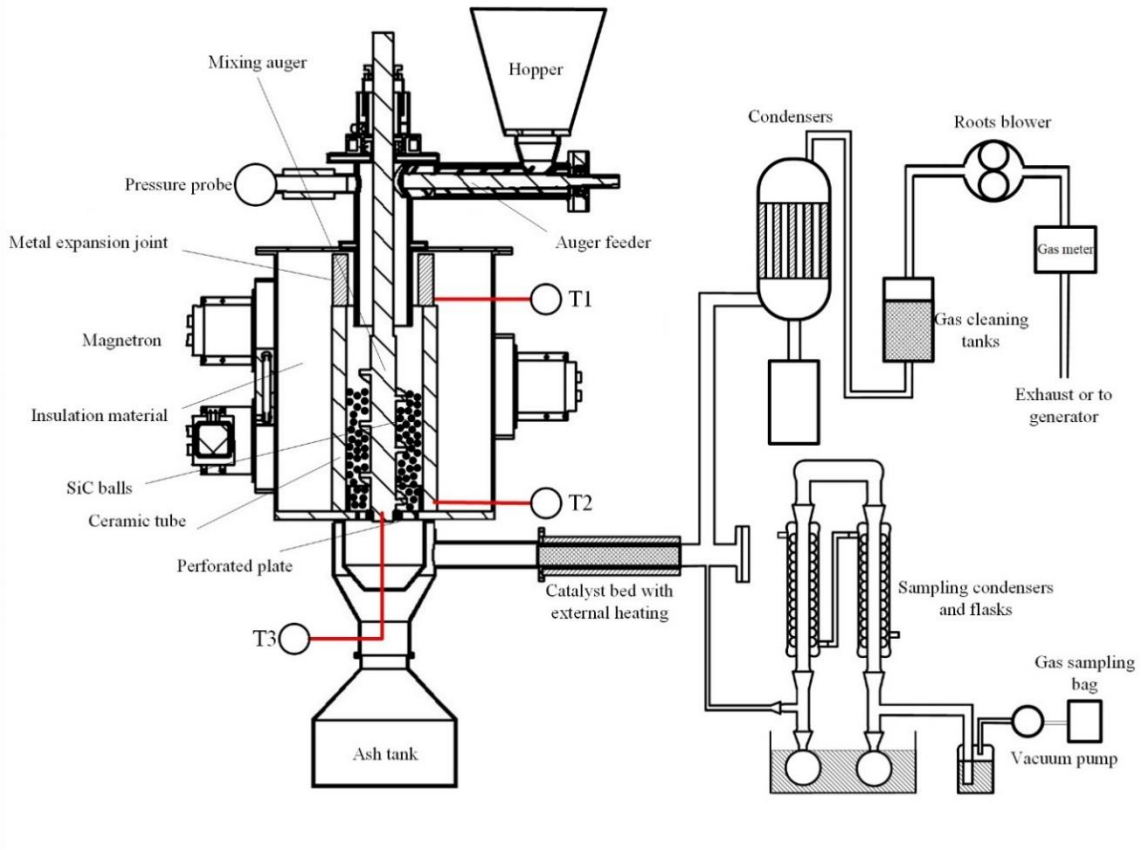

Figure 11 Schematic diagram of CMAP system

4.2.3. Sampling and analysis

The total flow rate of the produced gas was recorded by a pulse output gas meter (EKM Metering Inc.) downstream of the roots blower. A side stream of 1 liter per minute (LPM) of hot vapor exiting the catalytic reactor was routed into the glass condensers, and flasks were used to collect the condensable liquid and wax. To continuously monitor the product composition and yield, condensable samples (i.e. liquid and wax) are taken every 15 minutes by an ice water cooled glass condenser system, and the sampling time is 10

minutes each, to obtain enough sample for analysis and accurate weight. Non-condensable gas samples are taken around every 5 minutes in Tedlar gas sampling bags. The yield of non-condensable gas was calculated based on the chemical composition and flow rate data, while the yield of condensable fraction (including liquid and wax) was calculated based on the weight difference of the flasks before and after each sampling, noted as m_c. Since wax was obtained, together with a liquid product under some conditions, and the phase separation between these two components was often not clear, chloroform was used as a solvent to selectively dissolve the light hydrocarbons (liquid fraction) from the mixture. The undissolved portion, deemed as wax, was filtered and weighed, and then the weight percentage of wax (wax%) in the mixture was obtained. Finally, the percentage yield of each product was determined as follows:

$$Y_{gas} = Q \times \sum x_i M_i \div \left(V_{300K}^{1atm} \times \dot{m}_f\right)$$

$$Y_{wax} = m_c \times wax\% \times Q \div \dot{m}_f$$

$$Y_{liquid} = m_c \times (1 - wax\%) \times Q \div \dot{m}_f$$

$$Y_{unquantified} = 100 - Y_{gas} - Y_{wax} - Y_{liquid}$$

, where x_i and M_i are the volume percentage and molecular weight of a gas component in the produced gas, respectively; Q is the gas flow rate measured by the end gas meter; $\dot{m}_f$ is the feeding rate of the plastic feedstock; and V_{300K}^{1atm} is the gas molar volume at 300 K under atmospheric pressure, i.e. 24.6 L/mol.

The composition of non-condensable gas samples was determined by using a Varian Micro-GC (CP-4900) coupled with a thermal conductivity detector (TCD) and two

analytical columns, namely Molecular Sieve 5A and the PoraPLOT Q. Standard gas mixtures were used to establish calibration curves for quantitative analysis of gases, including: H_2, CO, CO_2, CH_4 and C_2-C_4 alkanes and alkenes.

The composition of the liquid product was analyzed by using Agilent 7890-5975C GC/MS equipped with a 30 m × 0.32 mm HP-5 MS capillary column of 0.25 μm thickness. The oven temperature is programmed as follows: holding at 50°C for 2 min, then a heating ramp of 5°C /min to 300°C, and lastly holding for 5 min. The chromatographic peaks were identified by using National Institute of Standards and Technology (NIST) database. Individual components were not calibrated in the GC-MS analysis; instead, the area percentage of the corresponding total ion current (TIC) peak was used to give an approximation of the weight percentage of each component.

The higher heating value (HHV, MJ/ Nm^3) of the combined product gas is calculated by:

$$HHV = [H_2] \times 12.7 + [CO] \times 12.7 + [CH_4] \times 39.6 + [C_2H_4] \times 64.5 + [C_2H_6] \times 68.2 + [C_3H_6] \times 91.5 + [C_3H_8] \times 98.5 + [C_4H_8] \times 120.8 + [C_4H_{10}] \times 130.3$$

where each [gas] is the volume percentage of that gas component. The higher heating value (HHV, MJ/kg) of the condensable fraction was determined by an oxygen bomb calorimeter (Model 1341, Parr Instrument Company).

At least ten permanent samples and three condensable fraction samples were taken during each experiment trial to obtain the data, with relative standard deviations (RSD) of less than 10%. The mean values of the data were used for analysis in this paper.

4.3.Results and Discussion

The effects of processing temperature, catalysis, and feedstock type on the product yields and quality were investigated in this study. Each experimental run lasted for at least 1 hour with a stable temperature profile, and the product distribution over the course of time was also consistent for experiments without catalysts. Fig. 12, for example, shows a typical profile of gas compositions, which evolved over time.

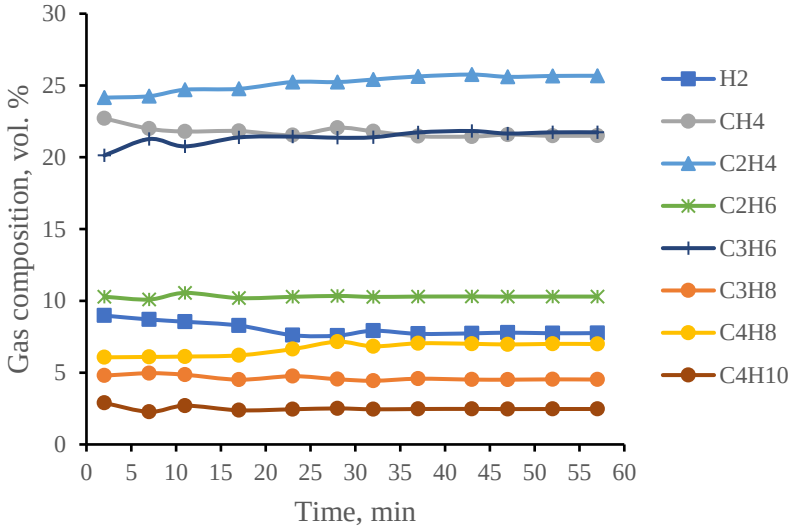

Figure 12 Evolution of gas composition profiles over the course of an experimental run at 620 ºC

4.3.1. Effect of temperature

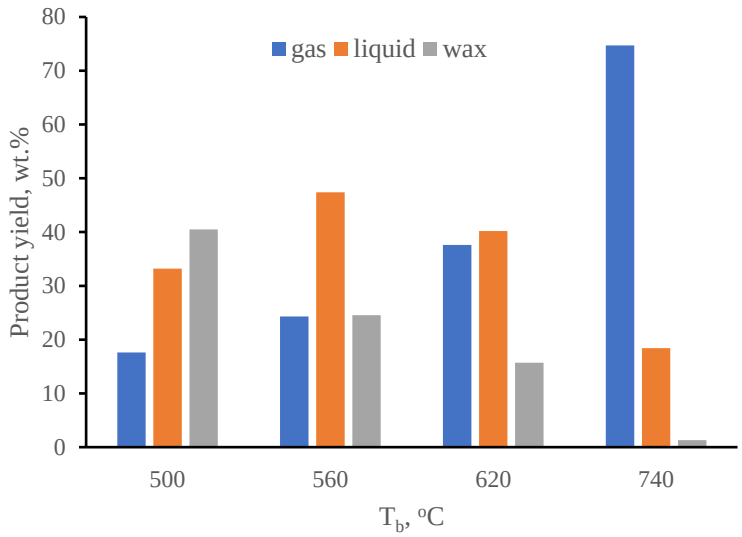
80
70
60
50
40
30
20
10
0
gas
liquid
wax
Product yield, wt.%
500
560
620
740
T_b, °C

(a)

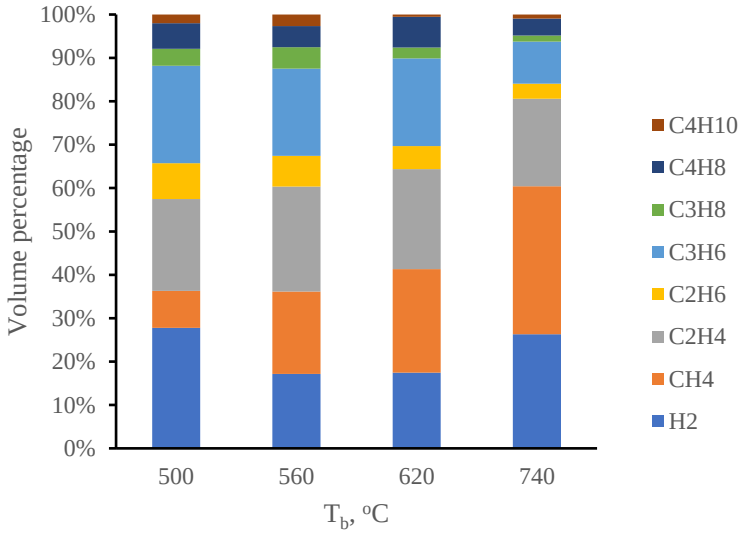
100%
90%
80%
70%
60%
50%
40%
30%
20%
10%
0%
Volume percentage
500
560
620
740
T_b, °C
C4H10
C4H8
C3H8
C3H6
C2H6
C2H4
CH4
H2

(b)

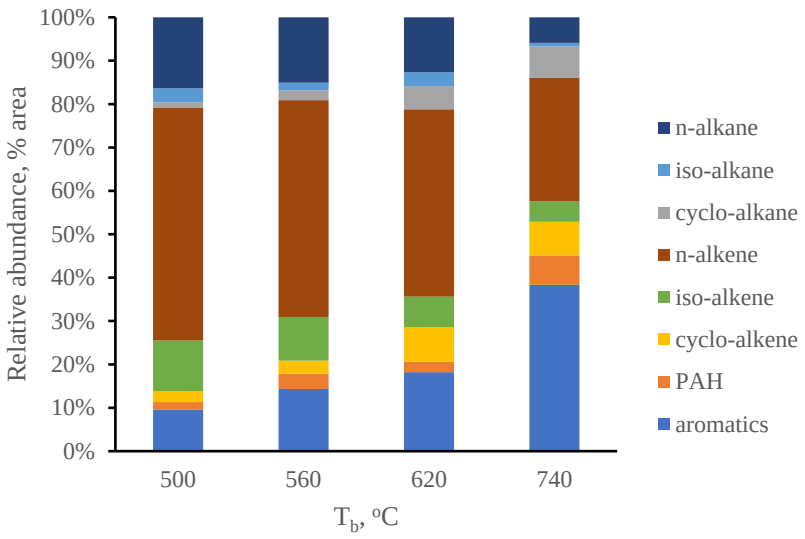

(c)

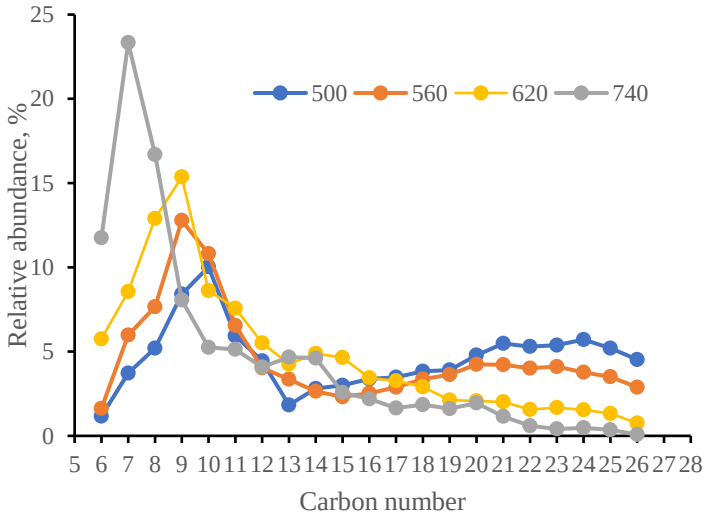

(d)

Figure 13 Product yields (a), gas product compositions (b), liquid product compositions (c) and liquid product carbon number distributions (d) of HDPE thermal pyrolysis under different temperature conditions

Table 8 Product yields of polyethylene thermal pyrolysis at 500 °C with different reactors

Reactor	Gas yield, %	Wax yield, %	Residence time, s	Reference
Fixed bed batch reactor	48.4	0	1200	Ding, Liu et al. (2019)
CMAP reactor	17.6	40.5	90	This study
Fluidized bed reactor	10.8	45.3	15	Williams and Williams (1999)
Conical spouted bed reactor	3.7	67.8	0.01	Elordi, Olazar et al. (2011)

Fig. 13(a) presents the product distribution (gas, liquid, and wax) under processing temperatures from 500°C to 740°C without the application of catalysts. The mass balance by adding three quantified fractions ranges from 89.2% to 95.3% for different temperature conditions. The highest liquid yield, 47.4 wt.%, was obtained at 560°C. As the processing temperature increased from 500 to 740°C, non-condensable gas yields increased from 17.6 to 74.7 wt.% while the wax yields decreased from 40.5 wt.% to negligible (1.3 wt.%). A comparison with other non-catalytic polyethylene pyrolysis studies, with various reactor designs, are shown in Table 8, and reveal that the CMAP system gives a gas yield and wax yield in between those of a batch reactor and a fluidization-based pyrolysis reactor. Specifically, the gas yields, under the same temperature of 500°C, rank from high to low as fixed bed reactor, CMAP reactor, fluidized bed reactor, and the conical spout bed reactor. The wax yields of these reactors follow the exact opposite order. Similar trends were also observed in other temperature conditions (Williams and Williams 1999, Elordi, Olazar et al. 2011, Ding, Liu et al. 2019). This trend could be explained by the difference in residence times among different reactors. A longer residence time means a more severe degree of thermal degradation, and therefore a higher gas yield and a lower wax yield, which has been proven by many

previous studies (Mastral, Esperanza et al. 2002, Zhao, Wang et al. 2019). The residence time of the CMAP reactor is roughly estimated to be around 90 seconds at the processing temperature of 500^{o}C based on the observed average time difference between starting to feed the plastics into the reactor and the detection of combustible gas exiting the reactor. In contrast, the residence time in a batch reactor is typically over 20 minutes; fluidized bed reactor is in the range of 1-25s; and conical spouted bed is 0.01s (Williams and Williams 1999, Mastral, Esperanza et al. 2002, Elordi, Olazar et al. 2011, Ding, Liu et al. 2019, Zhao, Wang et al. 2019). From the perspective of reducing wax yield, a longer residence time is preferred since this would lower the temperature necessary for cracking and thus the energy consumption of the process. A long residence time could be easily achieved with a fixed-bed batch process, which is, however, generally considered not suitable for scaled-up operations. For the fluidized bed reactors, a conflict, intrinsic to the fluidization principle, exists between a long residence time and a high heating rate, unless a circulating mechanism is applied, which is only efficient at very large scales (Milne, Behie et al. 1999). In contrast, the residence time in the CMAP system could be readily extended or reduced by adjusting the ball bed structure and the vacuum in the reactor. In this regard, due to the combination of the continuous operation design and a moderate residence time, the CMAP system offers some unique advantages over conventional reactor designs. Specifically, the continuous CMAP is more feasible for industrial scale operations compared to batch reactors, while it requires lower processing temperatures than the conventional continuous processes based on fluidization designs, to achieve the same level of cracking due to the longer residence time.

The composition of non-condensable gases under different processing temperatures are presented in Fig. 13(b). Trace amounts of N_2, CO and CO_2 (< 2 vol.%), probably generated by slight air leakage into the reactor due to vacuum, were also, occasionally detected in the product gas, but are not presented in this figure for simplicity. The gas components include H2, CH4, and C2-C4 alkanes and alkenes. The yield of CH4 disproportionally increased with temperature, as indicated by the increasing relative content of CH4 (i.e. 8.4% to 33.7%) relative to those of C2-C4 hydrocarbons (i.e. 63.1% to 39.2%). This tendency to produce lighter hydrocarbons under higher temperatures were also observed in several polyethylene pyrolysis studies (Lopez, De Marco et al. 2011, Zhao, Wang et al. 2019). This phenomenon could be explained by the chain-end scission mechanism proposed by several studies, which essentially states that a higher degradation temperature leads to higher probabilities of C-C bond dissociation at the end of carbon chains, rather than those towards the center of the chain (Murata, Hirano et al. 2002, Ueno, Nakashima et al. 2010). The higher heating values (HHV) of the gas products were calculated to be in the range of 45.3 to 46.9 MJ/kg, comparable to the heating values of common gas fuels such as propane (ca. 50 MJ/kg) and natural gas (ca. 45 MJ/kg).

Fig. 13(c) shows the detailed chemical composition of liquid products. Over 60 major components detected in the GC/MS analysis were divided into eight groups, based on their functional groups and molecular structure. N-alkenes was the most abundant group at temperatures below 620^{o}C, followed by n-alkanes and mono-aromatics, which is in agreement with many previous studies (Elordi, Olazar et al. 2011, Ding, Liu et al. 2019, Zhao, Wang et al. 2019). The n-alkenes/n-alkanes ratios were around 3 under all

conditions. The gas chromatograph gives a straightforward illustration of this result as it features a series of characteristic triplet peaks, which consist of three hydrocarbon compounds of the same carbon numbers eluted in the order of alkadiene, alkene and alkane, with the alkene peak being the largest. This pattern could be explained by the random scission mechanism of polyethylene thermal degradation. Essentially the chain scission leads to terminal free radicals transferring internally in the carbon backbone until an double bond is formed at one or both ends (Williams and Williams 1999, Ueno, Nakashima et al. 2010). As the temperature further increased to 740^{o}C, the relative ratio of mono-aromatic hydrocarbons significantly increased to 38.6% of the total liquid product. This is due to the increased rate of secondary reactions of primary pyrolysis products (e.g. n-alkanes and n-alkenes) via pathways such as the Diels-Alder reaction (Williams and Williams 1999). Overall, the increasing temperature leads to the production of lighter hydrocarbons as well as those more unsaturated and more thermodynamically stable hydrocarbons.

The liquid product is a mixture of various groups of hydrocarbons, each associated with its unique fuel properties. For example, one of the most important indexes for gasoline is the octane number (ON) as it relates to its antiknock performance in a gasoline engine. The octane numbers of different chemical categories rank as follows (high to low): aromatics > iso-aliphatics> cycloaliphatics > n-alkenes>n-alkanes (Ding, Liu et al. 2019, Sarıkoç 2020). In this regard, aromatics and n-alkenes are more desirable components than n-alkanes. However, it is also known that higher alkenes and aromatics content increase the tendency of deposition in engine injectors and intake valves, and their content also affects the engine emission performance (Yitao, SHUAI et al. 2009,

Hajbabaei, Karavalakis et al. 2013). Therefore, it is expected that post processing steps such as fractionation, blending, or hydrotreating are necessary to produce fuels that meet with regulation standards and specifications. In fact, regulations of commercial liquid fuels (e.g. gasoline, diesel, and jet fuels) regarding the chemical composition are rare, as regulations mostly involve physical specifications such as Reid vapor pressure, octane number (for gasoline), cetane number (for diesel), specific gravity, and flash point (Hajbabaei, Karavalakis et al. 2013). Therefore, refineries often have different formulations to mix various gasoline blending components to produce finished products that meet a range of specifications.

The liquid product carbon number distribution is shown in Fig. 13(d). The relative abundance of gasoline range hydrocarbons (C5-C12) increased from 38.9% to 74.3% and the peaks of the distribution curves generally shifted towards the left (lower carbon number) as the processing temperature increased from 500 to 740^{o}C. This trend can be explained, again, by the random scission mechanism of polyolefin degradation, which assumes a random cleavage in the carbon chains of macromolecular polymers to produce fragments of shorter carbon chain lengths, and the rate of bond cleavage positively correlates to temperature (Murata, Hirano et al. 2002, Zhao, Wang et al. 2019). Also noted from Fig. 3(d), is that the liquid products contained some wax range hydrocarbons (C20+). This indicates the wax yield could be underestimated while liquid yield overestimated under some conditions since chloroform, the solvent used to separate wax and liquid in this study, could slightly dissolve C20+ (wax) fractions.

4.3.2. Effect of plastic composition

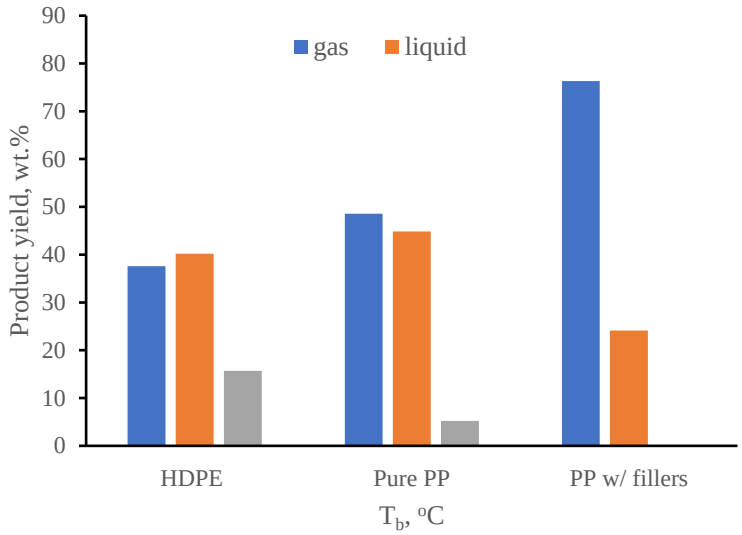

(a)

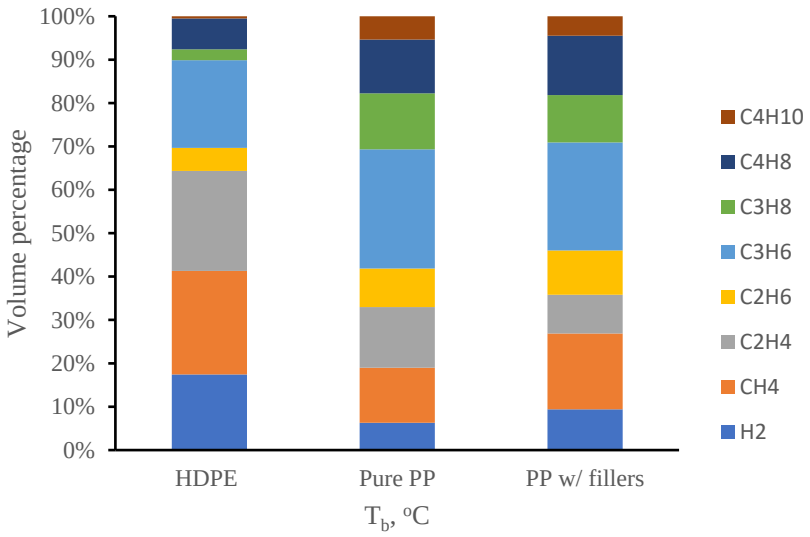

(b)

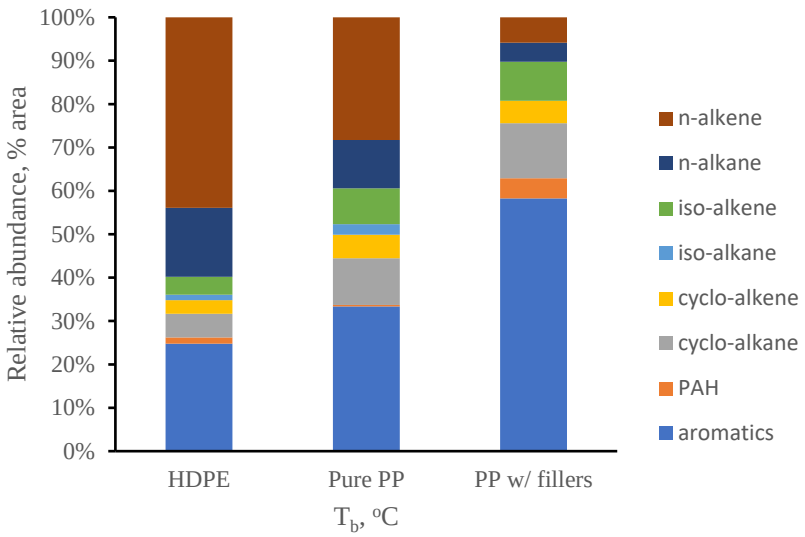

(c)

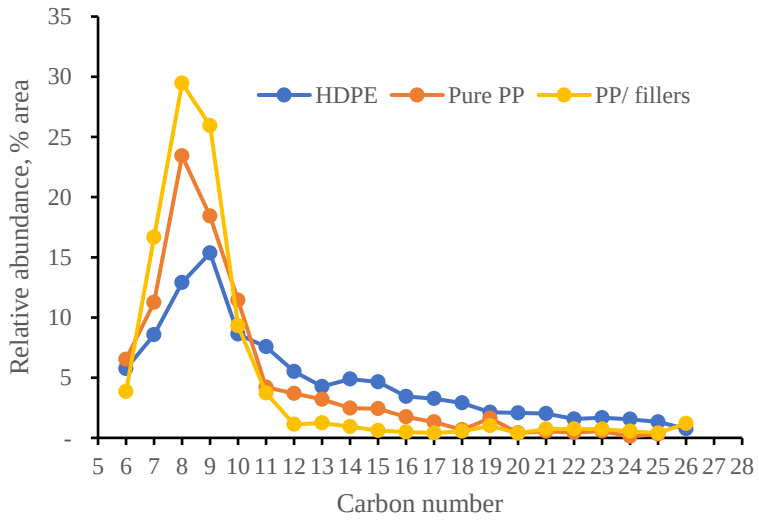

(d)

Figure 14 Product yields (a), gas product compositions (b), liquid product compositions (c) and liquid product carbon number distributions (d) of thermal pyrolysis of three different types of plastic feedstock at 620 °C

Fig. 14 (a) to (d) illustrate the product distribution and compositional analysis results from three different feedstocks, all at the processing temperature of 620°C. It is observed that pyrolysis of pure PP chips (without minerals) produced higher yields of gas (48.6%

vs. 37.6%) and liquid (44.8% vs. 40.2%) and less wax (5.2% vs. 15.7%) than HDPE, suggesting that PP is more susceptible to thermal degradation than HDPE. This is also reflected on the liquid composition difference. The liquid product from PP pyrolysis contained more aromatic content (33.4% vs 24.8%), less n-alkene content (28.3% vs. 44.0%), and more C5-C12 fraction (79.0% vs 64.3%); These results indicate a higher degree of thermal degradation and secondary reactions. A similar trend was also observed by Undri, Rosi et al. (2014) who found that PP was fully pyrolyzed while HDPE was only partially decomposed under the same experiment setting. These observations agree with many previous thermogravimetric analysis-based studies that demonstrated that activation energy for thermal degradation of HPDE was higher than PP (Aboulkas and El Bouadili 2010). In fact, resistance to thermal degradation of common plastic types generally follow the order of PVC<PS<PP<LDPE<HDPE (Peterson, Vyazovkin et al. 2001, Kim and Kim 2004, Wu, Chen et al. 2014). PP tends to produce more C3-C4 and less C1-C2 gas hydrocarbons than HDPE, probably due to their different monomers.

The product yields and compositions from pure PP and PP with fillers showed a significant difference. Specifically, the latter produced a much higher gas yield (76.3%) and a negligible wax yield. In addition, the liquid product also contained a higher aromatic content (57.9%) and a lower n-alkene content (5.8%). All these signs indicate a higher degree of degradation for PP with fillers, and this most likely resulted from the fillers which essentially acted as a catalyst. An ICP-MS analysis of the ash sample from PP with fillers detected elements including Mg, Si, and O, suggesting that the filler could be magnesium silicate (i.e. talc), a naturally occurring mineral and also a common filler

in polypropylene mainly to increase its stiffness (Stamhuis 1984). While no literature report was found, on the catalytic effect of magnesium silicate on pyrolysis reactions, it is known that naturally derived MgO materials are quite effective in *in-situ* catalytic upgrading of pyrolytic bio-oils, as alternatives to classical zeolite catalysts (Stefanidis, Karakoulia et al. 2016). Therefore, it is suspected that magnesium silicate, as a naturally occurring, mineral based filler, could be a cost-effective catalyst for the plastic pyrolysis process. In fact, based on literature reviews, the catalytic effect of inorganic fillers on plastic pyrolysis is rarely investigated, and may certainly deserve further study.

4.3.3. Effect of catalysis

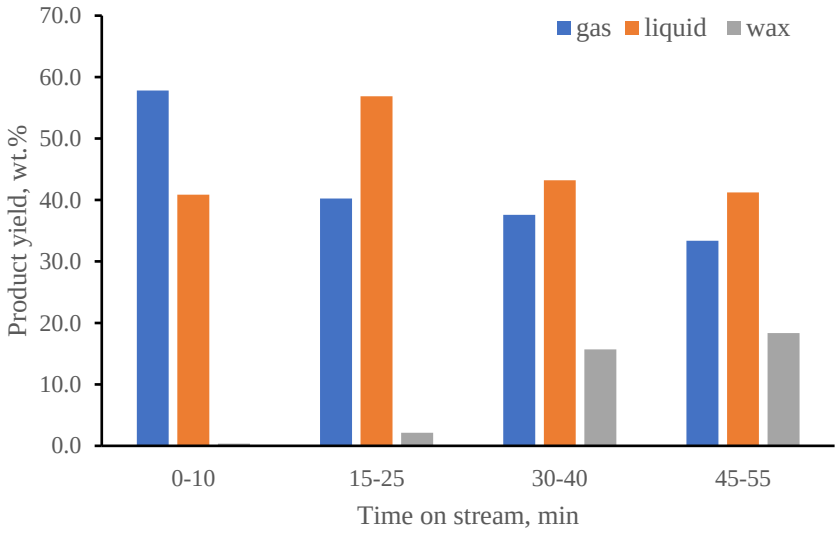

(a)

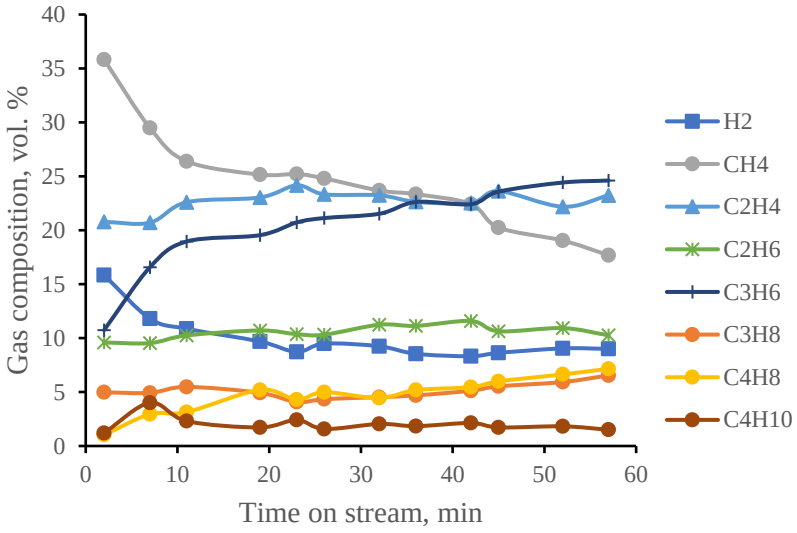
Gas composition, vol. %
Time on stream, min
H2
CH4
C2H4
C2H6
C3H6
C3H8
C4H8
C4H10

(b)

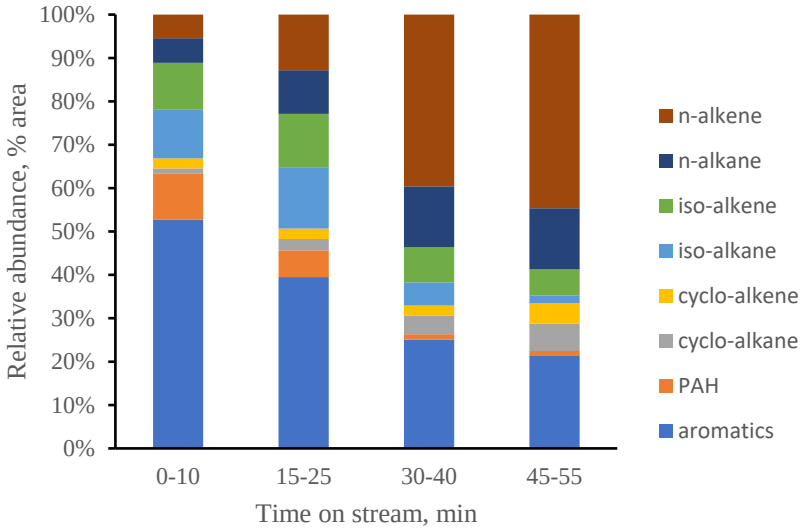
Relative abundance, % area
Time on stream, min
0-10
15-25
30-40
45-55
n-alkene
n-alkane
iso-alkene
iso-alkane
cyclo-alkene
cyclo-alkane
PAH
aromatics

(c)

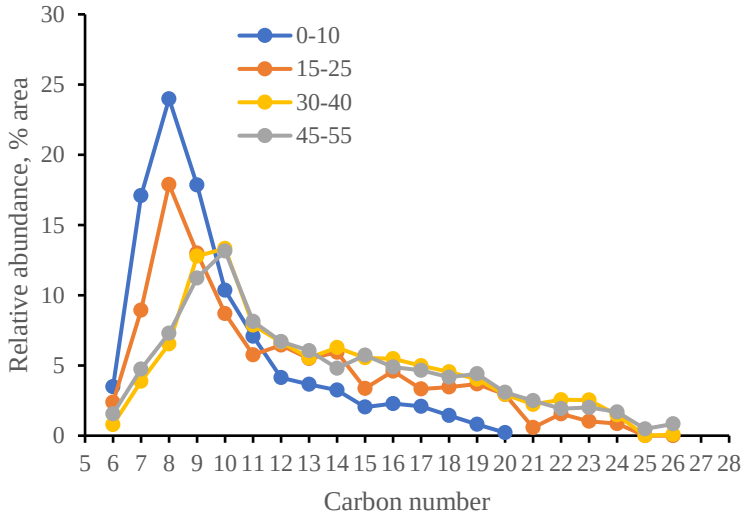

(d)

Figure 15 Time-on-stream evolution of product yields (a), gas product compositions (b), liquid product compositions (c) and liquid product carbon number distributions (d) of HDPE catalytic pyrolysis

To study the effect of catalysis on the process, 200g of ZSM-5 pellets were packed into a catalyst bed, and externally heated to 400^{o}C. HDPE chips were fed into the CMAP system at a rate of 2kg/h under a processing temperature of 620^{o}C. Product distribution was monitored continuously throughout the runs, which lasted for around 1 hour. Product yields and compositions as a function of time are illustrated in Fig.15(a) to Fig.15(d). The one-hour experimental run could be considered as composed of two stages, separated roughly at Time 30 minutes, based on the trend of yield change. During the first stage, the gas yields decreased from 57.8% to 40.2%, and the liquid yield increased to 56.9%, while wax yields remained negligible (from 0.3% to 2.1%). In contrast, the product yields remained relatively constant during the second stage, and very close to the product yields of a thermal pyrolysis run at the same temperature (without catalysts). Significant

changes over time were also observed in the liquid product composition. For instance, the aromatic hydrocarbon content gradually decreased (52.8% to 21.3%) while normal aliphatic hydrocarbons increased (11.1% to 58.7%) over time, with a marked change occurring after 25 minutes of run. In addition, the gasoline fraction content (C5-C12) also decreased from 84.0% to 52.8% during the process. All of these signs indicate a rapid loss of catalytic activity of ZSM-5 during this process, and specifically the catalytic activity was deemed diminished after 30 min, or equivalent to a plastic/catalyst ratio of 5. This is in accordance with many previous studies which reported the feedstock/ZSM-5 ratios, i.e. 2-10, for catalyst deactivation in an *ex-situ* catalytic setting (Olazar, Lopez et al. 2009, López, De Marco et al. 2011, Mullen, Dorado et al. 2018). The rapid deactivation is mainly caused by coke deposition on the catalyst surface, which blocks the access to the active acid sites of the catalysts. Fortunately, this deactivation can be partially reversed by a regeneration process which involves a calcination treatment, typically at 550^{o}C in air, to remove the coke deposition. Many studies have shown the recovered catalytic activity after regeneration, and thus the chance to reuse the catalysts for multiple cycles (López, De Marco et al. 2011, Zhou, Liu et al. 2018).

In order to evaluate the effect of catalysis on the process, the average product yields and compositions from the first 30 minutes of the catalytic pyrolysis run were compared with those in the thermal pyrolysis run, at the same processing temperature of 620^{o}C. The main difference observed, indicates that catalytic pyrolysis produced a higher liquid yield (48.9% vs. 40.2%) with a minimal wax yield (1.2% vs. 15.7%) as compared to the thermal pyrolysis process. The liquid product contains a considerably higher aromatic content (45.0% vs. 18.6%), a higher isomerized aliphatic content (24.6% vs. 10.4%), a

higher C5-C12 gasoline fraction (73.5% vs. 64.3%), and a lower n-alkene content (12.8% vs. 44.0%). This is in agreement with the well-known catalytic effects of ZSM-5 in cracking, isomerization, and aromatization owing to its balanced combination of microporous structure, acidity, and shape selectivity (Bagri and Williams 2002, López, De Marco et al. 2011, Rahimi and Karimzadeh 2011, Ratnasari, Nahil et al. 2017). Evidently, the incorporation of ZSM-5 catalysis in the process brings at least two benefits to the plastic pyrolysis process, including: 1) a higher quality liquid product featuring a narrow distribution of hydrocarbons, rich in gasoline-range aromatic compounds, and 2) a reduced temperature necessary to eliminate wax formation and thus a lower energy consumption of the whole process. However, it is also clear that ZSM-5 has several disadvantages, including: rapid deactivation, and relatively high cost. In addition, the high gas yield, and high aromatics content in the liquid product, make the process unsuitable to produce products of more interest to the petrochemical industry, such as naphtha, an intermediate feedstock to produce new plastics. Therefore, further studies are required to select or develop catalysts of higher activity and stability, lower cost, and more flexibility in selectively producing target products (Miandad, Barakat et al. 2016).

4.3.4. Energy balance analysis

Aside from product yields and quality, another critical aspect for evaluating the feasibility of an energy production process such as the fuel production from plastic waste pyrolysis, is the energy efficiency. An energy balance of this catalytic pyrolysis process on the CMAP system was established, based on the data obtained under the following specific conditions: HDPE feedstock, pyrolysis temperature of 620^{o}C, catalysis

temperature of 400°C, ZSM-5 pelletized catalyst, and a WHSV of 10 h^{-1}. All data were normalized to 1kg of HDPE input, as illustrated in Fig. 16.

1.9MJ of electrical energy for the magnetrons, and **3.1 MJ** of electrical energy for other parts (including the catalyst bed heating system, the water chiller, and electric motors for moving parts) were needed to continuously process 1kg of HDPE pellets. The process produced 4 fractions of products based on their carbon number ranges, namely **21.7 MJ** gas, **17.0 MJ** gasoline, **5.5 MJ** diesel, and **1.3 MJ** wax. Note that the heating values of the products are comparable to conventional fuels, reaching 46.5 and 46.0 MJ HHV/kg for the gas and liquid products, respectively. While the liquid product may require further processing to produce commercial grade liquid fuel or petrochemicals, the gas product could be readily used as an alternative to liquefied petroleum gas for power generation. The conversion efficiency could vary from 20% to 60% depending on the conversion technology adopted, e.g. a gas engine or a gas turbine. Considering 28% as the energy efficiency for a typical gas engine generator, **6.1MJ** electrical energy could be produced from the gas product alone, sufficient to support the electrical energy demand for the process, i.e. 1.9 + 3.1 = **5.0MJ**.

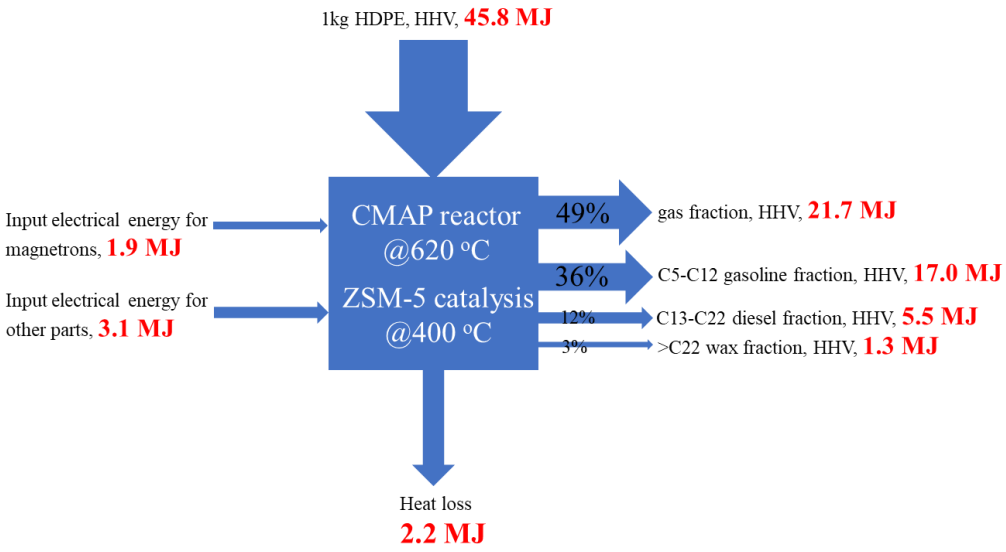

Figure 16 Energy balance of HDPE catalytic pyrolysis in the CMAP system

The theoretical energy consumption for pyrolyzing plastics, consisting of heat for increasing plastic temperature, pyrolysis reaction heat, and evaporation heat of hydrocarbon products, is reported to be between 1.05 to 1.32 MJ/kg polyethylene (Xingzhong 2006, Gao 2010). The higher energy input experimentally determined in this case, i.e. 1.9 MJ electrical energy, could arise from the energy conversion efficiency in the microwave heating process, i.e. from electrical energy to effective heat, and also the difference in production distributions between theoretical assumptions and the actual experimental results. The 3.1MJ electrical energy input for other parts could be reduced to a much lower level by increasing the plastic processing rate since the power consumption of these parts are constant, i.e. 1895W, regardless of the processing rate. Even with the additional 3.1 MJ electrical energy, the total energy efficiency of the process, defined as the total energy in the products (45.5 MJ) divided by the sum of feedstock energy input (45.8 MJ) and the electrical energy input (5.0 MJ), still reaches 89.6%, which is considerably higher than other types of reactors. For instance, the energy

efficiency for a rotary kiln based semi-batch process to recover energy from polyethylene is reported to be 65.4% and the heat loss is as high as 20.7 MJ per 1 kg PE processed (Zhang, Ji et al. 2020). The significantly higher heat loss in that process is likely caused by the semi-batch operation mode (volatiles swept out of reactor by room temperature carrier gas after 10 minutes of batch run) and the heat transfer limitation inherent to the conventional electric heating approach. In addition, Kaminsky and Sinn (1980) studied plastic pyrolysis in a pilot scale (19.1 kg/h) fluidized bed reactor and the heat required to process 1 kg of PP/PE mixture (1:1 ratio) was reported to be 11.0 MJ. The demand for a large amount of carrier gas and a higher operating temperature could contribute to the higher heat demand with the fluidized bed system. In fact, the CMAP system uses a minor vacuum instead of carrier gas to sweep the volatiles from the reactor to condensers. This should help reduce energy consumption, as experimentally proven by other studies (Mahari, Chong et al. 2018).

4.4. Summary

Pyrolysis of different types of plastic wastes was conducted in a novel continuous microwave-assisted pyrolysis system for fuel production. At 560^{o}C, the highest liquid product yield, 47.4%, was obtained for thermal pyrolysis of HDPE, together with 24.5% wax product. Higher pyrolysis temperatures promoted the cracking of wax and production of lighter and more thermodynamically stable hydrocarbons such as C1-C4 gases and aromatic hydrocarbons. Based on product yields and compositions, resistance to thermal degradation of three different plastic feedstocks rank as follows: HDPE, PP, and PP with fillers, and the mineral filler, i.e. talc, acted as a catalyst and showed noticeable cracking activity. Under a pyrolysis temperature of 620^{o}C, and incorporating

ZSM-5 catalysts in a secondary catalyst bed, enabled the elimination of wax product and an increase of liquid yield to 48.9%; this liquid product contained considerably higher contents of gasoline-range aromatic (45.0%) and isomerized aliphatic (24.6%) content. However, ZSM-5 catalysts also showed a tendency of rapid deactivation, lost its activity at a feedstock/catalyst ratio of 5. Energy balance analysis of the process showed that 5 MJ of electrical energy was required to process 1kg of HDPE with the CMAP system, giving a total energy efficiency as high as 89.6%. Furthermore, 6.1 MJ of electrical energy could potentially be generated from the gas products alone, making the process energy self-sufficient. Overall, the CMAP system, with its unique design, combining microwave heating with a mixing SiC ball bed, is a promising design for industrial application of energy recovery from plastic waste pyrolysis due to its advantages, including: 1) a higher energy efficiency, and 2) requirement of a lower processing temperature than conventional fluidized bed reactors.

Chapter 5 A Structured Catalyst of Silicon Carbide Foam Supported ZSM-5 for Microwave-assisted Pyrolysis of Biomass

5.1. Introduction

Biomass, as a renewable and abundant energy resource, has a great potential to be used as a feedstock for the production of chemicals and biofuels. Among the various conversion approaches, fast pyrolysis is a promising process and has been widely studied to convert biomass into liquids, commonly referred to as bio-oil (Zhou, Xia et al. 2011, Bridgwater 2012). However, bio-oil cannot be directly used in conventional engines because of a series of quality issues arising from its high oxygen content, including: low heating value, high water content, high acidity, and thermal instability (Czernik and Bridgwater 2004). Catalytic cracking, using zeolites, has been shown to be a promising approach for removing oxygen from bio-oil (Carlson, Vispute et al. 2008, French and Czernik 2010). ZSM-5, a synthetic zeolite, has received considerable attention because of its balanced performance, featuring a high selectivity towards aromatics production, and a moderate organic phase yield (Carlson, Tompsett et al. 2009, Jackson, Compton et al. 2009, Mihalcik, Mullen et al. 2011, Stefanidis, Kalogiannis et al. 2011).

Although ZSM-5 catalytic fast pyrolysis (CFP) has demonstrated promising results in micro-reactors (Carlson, Tompsett et al. 2009, French and Czernik 2010), significant process development is still needed before these results can be achieved at a scale feasible for commercial biofuel production. One of the key factors in CFP operation is the placement of ZSM-5 catalysts in the pyrolysis process. In this regard, most studies

carried out in industrially realistic systems, e.g. fluidized bed reactors, have focused on the *in-situ* CFP design, where catalysts are in direct contact with the biomass feedstock in the pyrolyzer (Carlson, Cheng et al. 2011, Mullen, Boateng et al. 2011, Zhang, Carlson et al. 2012, Du, Sun et al. 2014). However, as reviewed in Section 2.2.3, *in-situ* CFP design has encountered some serious problems when scaled up. The alternative, *ex-situ* design, where catalysts are placed in a separate catalyst bed, downstream of the pyrolysis reactor, could be a realistic solution. In general, *ex-situ* design requires less catalyst to achieve the same level of deoxygenation, but, at a marginal, additional cost of heating of the catalyst bed. The ex-situ design is also less prone deactivation due to coke formation, for three inherent advantages: 1) sufficient contact between pyrolysis vapor and the catalyst, 2) independent control of the catalytic temperature, and 3) indirect contact between biomass/char and the catalysts (Wang, Johnston et al. 2014, Gamliel, Du et al. 2015, Iisa, French et al. 2016, Hu, Xiao et al. 2017).

However, most bench scale *ex-situ* CFP studies, so far, configure the catalytic fixed bed reactors, by randomly packing several grams of catalyst powder (typically < 0.15 mm) or pellets (typically 1-2 mm) confined by a metal mesh or quartz wools (Zhang, Lei et al. 2015, Hu, Xiao et al. 2017, Liu, Zhang et al. 2017). These randomly packed bed reactors, with a small amount of fine catalyst powders and a simple reactor design, makes sense for lab-scale experiments that focus on testing the chemical performance of the catalysts. But, they will encounter severe limitations when applied to a full scale gasification system. For instance, pressure drop is a common problem in industrial applications of fixed bed reactors, and often causes premature system shutdowns. Excessive pressure drop is also reported, even in lab scale catalytic fixed bed reactors. Ferella, Stoehr et al.

(2013) investigated the effect of catalyst pellet size on tar removal performance with ~ 60g of alumina-based catalyst in a lab-scale fixed bed reactor. They observed significant performance improvement with catalysts of smaller pellet size, but further reducing pellet size was restrained by the increasing pressure drop. This is a classic example of the dilemma in packed bed reactors: the need for minimizing particle size to maximize the utilization of catalytic sites, which contradicts the demand for a larger particle size to reduce pressure drop (Pangarkar, Schildhauer et al. 2008, Gascon, Van Ommen et al. 2015). In addition, this inherent problem with packed beds, high pressure drop across the randomly packed bed, can be aggravated by fouling, especially for catalytic cracking reactions, which can cause carbon deposition on the catalyst surfaces. More importantly, fly ash that escapes from ash separation devices can enter the catalyst bed and cause permanent fouling of the catalyst (Liu, Wang et al. 2008). In the case of syngas production from pyrolysis or gasification processes, high pressure drop not only causes many operational challenges, but could also be a major safety concern, because the gas pressure build-up is a potential explosion hazard. Nevertheless, randomly packed beds are also related to more subtle problems, such as heat transfer limitations, non-homogeneous flow distributions and channeling through the packed bed, and undesirable secondary reactions, which substantially undermine the performance of the catalytic reactors (Eigenberger and Ruppel 2000, Gascon, Van Ommen et al. 2015).

A promising solution to the aforementioned problems may be a structured catalyst, consisting of a structured packing, coated with catalyst species, which could reduce the pressure drop and simultaneously enhance heat and mass transfer (Eigenberger and Ruppel 2000, Pangarkar, Schildhauer et al. 2008, Gascon, Van Ommen et al. 2015).

Typical examples of structured packings include monoliths, corrugated plate type packing, knitted wire packing, and open cell foams. The most widely used structured packing might be the corrugated plate type packing, or static mixers and catalyst bale. They can provide sufficient gas-liquid contact area and high heat transfer rate that are critical for separation processes such as vacuum distillation. However the metal material has limited its usage in low to medium temperature applications. Another commonly used packing is the ceramic monolith structure with parallel straight channels. They are typically used in environmental catalysis where large gas streams must be processed with low pressure drop, e.g. in purification of engine exhaust. Yet because of the dominant laminar pattern of the flow within the parallel walls, radial heat and mass transfer, i.e. from flow to the wall, becomes a limitation for monoliths to be used in high throughput isothermal catalytic processes, e.g. catalytic cracking (Eigenberger and Ruppel 2000).

Compared to others, ceramic foams, which are sponge-like ceramic materials consisting of interconnecting pores, seem to be a more suitable structured packing for very high temperature catalytic cracking. Ceramic foams typically have porosities ranging from 75 to 90%. Commercially available ceramic foams are typically of 5 to 100 PPI (pores per inch), corresponding to an average pore size of ca. 2.5 to 0.2 mm. Their interconnecting mega-porous geometry constitutes a tortuous flow path of the gas steam and therefore the hydrodynamic and thermal boundary layers are under constant disruption(Twigg and Richardson 2007, Pangarkar, Schildhauer et al. 2008). This gives rise to its most attractive property as a catalyst support: a combination of high permeability to gas flow and good heat and mass transfer characteristics, which has been demonstrated both by experiments and simulations. On the basis of equivalent surface to bed volume ratio,

foams demonstrated 2-5 times fast heat transfer rates, slightly higher mass transfer coefficients, and over 90% reduction of pressure drop, compared to randomly packed pellet beds (Richardson, Peng et al. 2000, Richardson, Remue et al. 2003, Lacroix, Nguyen et al. 2007). Experimental comparisons between three alumina based packing materials with similar geometric surface areas, namely bead packed bed, monolith, and foam, demonstrate that foam supports gave the overall best performance in terms of enhanced mass transfer and lower pressure drop, compared to packed beads, and a better heat transfer and substantial reduction in reactor size compared to the monolith (Giani, Groppi et al. 2005, Patcas, Garrido et al. 2007). The superiority of foams over monoliths in terms of the promotion of catalytic activity, has also been confirmed in many other studies (Ciambelli, Palma et al. 2010, Italiano, Balzarotti et al. 2016). Other advantages of ceramic foams as a catalyst support include: 1) capability to pre-shape per requirement: ceramic foams are made by carburization processes with polyurethane foams as a template, allowing them to be pre-formed into any desirable form and external porosity to fit into the reactor; 2) low cost: currently ceramic foams are mass-produced mainly for foundry filtration applications with a low cost; 3) wide temperature range: common materials used in commercial ceramic foams include Al_2O_3, ZrO_2, MgO, and SiC, all of which can be used in high temperatures, e.g. over 1700^{o}C for SiC.

In this study, a composite catalyst of ZSM-5 coating on SiC foam support, is investigated as a potential solution to the aforementioned problems. SiC is selected as the ceramic foam material because it has several appealing properties: high thermal conductivity, low thermal coefficient of expansion, and chemical inertness at elevated temperatures (Ivanova, Louis et al. 2007, Jiao, Jiang et al. 2012, Jiao, Yang et al. 2015, Duong-Viet,

Ba et al. 2016). Of equal importance, SiC is an excellent microwave absorbent and can potentially enable easy and precise temperature control of the catalyst bed when incorporated into a microwave assisted pyrolysis (MAP) system (Borges, Du et al. 2014).

The objective of this chapter was to study the feasibility of using the ZSM/SiC structured catalysts for *ex-situ* catalytic fast pyrolysis. The composite catalysts were prepared using a hydrothermal method and then tested in a MAP system. The pyrolysis results were compared with those from other configurations of catalyst placement. The effect of catalyst to biomass (C/B) ratio on the product yields, bio-oil composition, and catalyst deactivation behavior was investigated. The stability of the composite catalysts over regeneration cycles was also evaluated. To the best of the authors' knowledge, this is the first study using a composite catalyst to deal with the scale-up limitations of conventional packed beds for catalytic fast pyrolysis of biomass.

5.2. Materials and Methods

5.2.1. Materials

Silicon carbide foams with a pore size of 20 PPI were purchased from Tongda Carbide Co., Ltd (Zhuzhou, China). The foams were cut into cuboid pieces of 25 mm *25 mm* 14 mm in order to fit into the quartz catalytic reactor. Corn stover was obtained from a local farm in Saint Paul, MN, and was ground to 2 mm and dried before being used as the feedstock for the pyrolysis experiments. The proximate composition (wt. %) and elemental composition (wt. % on dry basis) were determined as follows: 6.72% moisture, 73.18% volatile matter, 16.11% fixed carbon, and 3.99% ash; 42.32 % C, 5.27 % H, 1.32 % N, and 45.10 % O.

5.2.2. Preparation and Characterization of ZSM-5/SiC Composite Catalysts

ZSM-5 coatings were prepared based on a hydrothermal synthesis method developed by Ivanova et al. (Ivanova, Louis et al. 2007). A precursor gel was first prepared by adding dropwise tetraethylorthosilicate (TEOS, 98%, Sigma-Aldrich) to an aqueous solution containing tetrapropylammonium hydroxide (TPAOH, 1 M, Sigma-Aldrich), sodium chloride, and sodium aluminate ($NaAlO_2$, 98%,Sigma-Aldrich) with the following molar ratios: 2.16 TPAOH: 5.62 TEOS: 3.43 NaCl: 0.13 $NaAlO_2$: 1000 H_2O. After 4 h of vigorous stirring of the gel, the foams were placed in a hydrothermal autoclave reactor filled with the gel and aged for another 4 h at room temperature before being transferred to the oven, maintained at 440 K (167^{o}C). After 48 h of synthesis reaction, the composite catalysts were washed with distilled water to remove loosely attached zeolites. The same procedure was repeated three times. After synthesis, the catalysts were calcinated at 500^{o}C to remove the organic template before being ion-exchanged with 1M NH_4Cl solution at 85^{o}C to replace the Na^+ with NH_4^+. Finally, the catalysts were calcinated again at 500^{o}C to obtain H-ZSM-5. In order to compare the catalytic performance of the ZSM-5/SiC foam composite to that of bulk ZSM-5, the same method was applied to synthesize ZSM-5 powders except without the SiC foam.

Specific surface areas (SSAs) of the foam supports and the catalysts were determined by N_2 adsorption/desorption measurement at 77 K on a PMI BET (Model BET201A) with a standard multipoint BET run. Prior to the measurement, the samples were heated at 313 K (40^{o}C) until an outgassing rate of under 0.005 torr/min was met under vacuum.

X-ray diffraction (XRD) patterns were recorded on a two-dimensional X-ray diffractometer (D8-Discover fitted with a Vantec 500 detector, Bruker) with Co Kα

radiation (1.78899 Å; 40 kV × 35 mA). Three measurement frames were collected for 300 seconds each, at 20/10, 50/25 and 80/40 º2θ/ ω, respectively. Area detector images were converted to one-dimensional intensity vs. 2θ data sets by using an averaging integration algorithm. The data was finally converted to Cu as X-ray source, using commercially available software (JADE 2010).

Scanning electron microscopy (SEM) images of the samples were recorded on a Hitachi SU8230 microscope working at an accelerating voltage of 0.8 kV in backscattered mode (BSE). Before imaging, the samples were coated with an indium layer by a Leica ACE600 sputter coater.

Elemental composition of the zeolites was analyzed using an inductively coupled argon plasma optical emission spectrometer (ICP-OES). The samples were first digested in acids using a microwave digestion system (NovaWave SA). The measurement was carried out on a Thermo Scientific iCAP 7600 ICP-OES Duo in conjunction with a CETAC ASX-520 auto sampler.

5.2.3. Microwave assisted pyrolysis (MAP) and analysis

An MAP system developed in our lab was employed in this study (Liu, Zhang et al. 2017, Fan, Chen et al. 2018). The schematic diagram of the system is presented in Fig. 17. A vacuum pump was used to evacuate the air from the reactor and maintain a vacuum of 100 mmHg before and during the experiments. A heating bed comprised of 700 g 30-grit silicon carbide was established in the bottom of the quartz reactor. Due to the excellent microwave absorbing ability, the SiC heating bed can be heated up rapidly under microwave radiation. After the desired temperatures were reached, biomass feedstock was introduced into the quartz reactor to start the experiment. Due to the simultaneous

heating of both the heating bed and the microwave radiation, a high heating rate was expected for the biomass. A stable heating bed temperature was established by repeatedly turning on and off the power.

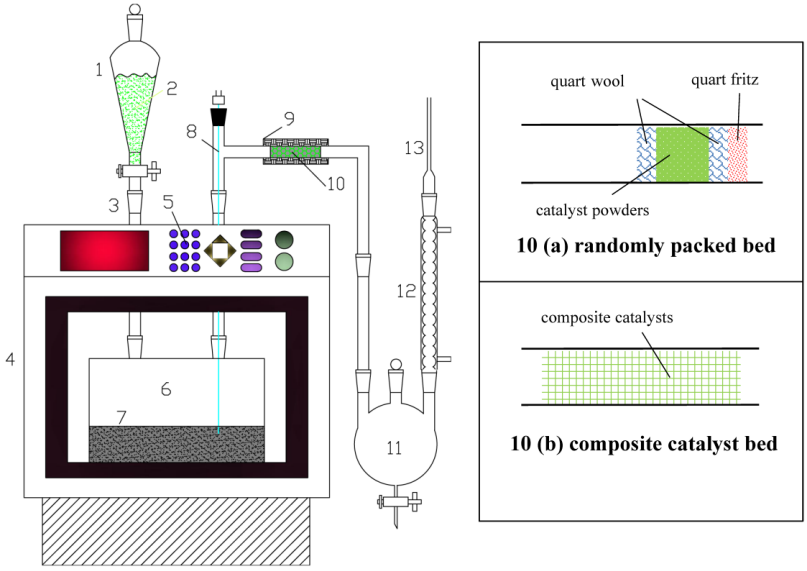

Figure 17 Schematic diagram of the experiment system setup: (1) feeder; (2) feedstock or a mixture of feedstock and catalysts; (3) quartz connector; (4) microwave oven; (5) control panel; (6) quartz reactor; (7) SiC bed; (8) thermocouple (K-type); (9) heating tape; (10) catalyst bed; (11) liquid fraction collectors; (12) condenser; (13) connection to vacuum pump

Three different configurations of catalyst placement were compared: *in-situ*, *ex-situ* with randomly packed bed, and *ex-situ* with composite catalysts. For *in-situ* catalysis, activated HZSM-5 powders (60 mesh) were mixed together with the biomass feedstock and introduced from the feeder (#1 in Fig. 17) into the reactor (#6) for pyrolysis while no heating was applied on the empty catalyst bed (#10); for *ex-situ* catalysis with randomly packed bed represented as 10 (a) in Fig. 17, catalyst powders were placed in a custom-

made quartz catalyst bed and secured in place by quartz wools at both ends and a quartz frit post the stream; for the *ex-situ* catalysis with composite catalyst bed represented as 10 (b), eight pieces of composite catalysts, which contain ~3.8 g H-ZSM5, were accommodated in the catalyst bed. The gaps between the composite catalysts and the inner reactor wall were filled with SiC grit and quartz wool to ensure the pyrolytic vapors would pass through the SiC foam pores. Both *ex-situ* configurations included additional heating, provided by a PID controlled heating tape. The pyrolysis temperature and the catalytic bed temperature were set at 550^{o}C and 425^{o}C, respectively, to achieve the optimal catalytic pyrolysis results according to our previous study (Liu, Zhang et al. 2017). The amounts of the biomass feedstock were varied to achieve the desired biomass to catalyst ratios (B/C) at 2, 4, and 10 for the *ex-situ* with composite catalyst experiments. Control experiments were also carried out, either with no catalyst, or with only SiC foams. To study the effect of regeneration on their catalytic activity, spent composite catalysts were regenerated by calcination in air at 500^{o}C for 8 h, and the same experiments were repeated 7 times at a constant C/B ratio of 1/4.

After each experimental run, the amount of char, coke, and bio-oil were determined by the weight difference, before and after the experiments, from the quartz reactor, the catalysts, and the condensers, respectively. The gas yield was calculated by difference, according to the mass balance as:

weight of gas = initial biomass amount – char mass – coke mass – bio-oil mass.

Composition of the bio-oil was characterized using GC/MS (Agilent 7890-5975C) with a HP-5 MS capillary column. The oven temperature was held at 50^{o}C for 2 min followed by a heating ramp to 260^{o}C at 5^{o}C/min, and then was held for another 5 min. The

injector was set at a temperature of 290°C and an injector size of 1 µL with a split ratio of 1:10. The carrier gas flow rate (helium) was 1.2 mL/min. Compounds were identified by comparison of the mass spectra with NIST library data. The content of each compound was semi-quantitatively determined by the corresponding peak area.

All experiments were performed at least in three replicates to obtain a relative standard deviation of less than 10%. The averages of data were used for analysis in this paper.

5.3. Results and Discussion

5.3.1. Catalysts Preparation and Characterization

After three synthesis steps, a homogeneous layer of white crystals was observed on the surface of the SiC foam support, and the average final loading of zeolites was 15.4 wt. %. The Si/Al ratio of the unsupported ZSM-5 powder was determined to be 34 using ICP-OES. BET specific surface areas (SSAs) of SiC support, the composite catalyst, and the unsupported ZSM-5 powder were determined to be 1.1, 76.7, and 470.4 m^2/g, respectively. The dramatic difference in the SSA values between the bare SiC support and the ZSM-5/SiC composite attributes to the porous ZSM-5 coatings. XRD patterns of the unsupported zeolite included in supplementary data is featured with the characteristic peaks of MFI structure at 7.9° and 8.9° and the characteristic triplet at ~23.5°, which agrees with the standard pattern of ZSM-5 (JCPSD card No: 44-0002). XRD patterns of the foam exhibit peaks at 35.6°, 60.0° and 71.7°, which is in agreement with standard patterns of β-SiC (JCPDS card No: 29-1129). Several minor peaks in the XRD pattern of SiC foam might indicate the existence of impurities in the commercial SiC foam. XRD pattern of ZSM-5/SiC composite catalyst contains all the features from both the SiC foam

and zeolite, confirming the successful coating of ZSM-5 structures on the SiC foam support.

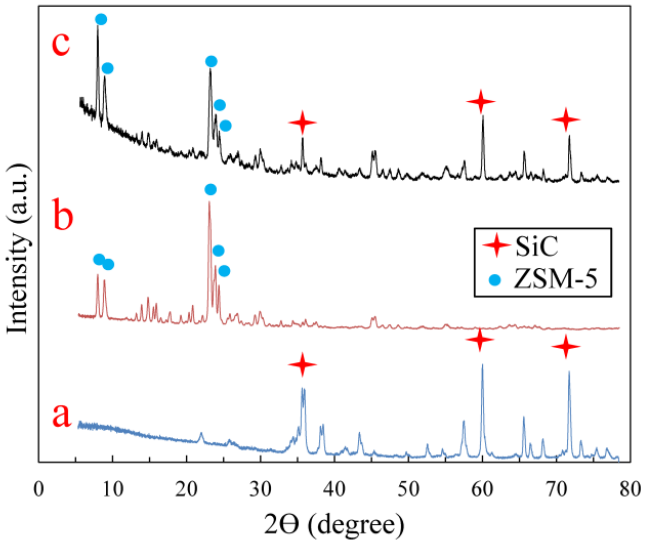

Figure 18 XRD patterns of (a) SiC foam, (b) ZSM-5 powder, and (c) ZSM-5/SiC foam composite

SEM micrographs of the composite catalyst, which are included in the supplementary data, confirm that the pores of the SiC foam are not blocked by zeolites. Zeolite crystals with a typical shape of hexagonal prisms and a uniform size of around 1 μm were observed to form a continuous and homogeneous thin layer that almost completely covers SiC foam surface. The thin layer arrangement would avoid mass transfer limitations in the randomly packed zeolites powders/pellets and allow easier access to the active sites of the zeolites. In addition, it can be seen from the micro-structures that most zeolite particles have been directly grown into, instead of loosely attached to, each other, which ultimately bond to the SiC foam matrix. Therefore, an efficient heat transfer of the composite catalyst, and a strong adherence of the zeolite layer to the foam support are expected.

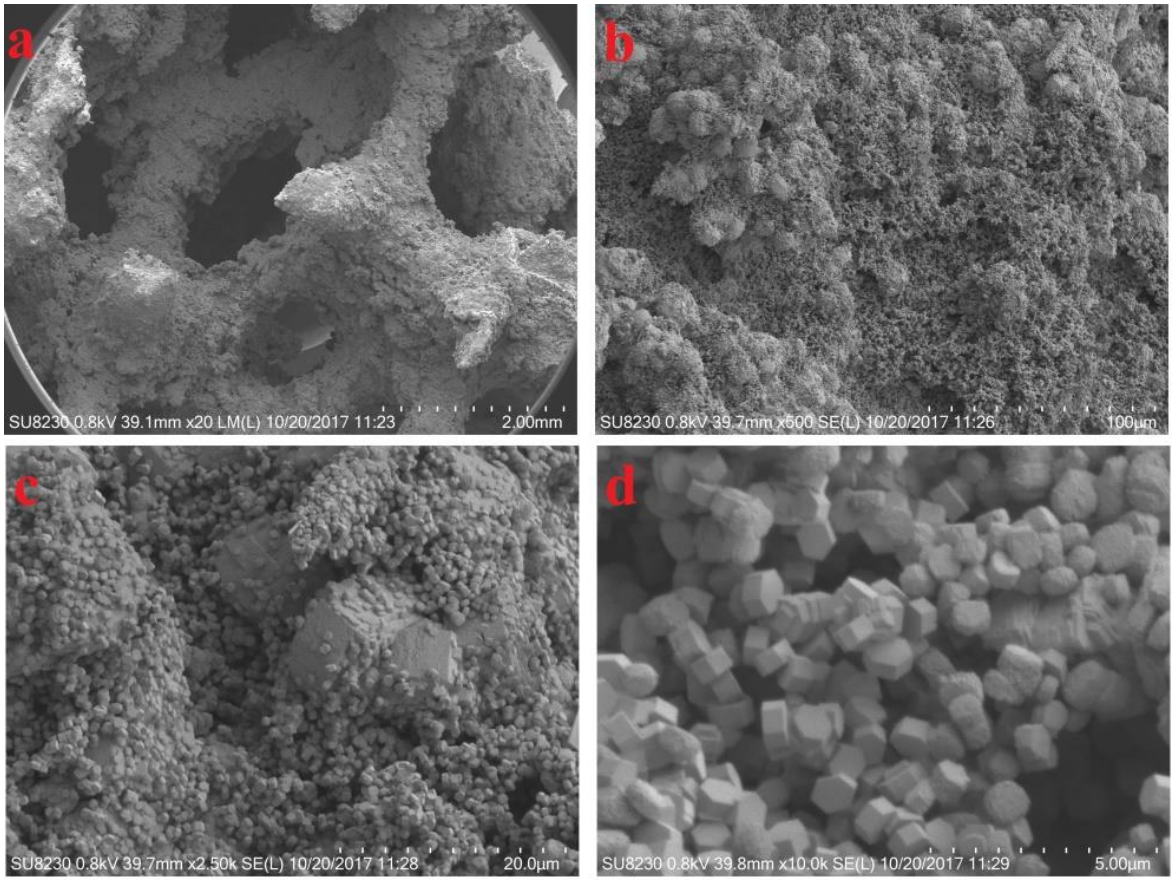

Figure 19 SEM micrographs of ZSM-5/SiC foam composites of different magnifications: 20 (a), 500 (b), 2500 (c), and 10000 (d).

5.3.2. Effect of Catalysts Placement

Three different configurations, including *in-situ*, *ex-situ* with randomly packed bed, and *ex-situ* with composite catalysts, along with two control experiments, either with bare SiC foam support, or without any catalysts, were compared at the same C/B ratio of 1/4. Fig 20 (a) shows the product yields under different MAP conditions. The addition of a bare SiC foam in the catalytic bed led to a lower bio-oil yield (36.5%) and correspondingly a higher gas yield (35.2%) compared with 40.2% and 31.4%, respectively, for the control experiment with no catalysts. This could be due to the secondary cracking reactions of

the pyrolytic vapors within the hot SiC foam matrix. The *ex-situ* composite catalyst configuration produced a product yield distribution which is very close to that from the bare SiC foam control, indicating a minimal negative effect of the catalyst coatings on the product yield distribution. In contrast, the *ex-situ* packed bed configuration delivered the lowest yield of bio-oil, 32.5%, and the highest gas yield, 41.5%, among the five conditions. The decreased bio-oil yield and increased gas yield compared with the *ex-situ* composite catalyst configuration could attribute to the enhanced secondary cracking reactions of the primary pyrolytic vapors, which stem from the higher pressure drop and thus longer residence time in the randomly packed catalyst bed. Lacroix et al. compared the pressure drops through foam (pore size: ϕ 1.8 mm) and spherical particles (d 1.45 mm) fixed bed (Lacroix, Nguyen et al. 2007). At a gas velocity of 1m/s, pressure drop per length recorded on the packed bed was about twice that of the foam, and the difference increased with increasing gas velocity. In our case, the 60 mesh ZSM-5 powders in the packed bed are smaller than 0.25 mm; therefore, the pressure drop difference relative to the foam is expected to be even greater. In addition, the coking yield of the packed bed and composite catalyst bed were determined to be 3.4% and 2.0%, respectively, which indicates that packed bed configuration is more prone to catalyst deactivation than the composite catalyst bed.

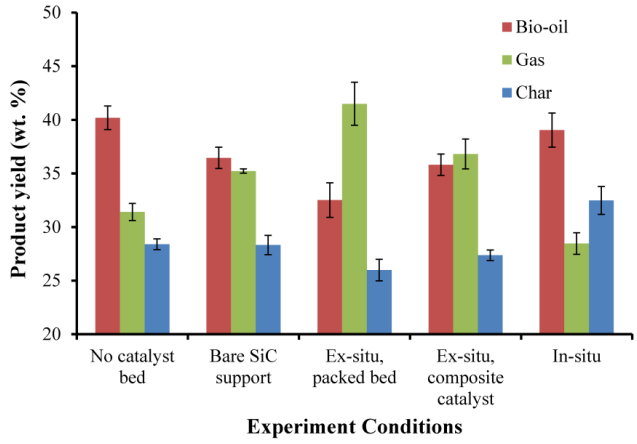

(a)

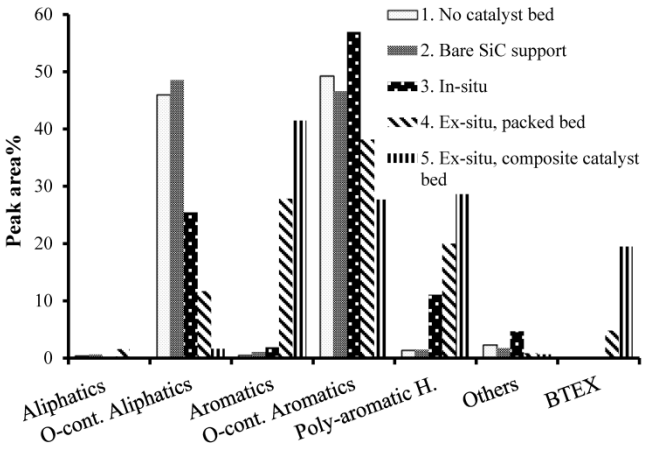

(b)

Figure 20 Product yields (a) and bio-oil compositions (b) under different MAP conditions

The *in-situ* addition of catalysts produced the highest yield of solid residue of 32.5% in contrast to an almost constant char yield around 28% in the other configurations, while the bio-oil yield, 39%, is comparable to that in the control experiment without catalysts. The higher solid residue yield agrees with several other studies (Wang, Johnston et al. 2014, Hu, Xiao et al. 2017), and it possibly arises from the coking on the catalysts, which

was difficult to separate from the char in both lab-scale and pilot scale *in-situ* configurations(Paasikallio, Lindfors et al. 2014, Yildiz, Ronsse et al. 2016). To better understand the impact of two different configurations on catalysts recycling, spent catalysts from both the *in-situ* and *ex-situ* packed bed configurations were regenerated and the mineral contents were determined using ICP-OES. The results are summarized in Table 9. Dramatic content increases were observed for all selected minerals except Al in the regenerated catalysts from *in-situ* experiments compared with the fresh catalysts. Specifically, the contents of Si and K, the two most abundant inorganic elements in corn stover, increased over 1 wt. % after only one recycle. Mineral depositions largely come from ash that remained after combustion of the coked catalysts and the char, and they may continue to accumulate during extended reaction and regeneration cycles to such an extent that results in irreversible deactivation of the catalysts (Duduković, Larachi et al. 2002, Pangarkar, Schildhauer et al. 2008, Gascon, Van Ommen et al. 2015). It is worthwhile to note that slight increases in some mineral contents were also observed for the regenerated catalysts in *ex-situ* packed beds. The metals may have been carried into the *ex-situ* packed bed by either solid particles or vapor. Nevertheless, catalyst contamination due to mineral deposition is expected to be more serious for the *in-situ* configuration.

Table 9 Contents of selected elements in fresh and regenerated (Re.) ZSM-5 samples

Sample	Si wt. %	Al wt. %	Ca ppm	Cu ppm	Fe ppm	K ppm	Mg ppm	Na ppm	P ppm	S ppm
Fresh ZSM-5	44.5	1.3	0	0	0	0	0	122	0	0
Re. *ex-situ* ZSM-5	44.5	1.3	31	0	0	57	11	135	0	12
Re. *in-situ* ZSM-5	45.7	1.2	1090	10	636	11281	1030	209	566	260

Chemical compositions of bio-oil organic phases were analyzed using GC/MS. 60 major peaks were selected for analysis and the identified components were categorized into six groups, namely, aliphatic hydrocarbons, aromatic hydrocarbons, oxygen-containing aliphatic compounds, oxygen-containing aromatic compounds, polycyclic aromatic compounds (PAHs), and others. The results are summarized in Fig. 20(b). Bio-oil compositions for the two controls are very similar, comprising of ca. 47% oxygen-containing aliphatics and ca. 48% oxygen-containing aromatics. The first group mainly includes furan derivatives and acids, such as furfural, furan-3-methanol, butyrolactone, and propionic acid, etc., which are known as primary decomposition products from cellulosic materials (Carlson, Vispute et al. 2008, Carlson, Jae et al. 2009). The second group mainly includes phenolic derivatives such as phenol, benzofuran, 2-methoxy-4-vinylphenol, and 4-ethylphenol, etc., which are primary products derived from lignin (Bu, Lei et al. 2011). When ZSM-5 was added *in-situ*, oxygen-containing aliphatics proportions almost halved, and PAH content significantly increased to 11% while negligible aromatics were produced. Interestingly, this result is very similar to that from an *ex-situ* catalysis experiment of corn stover where a lower pyrolysis temperature, 450^{o}C, was used (Liu, Zhang et al. 2017). This is probably because the addition of catalysts in the biomass increases thermal resistance and thus leads to a lower heating rate than that which could be achieved with mere biomass under the same experimental conditions. For a large-scale pyrolysis system, this means that additional heat or a higher reaction temperature might be needed to achieve the same heating rate in an *in-situ* design compared to the *ex-situ design*. Other possible reasons for the poorer bio-oil quality with the *in-situ* configuration, include the surface blockage due to char buildup

(Elordi, Olazar et al. 2011) and more rapid catalyst deactivation due to coking (Iisa, French et al. 2016). This is also why, usually much higher catalyst/biomass ratios are used in other *in-situ* CFP studies (Carlson, Cheng et al. 2011, Wang, Johnston et al. 2014, Gamliel, Du et al. 2015).

Compared with the *in-situ* configuration, both *ex-situ* experiments delivered bio-oils of higher quality in terms of considerable amounts of aromatics and significantly lower contents of oxygen-containing aliphatics. In particular, the composite catalyst bed configuration produced the best bio-oil, which contained 41.5% aromatics and only 1.6% oxygen-containing aliphatics in contrast to 27.8% and 11.7%, respectively, for the randomly packed bed configuration. This indicates a significantly higher selectivity towards the production of aromatics with ZSM-5 in the composite catalyst bed. In addition, bio-oils from the composite catalyst configuration contained considerable amounts of valuable mono-aromatic petrochemicals, including *p*-xylene (13.2%), *o*-xylene (2.5%), toluene (2.5%), and ethylbenzene (1.1%), which added up to a total of ~19% BTEX, as opposed to 4.8% from the packed-bed bio-oil. The differences in the bio-oil quality may be attributed to another fundamental advantage of the composite catalyst over the randomly packed bed of ZSM-5 powders: the dispersed catalysts in the form of thin layers are more accessible to the pyrolytic vapors and thus can be more effective than those in randomly packed beds. Ivanova et al. (Ivanova, Louis et al. 2007) and Jiao et al. (Jiao, Yang et al. 2015) both synthesized ZSM-5/SiC composite catalysts and compared them with a randomly packed bed of ZSM-5 for methanol-to-olefins conversion. Their results showed that the composite catalysts were significantly more stable than the packed beds, and Jiao et al. (Jiao, Yang et al. 2015) attributed it to reduced

internal diffusion limitations within the composite catalysts, which allows easier escape of intermediate products, and thus alleviates deactivation due to coking.

5.3.3. Effect of Catalyst to Biomass Ratios (C/B)

In order to investigate the effect of C/B ratios on the catalytic performance of the composite catalyst, biomass input amounts were varied to obtain a series of C/B ratios from 0 to 1/2. It can be seen from Fig. 21(a) that while the char yield remained almost constant, bio-oil yield decreased from 40.2% to 33.5% and gas yield increased from 31.4% to 39.7% as the C/B ratio increased from 0 to 1/2. This trend agrees with many other CFP studies, either *in-situ* or *ex-situ* (Carlson, Cheng et al. 2011, Compton, Jackson et al. 2011, Wang, Johnston et al. 2014). The lower bio-oil yield together with the higher gas yield correlates to an enhanced catalytic conversion by ZSM-5. As primary pyrolytic vapor enters the pore structure of ZSM-5, oxygen is removed in the forms of CO, CO_2, and H_2O, through decarbonylation, decarboxylation, and dehydration reactions, which ultimately lead to the higher gas yield and lower bio-oil yield (Carlson, Jae et al. 2009). This is also supported by the bio-oil composition results shown in Fig. 21(b). With the increase of C/B from 0 to 1/2, proportions of oxygenates, mainly primary decomposition products, generally decreased while those of hydrocarbons predictably increased, which suggests an enhanced oxygen removal effect for the bio-oil at higher C/B ratios. Overall, the loss of the bio-oil yield can be compensated for, by the improved bio-oil quality at high C/B ratios. It is worthwhile to point out that, while the coke yield increased from 1.6% to 2.3% with the increasing C/B ratios, the absolute coke amount on the given composite catalyst bed decreased with increasing C/B ratios. In other words, coke as an undesirable product from ZSM-5 catalytic reactions gradually accumulates in the

composite packed bed as the pyrolysis reaction proceeds. Coke blocks the active sites within the pore structure of ZSM-5 and leads to rapid deactivation of the catalysts, as suggested by the poorer bio-oil quality at lower C/B ratios. This is one of the most critical issues facing application of ZSM-5 in CFP processes (Mullen, Boateng et al. 2011).

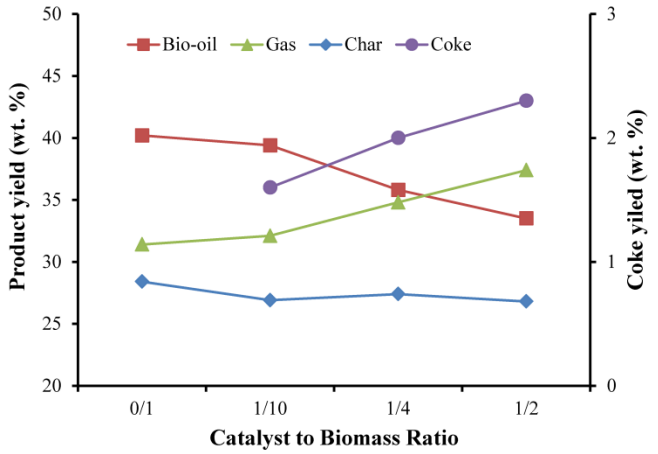

(a)

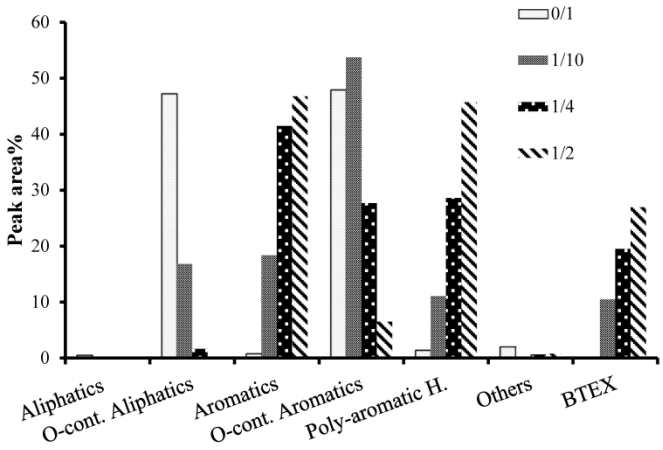

(b)

Figure 21 Product yields (a) and bio-oil compositions (b) under different catalyst to biomass ratios

5.3.4. Catalyst Deactivation

In order to further study the deactivation behavior of the *ex-situ* composite catalyst over time, a series of five consecutive experiments were conducted as follows: one run of experiment at a C/B ratio of 1/2, analyzing the products, adding the second batch of biomass of the same amount for the second run while keeping the same catalysts; repeating the cycles for five runs. In order to maintain the oxygen-free environment during the consecutive runs, only bio-oil was able to be collected and analyzed after each run. The average char yield and coke yield after five runs were determined to be 26.4% and 2.3% respectively. The bio-oil yields and compositions are shown in Fig. 22. It can be seen from Fig. 22(a) that as the catalysts were used consecutively, bio-oil yield from each run increased from 31.1% to 41.6%. Again, this is because the catalytic activity of ZSM-5 is gradually lost during the process due to coking. Less oxygen was removed from the bio-oil as the catalytic activity decreased and therefore, the bio-oil yields increased. This loss of catalytic activity can be further revealed by the change of bio-oil compositions over time as shown in Fig. 22(b). Specifically, the proportion of aromatics dramatically decreased from 46.8% to 9.7% after only three runs, and it further decreased to only 1.7% after 5 runs. This means the selectivity to aromatics production is almost completely lost for the *ex-situ* composite catalyst after 5 runs, corresponding to an overall C/B of 1/10, at which point the catalyst can be deemed as completely deactivated. Nevertheless, deactivation of ZSM-5 in the *in-situ* pyrolysis configuration is usually much more rapid. For example, Iisa et al. reported in a fluidized bed CFP study that ZSM-5 was deemed deactivated at a C/B of 1/1.5 (Iisa, French et al. 2016), Carlson et al. reported that catalytic activity of HZSM-5 began to decrease due to coke formation after

40 min of operation at a weight hourly space velocity (WHSV) of 0.1, corresponding to a C/B of 15/1. In contrast, the ex-situ composite catalyst deactivates at a much lower C/B ratio, meaning that the same amount of catalyst in *ex-situ* composite catalyst configuration can handle much more biomass than in the *in-situ* configuration. In other words, the stability of the ZSM-5 catalyst in a CFP process can be significantly improved with the *ex-situ* composite catalyst configuration. Direct comparison between these two configurations will be conducted in the future, based on a pilot-scale continuous MAP system recently developed in our lab.

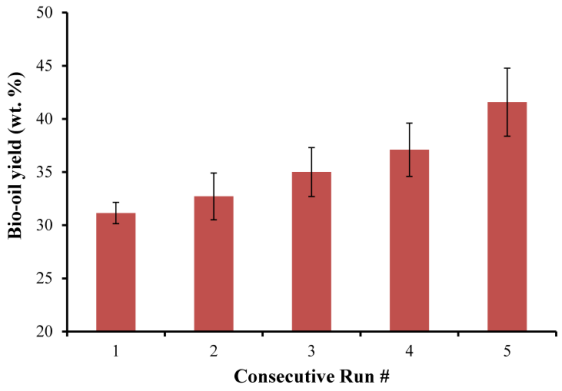

(a)

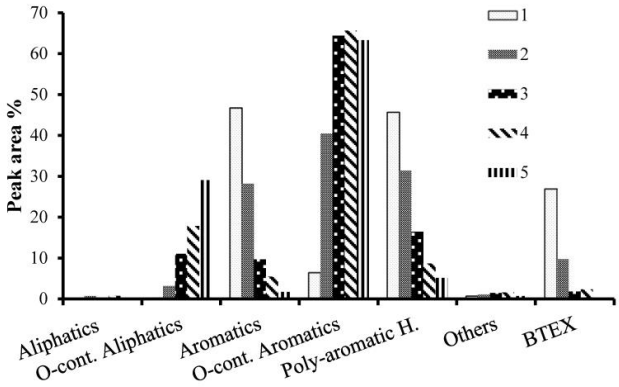

(b)

Figure 22 Bio-oil yields (a) and composition (b) in consecutive experiment runs.

5.3.5. Catalyst Regeneration and Recycling

Due to the rapid deactivation by coking, it is necessary to regenerate and recycle the coked catalysts to reduce the operational cost of the CFP process. In order to study the stability of the catalysts during repeated reaction-regeneration cycles, spent composite catalysts were regenerated by calcination in air at 500^{o}C for 8 h, and the pyrolysis experiments were repeated 7 times at a constant C/B of 1/4. ZSM-5 coating weight slightly decreased from 3.887 g to 3.763 g after 7 cycles, which indicates a strong adherence of the coating to the support. The weight loss is possibly caused by attrition during handling of the composite catalysts. Fig. 23(a) and 23(b) summarize the products yields and bio-oil compositions, respectively, of the 7 cycles. It can be seen that, overall both yields and bio-oil compositions remained stable. There are a slight increase of bio-oil yields (from 35.4% to 37.0%) and a slight decrease of aromatics proportion in the bio-oil (from 39.8% to 35.2%), which might indicate a slight loss in the catalytic activity of the composite catalysts. No significant difference (ANOVA, $p<0.05$) was observed for the 7 coke yields with an average of 2.1 wt.%, and therefore the data were not shown in Figure 23. Vitolo et al. also studied the stability of ZSM-5 in a packed bed configuration, subject to repeated reaction-regeneration cycles, and they reported an irreversible loss of catalytic activity after only five cycles(Vitolo, Bresci et al. 2001). They attributed the irreversible deactivation to the loss of acidic sites, which is believed to be caused by localized overheating during the coke combustion process (Shao, Zhang et al. 2018). In contrast, the hot spot or localized overheating issue can be alleviated in the ZSM-5/SiC composite catalyst because the SiC foam support is an excellent heat conducting material

and can rapidly take away the reaction heat generated from coke combustion. This may partially explain its stability over extended reaction-regeneration cycles.

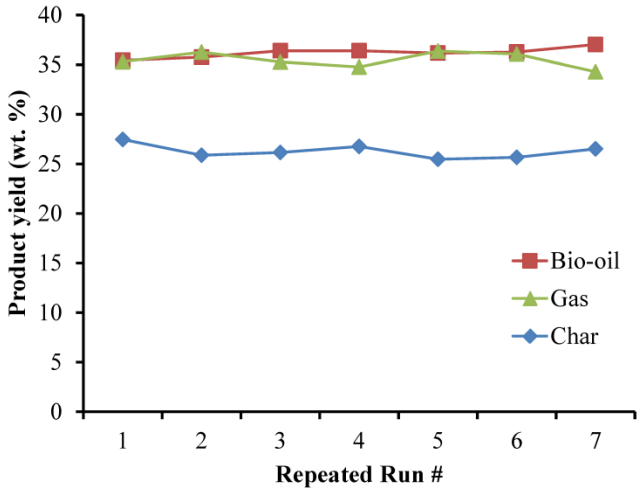

(a)

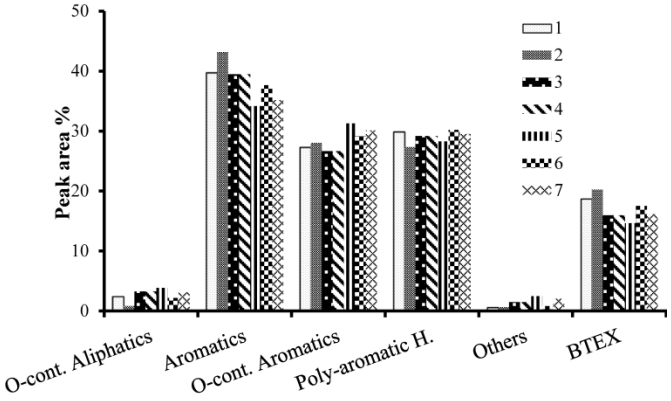

(b)

Figure 23 Product yields (a) and compositions (b) in seven reaction-regeneration cycles.

The specific surface area of the regenerated catalyst was determined to be 75.3 g/m^2, slightly lower than that of the fresh catalyst, 76.7 g/m^2, indicating a well preserved porosity and the removal of coke products from the porous structures after regeneration.

The decrease may come from the slight loss of ZSM-5 crystals from the composite catalyst. Additional SEM micrographs and XRD patterns of the regenerated composite catalysts which are included in the supplementary data show no significant changes compared with fresh ones, suggesting the crystal structures have been well-preserved after seven reaction-regeneration cycles.

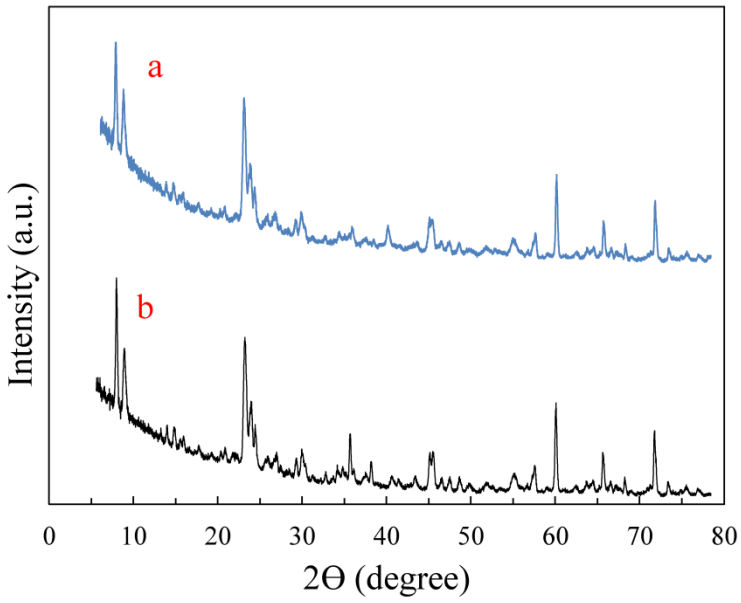

Figure 24 XRD patterns of the regenerated (a) and the fresh (b) ZSM-5/SiC catalysts

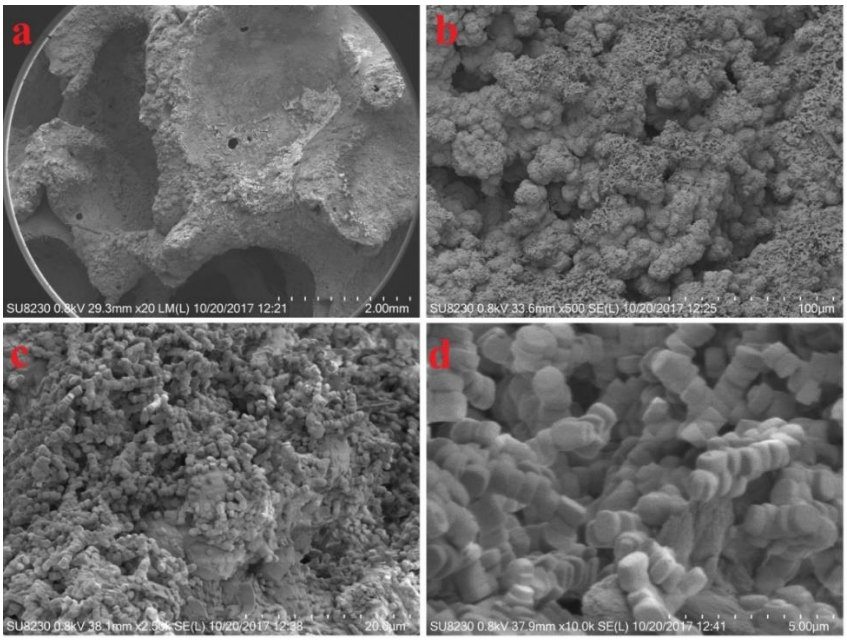

Figure 25 SEM micrographs of regenerated ZSM-5/SiC foam composite catalysts under different magnifications: 20 (a), 500 (b), 2500 (c), and 10000 (d).

5.4. Summary

In order to address a series of issues facing the application of catalysts in scaled-up catalytic fast pyrolysis systems, a composite catalyst of ZSM-5 coatings on SiC foam supports was developed, using a hydrothermal method. The composite catalyst was then tested in a microwave-assisted pyrolysis system for *ex-situ* catalytic upgrading of the pyrolytic vapors. Compared with *in-situ* and *ex-situ* randomly packed bed configurations, *ex-situ* composite catalyst significantly improved the bio-oil quality while maintaining its yield, possibly because its structure reduced the pressure drop and enhanced the mass transfer within the catalytic bed. Experiments with varied catalyst to biomass ratios (C/B) showed that a higher C/B ratio can improve the quality of bio-oil at the cost of its yield. In addition, the composite catalyst was found to become completely deactivated at a C/B of 1/10, which is lower than other configurations found in literature. This means the

composite catalyst configuration can treat more biomass than other configurations, given the same amount of catalysts. Furthermore, the composite catalysts could be repeatedly regenerated and reused, and results showed that its material properties and catalytic activity was well preserved even after seven reaction-regeneration cycles. These results suggest that the ZSM-5/SiC composite catalyst is effective, stable, and also offers the advantages of reduced pressure drop, and enhanced heat and mass transfer, compared to the randomly packed bed. Therefore, it serves as a promising candidate for catalysts applied in large scale *ex-situ* CFP operations.

Chapter 6 Conclusions and Future Remarks

6.1. Conclusions

With the goal of improving the feasibility and scalability of the microwave-assisted pyrolysis process, a novel system of continuous microwave-assisted pyrolysis (CMAP) featuring a mixing SiC ball bed was developed and tested for fuel production from biomass and plastic wastes. Energy balance analysis and comparisons with data reported in literature showed that the CMAP system had a higher energy efficiency and required lower processing temperatures than conventional fluidized bed reactors, to obtain similar products. Therefore, the CMAP system offers a very promising design for future industrial applications of energy recovery from biomass and plastic wastes. Plastic wastes, especially polyolefin base plastics, have much higher heating values, and relatively simpler compositions, compared to biomass, thus making them a more desirable feedstock to produce high quality fuels, in an energy-efficient manner. The application of catalysts in the CMAP process has shown a significant impact on product yields and composition, but it also suffers from rapid deactivation, and thus calls for further research. In order to address a series of issues facing the application of catalysts in scaled-up pyrolysis systems, a structured catalyst of SiC foam, used to support ZSM-5 zeolite catalyst, was developed and tested for *ex-situ* catalytic upgrading of biomass pyrolytic vapors. Results suggest that the structured catalyst is more active and stable, compared to a randomly packed bed of catalysts, while also having the advantages of reduced pressure drop, and enhanced heat and mass transfer. Therefore, this structured

catalyst serves as a promising candidate for catalysts applied in large-scale pyrolysis operations. More specific conclusions from each chapter are summarized below:

Chapter 3: A continuous microwave assisted pyrolysis (CMAP) prototype system was developed and tested for syngas production from wood pellets. This system featured a silicon carbide ball reactor bed and a mixing mechanism, enabling rapid and uniform heating, and continuous operation of the process. Higher processing temperatures promoted the production of gas products, especially CO and H_2, and lowered the yields of tar, water, and char. Specifically, at a temperature of 800^oC, producer gas with a high energy content of 18.0 MJ/ Nm^3, and a high syngas (H_2+CO) content of 67 vol% was obtained at a gas yield of 72.2 wt. %, or 0.80 Nm^3/kg d.a.f. wood pellets. Downstream condensation and physical adsorption lowered the tar concentration from 7.83 g/Nm^3 at the exit of the pyrolysis reactor, to below the detection limit, at the end of the process. The higher gas yields and improved quality from this process, compared to pyrolysis with conventional heating at similar temperature levels, could be attributed to two factors: 1) the heterogenous reactions between primary tar and biochar enhanced by microwave irradiation, and 2) the absence of a carrier gas, such as N_2 in the process that would have otherwise diluted the producer gas. In terms of energy efficiency, a cold gas efficiency of 73.3% was achieved at 800^oC, which comes at the cost of 7.2 MJ, or 2 kWh of electrical energy per kg of wood pellets. Further measures to improve the energy efficiency could potentially reduce the electrical consumption to 3.45 MJ/kg of wood, enabling a net electricity production from the process.

Chapter 4: Pyrolysis of different types of plastic wastes was conducted in the CMAP system, for fuel production. At 560^oC, the highest liquid product yield, 47.4%, was

obtained for thermal pyrolysis of HDPE, together with 24.5% wax product. Higher pyrolysis temperatures promoted the cracking of the wax and production of lighter and more thermodynamically stable hydrocarbons such as C1-C4 gases and aromatic hydrocarbons. Based on product yields and compositions, resistance to thermal degradation of three different plastic feedstocks rank as follows: HDPE, PP, and PP with fillers (the mineral filler, i.e. talc). The filler mineral, talc, acted as a catalyst and showed noticeable cracking activity. Under a temperature of 620^{o}C, incorporating ZSM-5 catalysts in a secondary catalyst bed, enabled the elimination of the wax product, resulting in an increase of liquid yield to 48.9%, and these liquid products contained considerably higher contents of gasoline-range aromatics (45.0%) and isomerized aliphatics (24.6%). However, ZSM-5 catalysts also showed a tendency for rapid deactivation, with loss of its activity at a feedstock/catalyst ratio of 5. Energy balance analysis of the process showed that **5.0 MJ of electrical energy** was required to process 1kg of HDPE with the CMAP system, giving a total energy efficiency as high as 89.6%. Furthermore, **6.1 MJ of electrical energy** could potentially be generated from the gas products alone, making the process energy self-sufficient.

Chapter 5: A structured catalyst of ZSM-5 coatings on a SiC foam support was developed for catalyst applications, for future, scaled-up pyrolysis systems. A hydrothermal synthesis method was used to synthesize the catalysts, which resulted in a thin layer of ZSM-5 crystals firmly attached to the structure of a microporous SiC foam material. The structured catalysts were studied and compared with other catalytic reactor configurations, for catalytic upgrading of biomass pyrolytic vapors in a lab-scale microwave-assisted pyrolysis system. Comparing *in-situ* to *ex-situ* randomly packed bed

configurations, the *ex-situ* structured catalyst significantly improved the bio-oil quality while maintaining the liquid yield. A higher catalyst-to-biomass ratio (C/B) was shown to improve the quality of bio-oil, but at the cost of its yield. The structured catalyst was found to become completely deactivated at a C/B of 1/10, which is lower than other configurations found in literature, meaning the structured catalyst can treat more biomass than other configurations, given the same amount of catalyst. Furthermore, the composite catalyst (ZSM-5 on SiC foam) could be repeatedly regenerated and reused; results showed that its material properties and catalytic activity was well preserved after seven reaction-regeneration cycles. These results suggest that the ZSM-5/SiC structured catalyst is as a promising candidate for catalytic applications in large scale pyrolysis processes.

6.2.Future Work

Energy-efficient and environmentally friendly tar removal remains a key technological barrier to industrial scale biomass gasification and pyrolysis technologies for syngas production. This challenge could potentially be solved by application of catalysts. Nickel (Ni) based catalysts are known to be effective in catalytic cracking of tars, but it will take further research efforts to improve the performance of these Ni catalysts to a satisfactory level for industrial applications. The “recipe” for Ni catalysts could be optimized by improving three essential components of a catalyst: catalyst support, promoter, and Ni loading methods. The optimized recipe could be further combined with ceramic foam materials to obtain a structured catalyst that could be tested on the CMAP system.

Finding a cheap and active catalyst for plastic pyrolysis is also an important research topic. While conventional zeolite catalysts such as ZSM-5 are very active in cracking, isomerization, and aromatization reactions, it is also clear that ZSM-5 has several

disadvantages, including rapid deactivation, and relatively high cost. In addition, the high gas yield and high aromatics content in the liquid product make the process undesirable to produce higher value products such as naphtha, which is an intermediate feedstock to produce plastics, and is of more interest to the petrochemical industry. Therefore, further studies are required to select and develop catalysts of higher activity and stability, lower cost, and more flexibility in selectively producing target products.

Due to the inevitable deactivation of catalysts in the plastic pyrolysis process, catalyst regeneration is a critical factor to the economics of this process. Conventionally, these deactivated catalysts could be partially regenerated by burning off coke deposits at high temperatures, e.g. 500^{o}C. Yet the high temperature also leads to irreversible structure damage to the zeolite materials, and therefore the catalysts would eventually become irreversibly deactivated after several reaction-regeneration cycles. Therefore, it may be necessary to develop a regeneration process that can operate at lower temperatures. Non-thermal plasma seems to be a very interesting potential solution, as it has been shown to be a highly oxidative process under near-ambient temperatures. It is recommended that future studies be conducted to investigate the feasibility of regenerating spent catalysts under near-ambient temperatures to improve the long-term stability of these catalysts.

Bibliography

1. Aboulkas, A. and A. El Bouadili (2010). "Thermal degradation behaviors of polyethylene and polypropylene. Part I: Pyrolysis kinetics and mechanisms." Energy Conversion and Management **51**(7): 1363-1369.
2. Alamia, A., et al. (2017). "Performance of large-scale biomass gasifiers in a biorefinery, a state-of-the-art reference." International Journal of Energy Research **41**(14): 2001-2019.
3. Alvarez, J., et al. (2017). "Evaluation of the properties of tyre pyrolysis oils obtained in a conical spouted bed reactor." Energy **128**: 463-474.
4. Arabiourrutia, M., et al. (2012). "Characterization of the waxes obtained by the pyrolysis of polyolefin plastics in a conical spouted bed reactor." Journal of Analytical and Applied Pyrolysis **94**: 230-237.
5. Arena, U. and M. L. Mastellone (2000). "Defluidization phenomena during the pyrolysis of two plastic wastes." Chemical Engineering Science **55**(15): 2849-2860.
6. Arpia, A. A., et al. (2020). "Sustainable biofuel and bioenergy production from biomass waste residues using microwave-assisted heating: A comprehensive review." Chemical Engineering Journal: 126233.
7. Asadullah, M. (2014). "Barriers of commercial power generation using biomass gasification gas: A review." Renewable and Sustainable Energy Reviews **29**: 201-215.
8. Asadullah, M. (2014). "Biomass gasification gas cleaning for downstream applications: A comparative critical review." Renewable and Sustainable Energy Reviews **40**: 118-132.
9. Asomaning, J., et al. (2018). "Recent developments in microwave-assisted thermal conversion of biomass for fuels and chemicals." Renewable and Sustainable Energy Reviews **92**: 642-657.
10. Atuonwu, J. C. and S. A. Tassou (2018). "Quality assurance in microwave food processing and the enabling potentials of solid-state power generators: A review." Journal of food engineering **234**: 1-15.
11. Auxilio, A. R., et al. (2017). "An experimental study on thermo-catalytic pyrolysis of plastic waste using a continuous pyrolyser." Waste Management **67**: 143-154.
12. Bagri, R. and P. T. Williams (2002). "Catalytic pyrolysis of polyethylene." Journal of Analytical and Applied Pyrolysis **63**(1): 29-41.
13. Benedikt, F., et al. (2018). "Fuel flexible gasification with an advanced 100 kW dual fluidized bed steam gasification pilot plant." Energy **164**: 329-343.
14. Beneroso, D., et al. (2013). "Microwave pyrolysis of microalgae for high syngas production." Bioresource Technology **144**: 240-246.
15. Beneroso, D., et al. (2016). "Microwave-induced cracking of pyrolytic tars coupled to microwave pyrolysis for syngas production." Bioresource Technology **218**: 687-691.

16. Beneroso, D., et al. (2017). "Microwave pyrolysis of biomass for bio-oil production: Scalable processing concepts." Chemical Engineering Journal **316**: 481-498.

17. Boateng, A. A., et al. (2007). "Bench-scale fluidized-bed pyrolysis of switchgrass for bio-oil production." Industrial & Engineering Chemistry Research **46**(7): 1891-1897.

18. Borges, F. C., et al. (2014). "Fast microwave assisted pyrolysis of biomass using microwave absorbent." Bioresource Technology **156**: 267-274.

19. Brage, C., et al. (2000). "Tar evolution profiles obtained from gasification of biomass and coal." Biomass and bioenergy **18**(1): 87-91.

20. Bridgwater, A. (1995). "The technical and economic feasibility of biomass gasification for power generation." Fuel **74**(5): 631-653.

21. Bridgwater, A. V. (2012). "Review of fast pyrolysis of biomass and product upgrading." Biomass and bioenergy **38**: 68-94.

22. Briesemeister, L., et al. (2017). "Air-blown entrained-flow gasification of biomass: influence of operating conditions on tar generation." Energy & fuels **31**(10): 10924-10932.

23. Bu, Q., et al. (2011). "Phenol and phenolics from lignocellulosic biomass by catalytic microwave pyrolysis." Bioresource technology **102**(13): 7004-7007.

24. Carlson, T. R., et al. (2011). "Production of green aromatics and olefins by catalytic fast pyrolysis of wood sawdust." Energy & Environmental Science **4**(1): 145-161.

25. Carlson, T. R., et al. (2009). "Mechanistic Insights from Isotopic Studies of Glucose Conversion to Aromatics Over ZSM-5." ChemCatChem **1**(1): 107-110.

26. Carlson, T. R., et al. (2009). "Aromatic production from catalytic fast pyrolysis of biomass-derived feedstocks." Topics in Catalysis **52**(3): 241.

27. Carlson, T. R., et al. (2008). "Green gasoline by catalytic fast pyrolysis of solid biomass derived compounds." ChemSusChem **1**(5): 397-400.

28. Carpenter, D. L., et al. (2010). "Pilot-scale gasification of corn stover, switchgrass, wheat straw, and wood: 1. Parametric study and comparison with literature." Industrial & Engineering Chemistry Research **49**(4): 1859-1871.

29. Castello, D., et al. (2018). "Continuous hydrothermal liquefaction of biomass: A critical review." Energies **11**(11): 3165.

30. Chandel, A. K., et al. (2018). "The path forward for lignocellulose biorefineries: bottlenecks, solutions, and perspective on commercialization." Bioresource Technology **264**: 370-381.

31. Cheah, S., et al. (2016). "Effects of thermal pretreatment and catalyst on biomass gasification efficiency and syngas composition." Green Chemistry **18**(23): 6291-6304.

32. Chen, G., et al. (2018). "Investigation on model compound of biomass gasification tar cracking in microwave furnace: Comparative research." Applied Energy **217**: 249-257.

33. Cherubini, F. (2010). "The biorefinery concept: using biomass instead of oil for producing energy and chemicals." Energy conversion and management **51**(7): 1412-1421.

34. Choi, S., et al. (2015). "Biorefineries for the production of top building block chemicals and their derivatives." Metabolic engineering **28**: 223-239.

35. Ciambelli, P., et al. (2010). "Comparison of ceramic honeycomb monolith and foam as Ni catalyst carrier for methane autothermal reforming." Catalysis Today **155**(1-2): 92-100.

36. Commandré, J.-M., et al. (2011). "Pyrolysis of wood at high temperature: the influence of experimental parameters on gaseous products." Fuel Processing Technology **92**(5): 837-844.

37. Compton, D. L., et al. (2011). "Catalytic pyrolysis of oak via pyroprobe and bench scale, packed bed pyrolysis reactors." Journal of Analytical and Applied Pyrolysis **90**(2): 174-181.

38. Corella, J., et al. (2007). "A review on dual fluidized-bed biomass gasifiers." Industrial & Engineering Chemistry Research **46**(21): 6831-6839.

39. Czernik, S. and A. Bridgwater (2004). "Overview of applications of biomass fast pyrolysis oil." Energy & fuels **18**(2): 590-598.

40. Daugaard, D. E. and R. C. Brown (2003). "Enthalpy for pyrolysis for several types of biomass." Energy & fuels **17**(4): 934-939.

41. De Bhowmick, G., et al. (2018). "Lignocellulosic biorefinery as a model for sustainable development of biofuels and value added products." Bioresource Technology **247**: 1144-1154.

42. de Rezende Pinho, A., et al. (2017). "Fast pyrolysis oil from pinewood chips co-processing with vacuum gas oil in an FCC unit for second generation fuel production." Fuel **188**: 462-473.

43. De, S., et al. (2015). "Hydrodeoxygenation processes: Advances on catalytic transformations of biomass-derived platform chemicals into hydrocarbon fuels." Bioresource Technology **178**: 108-118.

44. De Smet, M. (2016). "The New Plastics Economy—Rethinking the Future of Plastics & Catalysing Action." Cowes, Isle of Wight, UK: Ellen MacArthur Foundation.

45. Devi, L., et al. (2003). "A review of the primary measures for tar elimination in biomass gasification processes." Biomass and bioenergy **24**(2): 125-140.

46. Di Blasi, C., et al. (1999). "Product distribution from pyrolysis of wood and agricultural residues." Industrial & Engineering Chemistry Research **38**(6): 2216-2224.

47. Ding, K., et al. (2019). "Catalytic microwave-assisted pyrolysis of plastic waste over NiO and HY for gasoline-range hydrocarbons production." Energy Conversion and Management **196**: 1316-1325.

48. Domínguez, A., et al. (2008). "Bio-syngas production with low concentrations of CO2 and CH4 from microwave-induced pyrolysis of wet and dried sewage sludge." Chemosphere **70**(3): 397-403.

49. Dominguez, A., et al. (2007). "Conventional and microwave induced pyrolysis of coffee hulls for the production of a hydrogen rich fuel gas." Journal of Analytical and Applied Pyrolysis **79**(1-2): 128-135.

50. Du, S., et al. (2014). "Catalytic pyrolysis of miscanthus× giganteus in a spouted bed reactor." Bioresource technology **169**: 188-197.

51. Dudley, G. B., et al. (2015). "On the existence of and mechanism for microwave-specific reaction rate enhancement." Chemical science **6**(4): 2144-2152.

52. Duduković, M. P., et al. (2002). "Multiphase catalytic reactors: a perspective on current knowledge and future trends." Catalysis reviews **44**(1): 123-246.

53. Dufour, A., et al. (2009). "Synthesis gas production by biomass pyrolysis: Effect of reactor temperature on product distribution." International Journal of Hydrogen Energy **34**(4): 1726-1734.

54. Duong-Viet, C., et al. (2016). "Silicon carbide foam as a porous support platform for catalytic applications." New Journal of Chemistry **40**(5): 4285-4299.

55. Efika, C. E., et al. (2012). "Syngas production from pyrolysis–catalytic steam reforming of waste biomass in a continuous screw kiln reactor." Journal of Analytical and Applied Pyrolysis **95**: 87-94.

56. Eigenberger, G. and W. Ruppel (2000). "Catalytic Fixed-Bed Reactors." Ullmann's Encyclopedia of Industrial Chemistry.

57. Ellison, C., et al. (2017). "Dielectric properties of biomass/biochar mixtures at microwave frequencies." Energies **10**(4): 502.

58. Elordi, G., et al. (2009). "Catalytic pyrolysis of HDPE in continuous mode over zeolite catalysts in a conical spouted bed reactor." Journal of Analytical and Applied Pyrolysis **85**(1-2): 345-351.

59. Elordi, G., et al. (2011). "Product yields and compositions in the continuous pyrolysis of high-density polyethylene in a conical spouted bed reactor." Industrial & Engineering Chemistry Research **50**(11): 6650-6659.

60. Elordi, G., et al. (2011). "Role of pore structure in the deactivation of zeolites (HZSM-5, Hβ and HY) by coke in the pyrolysis of polyethylene in a conical spouted bed reactor." Applied Catalysis B: Environmental **102**(1-2): 224-231.

61. Enestam, S., et al. (2013). "Are NaCl and KCl equally corrosive on superheater materials of steam boilers?" Fuel **104**: 294-306.

62. Fan, L., et al. (2018). "In-situ and ex-situ catalytic upgrading of vapors from microwave-assisted pyrolysis of lignin." Bioresource technology **247**: 851-858.

63. Ferella, F., et al. (2013). "Zirconia and alumina based catalysts for steam reforming of naphthalene." Fuel **105**: 614-629.

64. French, R. and S. Czernik (2010). "Catalytic pyrolysis of biomass for biofuels production." Fuel Processing Technology **91**(1): 25-32.

65. Friedl, A., et al. (2005). "Prediction of heating values of biomass fuel from elemental composition." Analytica Chimica Acta **544**(1-2): 191-198.

66. Fuchs, J., et al. (2019). "Dual fluidized bed gasification of biomass with selective carbon dioxide removal and limestone as bed material: A review." Renewable and Sustainable Energy Reviews **107**: 212-231.

67. Fuentes-Cano, D., et al. (2018). "The influence of volatiles to carrier gas ratio on gas and tar yields during fluidized bed pyrolysis tests." Fuel **226**: 81-86.

68. Gamliel, D. P., et al. (2015). "Investigation of in situ and ex situ catalytic pyrolysis of miscanthus× giganteus using a PyGC–MS microsystem and comparison with a bench-scale spouted-bed reactor." Bioresource Technology **191**: 187-196.

69. Gao, F. (2010). "Pyrolysis of waste plastics into fuels."

70. Garcia-Nunez, J., et al. (2017). "Historical developments of pyrolysis reactors: a review." Energy & fuels **31**(6): 5751-5775.

71. Gascon, J., et al. (2015). "Structuring catalyst and reactor–an inviting avenue to process intensification." Catalysis Science & Technology **5**(2): 807-817.

72. Giani, L., et al. (2005). "Mass-transfer characterization of metallic foams as supports for structured catalysts." Industrial & engineering chemistry research **44**(14): 4993-5002.

73. Gollakota, A., et al. (2018). "A review on hydrothermal liquefaction of biomass." Renewable and Sustainable Energy Reviews **81**: 1378-1392.

74. Grant, E. and B. J. Halstead (1998). "Dielectric parameters relevant to microwave dielectric heating." Chemical society reviews **27**(3): 213-224.

75. Griffin, M. B., et al. (2018). "Driving towards cost-competitive biofuels through catalytic fast pyrolysis by rethinking catalyst selection and reactor configuration." Energy & Environmental Science **11**(10): 2904-2918.

76. Guo, F., et al. (2014). "Effect of design and operating parameters on the gasification process of biomass in a downdraft fixed bed: An experimental study." International Journal of Hydrogen Energy **39**(11): 5625-5633.

77. Hajbabaei, M., et al. (2013). "Impact of olefin content on criteria and toxic emissions from modern gasoline vehicles." Fuel **107**: 671-679.

78. Han, J. and H. Kim (2008). "The reduction and control technology of tar during biomass gasification/pyrolysis: an overview." Renewable and Sustainable Energy Reviews **12**(2): 397-416.

79. Hanchate, N., et al. (2020). "Biomass Gasification using Dual Fluidized Bed Gasification Systems: A Review." Journal of Cleaner Production: 123148.

80. Hansen, J., et al. (2016). "Ice melt, sea level rise and superstorms: evidence from paleoclimate data, climate modeling, and modern observations that 2 A degrees C global warming could be dangerous." Atmospheric Chemistry and Physics **16**(6): 3761-3812.

81. Haque, K. E. (1999). "Microwave energy for mineral treatment processes—a brief review." International journal of mineral processing **57**(1): 1-24.

82. He, J., et al. (2019). "Prospects, obstacles and solutions of biomass power industry in China." Journal of Cleaner Production **237**: 117783.

83. He, M., et al. (2010). "Syngas production from pyrolysis of municipal solid waste (MSW) with dolomite as downstream catalysts." Journal of Analytical and Applied Pyrolysis **87**(2): 181-187.

84. Hertzog, J., et al. (2018). "Catalytic fast pyrolysis of biomass over microporous and hierarchical zeolites: Characterization of heavy products." ACS Sustainable Chemistry & Engineering **6**(4): 4717-4728.

85. Horikoshi, S. and N. Serpone (2014). "Role of microwaves in heterogeneous catalytic systems." Catalysis Science & Technology **4**(5): 1197-1210.

86. Hu, C., et al. (2017). "Ex-situ catalytic fast pyrolysis of biomass over HZSM-5 in a two-stage fluidized-bed/fixed-bed combination reactor." Bioresource Technology **243**: 1133-1140.

87. Huang, Y.-F., et al. (2016). "Microwave pyrolysis of lignocellulosic biomass: Heating performance and reaction kinetics." Energy **100**: 137-144.

88. Huang, Y., et al. (2010). "Hydrogen-rich fuel gas from rice straw via microwave-induced pyrolysis." Bioresource Technology **101**(6): 1968-1973.

89. IEA (2019). World Energy Outlook 2019. IEA, Paris.

90. IEA (2020). Global Energy Review 2019. Paris IEA.

91. IEA (2020). World Energy Outlook 2020. Paris

92. Iisa, K., et al. (2016). "Catalytic pyrolysis of pine over HZSM-5 with different binders." Topics in Catalysis **59**(1): 94-108.

93. Iisa, K., et al. (2016). "In situ and ex situ catalytic pyrolysis of pine in a bench-scale fluidized bed reactor system." Energy & fuels **30**(3): 2144-2157.

94. Iliopoulou, E. F., et al. (2012). "Catalytic upgrading of biomass pyrolysis vapors using transition metal-modified ZSM-5 zeolite." Applied Catalysis B: Environmental **127**: 281-290.

95. Italiano, C., et al. (2016). "Preparation of structured catalysts with Ni and Ni–Rh/CeO2 catalytic layers for syngas production by biogas reforming processes." Catalysis Today **273**: 3-11.

96. Ivanova, S., et al. (2007). "ZSM-5 coatings on β-SiC monoliths: possible new structured catalyst for the methanol-to-olefins process." The Journal of Physical Chemistry C **111**(11): 4368-4374.

97. Jackson, M. A., et al. (2009). "Screening heterogeneous catalysts for the pyrolysis of lignin." Journal of Analytical and Applied Pyrolysis **85**(1): 226-230.

98. Jacob, J., et al. (1995). "Thermal and non-thermal interaction of microwave radiation with materials." Journal of materials science **30**(21): 5321-5327.

99. Jae, J., et al. (2014). "Catalytic fast pyrolysis of lignocellulosic biomass in a process development unit with continual catalyst addition and removal." Chemical Engineering Science **108**: 33-46.

100. Jae, J., et al. (2011). "Investigation into the shape selectivity of zeolite catalysts for biomass conversion." Journal of Catalysis **279**(2): 257-268.

101. Jia, L., et al. (2017). "Catalytic fast pyrolysis of biomass: superior selectivity of hierarchical zeolites to aromatics." Green Chemistry **19**(22): 5442-5459.

102. Jiang, H., et al. (2020). "Chemical Recycling of Plastics by Microwave-Assisted High-Temperature Pyrolysis." Global Challenges **4**(4): 1900074.

103. Jiao, Y., et al. (2012). "Controllable synthesis of ZSM-5 coatings on SiC foam support for MTP application." Microporous and Mesoporous Materials **162**: 152-158.

104. Jiao, Y., et al. (2015). "Hierarchical ZSM-5/SiC nano-whisker/SiC foam composites: Preparation and application in MTP reactions." Journal of Catalysis **332**: 70-76.

105. Jing, X., et al. (2020). "Heating strategies for the system of PP and Spherical Activated Carbon during microwave cracking for obtaining value-added products." Fuel Processing Technology **199**: 106265.

106. Jing, X., et al. (2020). "Recycling waste plastics packaging to value-added products by two-step microwave cracking with different heating strategies." Fuel Processing Technology **201**: 106346.

107. Jing, X., et al. (2014). "Study on mild cracking of polyolefins to liquid hydrocarbons in a closed batch reactor for subsequent olefin recovery." Polymer degradation and stability **109**: 79-91.

108. Kabir, G. and B. Hameed (2017). "Recent progress on catalytic pyrolysis of lignocellulosic biomass to high-grade bio-oil and bio-chemicals." Renewable and Sustainable Energy Reviews **70**: 945-967.

109. Kaminsky, W. and H. Sinn (1980). Pyrolysis of plastic waste and scrap tires using a fluidized-bed process, ACS Publications.

110. Kan, T., et al. (2016). "Lignocellulosic biomass pyrolysis: A review of product properties and effects of pyrolysis parameters." Renewable and Sustainable Energy Reviews **57**: 1126-1140.

111. Kappe, C. O. (2004). "Controlled microwave heating in modern organic synthesis." Angewandte Chemie International Edition **43**(46): 6250-6284.

112. Karl, J. and T. Pröll (2018). "Steam gasification of biomass in dual fluidized bed gasifiers: A review." Renewable and Sustainable Energy Reviews **98**: 64-78.

113. Kassargy, C., et al. (2018). "Gasoline and diesel-like fuel production by continuous catalytic pyrolysis of waste polyethylene and polypropylene mixtures over USY zeolite." Fuel **224**: 764-773.

114. Khaghanikavkani, E. and M. M. Farid (2013). "Mathematical modelling of microwave pyrolysis." International Journal of Chemical Reactor Engineering **11**(1): 543-559.

115. Kim, S.-S. and S. Kim (2004). "Pyrolysis characteristics of polystyrene and polypropylene in a stirred batch reactor." Chemical Engineering Journal **98**(1-2): 53-60.

116. Kim, Y. D., et al. (2013). "Air-blown gasification of woody biomass in a bubbling fluidized bed gasifier." Applied Energy **112**: 414-420.

117. Klinger, J. L., et al. (2018). "Effect of biomass type, heating rate, and sample size on microwave-enhanced fast pyrolysis product yields and qualities." Applied Energy **228**: 535-545.

118. Kobayashi, J., et al. (2019). "Selective Dechlorination of Polyvinyl Chloride by Microwave Irradiation." Journal of Chemical Engineering of Japan **52**(7): 656-661.

119. Kokel, A., et al. (2017). "Application of microwave-assisted heterogeneous catalysis in sustainable synthesis design." Green Chemistry **19**(16): 3729-3751.

120. Kremsner, J. M. and C. O. Kappe (2006). "Silicon carbide passive heating elements in microwave-assisted organic synthesis." The Journal of organic chemistry **71**(12): 4651-4658.

121. Lacroix, M., et al. (2007). "Pressure drop measurements and modeling on SiC foams." Chemical Engineering Science **62**(12): 3259-3267.

122. Lam, S. S., et al. (2015). "Catalytic microwave pyrolysis of waste engine oil using metallic pyrolysis char." Applied Catalysis B: Environmental **176**: 601-617.

123. Lam, S. S., et al. (2019). "Microwave vacuum pyrolysis of waste plastic and used cooking oil for simultaneous waste reduction and sustainable energy conversion: Recovery of cleaner liquid fuel and techno-economic analysis." Renewable and Sustainable Energy Reviews **115**: 109359.

124. Lettner, F., et al. (2007). "Biomass gasification–State of the art description." Intelligent Energy Europe, Austria.

125. Li, C., et al. (2016). "Impact of feedstock quality and variation on biochemical and thermochemical conversion." Renewable and Sustainable Energy Reviews **65**: 525-536.

126. Li, L., et al. (2013). "Influence of microwave power, metal oxides and metal salts on the pyrolysis of algae." Bioresource Technology **142**: 469-474.

127. Lin, Q., et al. (2012). "Scale-up of microwave heating process for the production of bio-oil from sewage sludge." Journal of Analytical and Applied Pyrolysis **94**: 114-119.

128. Liu, H., et al. (2008). "Scale up and stability test for oxidative coupling of methane over Na2WO4-Mn/SiO2 catalyst in a 200 ml fixed-bed reactor." Journal of Natural Gas Chemistry **17**(1): 59-63.

129. Liu, S., et al. (2017). "Bio-oil production from sequential two-step catalytic fast microwave-assisted biomass pyrolysis." Fuel **196**: 261-268.

130. Liu, Y. and H. Ohara (2017). "Energy-efficient fluidized bed drying of low-rank coal." Fuel Processing Technology **155**: 200-208.

131. López, A., et al. (2011). "Deactivation and regeneration of ZSM-5 zeolite in catalytic pyrolysis of plastic wastes." Waste Management **31**(8): 1852-1858.

132. Lopez, A., et al. (2011). "Influence of time and temperature on pyrolysis of plastic wastes in a semi-batch reactor." Chemical Engineering Journal **173**(1): 62-71.

133. López, A., et al. (2011). "Catalytic pyrolysis of plastic wastes with two different types of catalysts: ZSM-5 zeolite and Red Mud." Applied Catalysis B: Environmental **104**(3-4): 211-219.

134. Lopez, G., et al. (2017). "Thermochemical routes for the valorization of waste polyolefinic plastics to produce fuels and chemicals. A review." Renewable and Sustainable Energy Reviews **73**: 346-368.

135. Ludlow-Palafox, C. and H. A. Chase (2001). "Microwave-induced pyrolysis of plastic wastes." Industrial & Engineering Chemistry Research **40**(22): 4749-4756.

136. Luo, H., et al. (2018). "Microwave-assisted in-situ elimination of primary tars over biochar: Low temperature behaviours and mechanistic insights." Bioresource Technology **267**: 333-340.

137. Ma, H.-K., et al. (2015). "Waste heat recovery using a thermoelectric power generation system in a biomass gasifier." Applied thermal engineering **88**: 274-279.

138. Mahari, W. A. W., et al. (2018). "Microwave co-pyrolysis of waste polyolefins and waste cooking oil: influence of N2 atmosphere versus vacuum environment." Energy Conversion and Management **171**: 1292-1301.

139. Maity, S. K. (2015). "Opportunities, recent trends and challenges of integrated biorefinery: Part I." Renewable and Sustainable Energy Reviews **43**: 1427-1445.

140. Mašek, O., et al. (2008). "A study on pyrolytic gasification of coffee grounds and implications to allothermal gasification." Biomass and bioenergy **32**(1): 78-89.

141. Mastral, F., et al. (2002). "Pyrolysis of high-density polyethylene in a fluidised bed reactor. Influence of the temperature and residence time." Journal of Analytical and Applied Pyrolysis **63**(1): 1-15.

142. Menéndez, J., et al. (2010). "Microwave heating processes involving carbon materials." Fuel Processing Technology **91**(1): 1-8.

143. Miandad, R., et al. (2016). "Catalytic pyrolysis of plastic waste: A review." Process Safety and Environmental Protection **102**: 822-838.

144. Mihalcik, D. J., et al. (2011). "Screening acidic zeolites for catalytic fast pyrolysis of biomass and its components." Journal of Analytical and Applied Pyrolysis **92**(1): 224-232.

145. Milne, B. J., et al. (1999). "Recycling of waste plastics by ultrapyrolysis using an internally circulating fluidized bed reactor." Journal of Analytical and Applied Pyrolysis **51**(1-2): 157-166.

146. Milne, T. A., et al. (1998). Biomass gasifier"Tars": their nature, formation, and conversion, National Renewable Energy Laboratory, Golden, CO (US).

147. Mishra, R. R. and A. K. Sharma (2016). "Microwave–material interaction phenomena: heating mechanisms, challenges and opportunities in material processing." Composites Part A: Applied Science and Manufacturing **81**: 78-97.

148. Mokhtar, N., et al. (2018). "EFFECTS OF MICROWAVE ABSORBERS ON THE PRODUCTS OF MICROWAVE PYROLYSIS OF OILY SLUDGE." Journal of Engineering Science and Technology **13**(10): 3313-3330.

149. Morf, P., et al. (2002). "Mechanisms and kinetics of homogeneous secondary reactions of tar from continuous pyrolysis of wood chips." Fuel **81**(7): 843-853.

150. Moriarty, K. L., et al. (2018). 2016 Bioenergy Industry Status Report, National Renewable Energy Lab.(NREL), Golden, CO (United States).

151. Moriwaki, S., et al. (2006). "Dehydrochlorination of poly (vinyl chloride) by microwave irradiation." Applied thermal engineering **26**(7): 745-750.

152. Mukarakate, C., et al. (2014). "Real-time monitoring of the deactivation of HZSM-5 during upgrading of pine pyrolysis vapors." Green Chemistry **16**(3): 1444-1461.

153. Mullen, C. A. and A. A. Boateng (2013). "Accumulation of inorganic impurities on HZSM-5 zeolites during catalytic fast pyrolysis of switchgrass." Industrial & Engineering Chemistry Research **52**(48): 17156-17161.

154. Mullen, C. A., et al. (2011). "Catalytic fast pyrolysis of white oak wood in a bubbling fluidized bed." Energy & fuels **25**(11): 5444-5451.

155. Mullen, C. A., et al. (2018). "Catalytic co-pyrolysis of switchgrass and polyethylene over HZSM-5: catalyst deactivation and coke formation." Journal of Analytical and Applied Pyrolysis **129**: 195-203.

156. Murata, K., et al. (2002). "Basic study on a continuous flow reactor for thermal degradation of polymers." Journal of Analytical and Applied Pyrolysis **65**(1): 71-90.

157. Nakada, S., et al. (2014). "Global bioenergy: supply and demand projections." International Renewable Energy Agency (IRENA), Abu Dhabi.

158. Olazar, M., et al. (2009). "Influence of FCC catalyst steaming on HDPE pyrolysis product distribution." Journal of Analytical and Applied Pyrolysis **85**(1-2): 359-365.

159. Paasikallio, V., et al. (2014). "Product quality and catalyst deactivation in a four day catalytic fast pyrolysis production run." Green Chemistry **16**(7): 3549-3559.

160. Palma, C. F. (2013). "Modelling of tar formation and evolution for biomass gasification: A review." Applied Energy **111**: 129-141.

161. Pangarkar, K., et al. (2008). "Structured packings for multiphase catalytic reactors." Industrial & Engineering Chemistry Research **47**(10): 3720-3751.

162. Park, Y., et al. (2016). "Energy Efficiency of Fluidized Bed Drying for Wood Particles1." J. Korean Wood Sci. Technol **44**(6): 821-827.

163. Parvez, A. M., et al. (2019). "Conventional and microwave-assisted pyrolysis of gumwood: A comparison study using thermodynamic evaluation and hydrogen production." Fuel Processing Technology **184**: 1-11.

164. Patcas, F. C., et al. (2007). "CO oxidation over structured carriers: A comparison of ceramic foams, honeycombs and beads." Chemical Engineering Science **62**(15): 3984-3990.

165. Pavlas, M., et al. (2010). "Heat integrated heat pumping for biomass gasification processing." Applied thermal engineering **30**(1): 30-35.

166. Payakkawan, P., et al. (2014). "Design, fabrication and operation of continuous microwave biomass carbonization system." Renewable energy **66**: 49-55.

167. Peterson, J. D., et al. (2001). "Kinetics of the thermal and thermo-oxidative degradation of polystyrene, polyethylene and poly (propylene)." Macromolecular Chemistry and Physics **202**(6): 775-784.

168. Prathiba, R., et al. (2018). "Pyrolysis of polystyrene waste in the presence of activated carbon in conventional and microwave heating using modified thermocouple." Waste Management **76**: 528-536.

169. Rabou, L. P., et al. (2009). "Tar in biomass producer gas, the Energy research Centre of the Netherlands (ECN) experience: an enduring challenge." Energy & fuels **23**(12): 6189-6198.

170. Radlein, D. and A. Quignard (2013). "A short historical review of fast pyrolysis of biomass." Oil & Gas Science and Technology–Revue d'IFP Energies nouvelles **68**(4): 765-783.

171. Ragaert, K., et al. (2017). "Mechanical and chemical recycling of solid plastic waste." Waste Management **69**: 24-58.

172. Ragauskas, A. J., et al. (2006). "The path forward for biofuels and biomaterials." Science **311**(5760): 484-489.

173. Rahimi, N. and R. Karimzadeh (2011). "Catalytic cracking of hydrocarbons over modified ZSM-5 zeolites to produce light olefins: A review." Applied Catalysis A: General **398**(1-2): 1-17.

174. Ramirez, A., et al. (2019). "Escaping undesired gas-phase chemistry: Microwave-driven selectivity enhancement in heterogeneous catalytic reactors." Science advances **5**(3): eaau9000.

175. Ratnasari, D. K., et al. (2017). "Catalytic pyrolysis of waste plastics using staged catalysis for production of gasoline range hydrocarbon oils." Journal of Analytical and Applied Pyrolysis **124**: 631-637.

176. Regalbuto, J. R. (2009). "Cellulosic biofuels—got gasoline?" Science **325**(5942): 822-824.

177. Rezaei, P. S., et al. (2014). "Production of green aromatics and olefins by catalytic cracking of oxygenate compounds derived from biomass pyrolysis: A review." Applied Catalysis A: General **469**: 490-511.

178. Richardson, J., et al. (2000). "Properties of ceramic foam catalyst supports: pressure drop." Applied Catalysis A: General **204**(1): 19-32.

179. Richardson, J., et al. (2003). "Properties of ceramic foam catalyst supports: mass and heat transfer." Applied Catalysis A: General **250**(2): 319-329.

180. Ruan, R. R., et al. (2008). "Size matters: small distributed biomass energy production systems for economic viability." International Journal of Agricultural and Biological Engineering **1**(1): 64-68.

181. Ruiz, J., et al. (2013). "Biomass gasification or combustion for generating electricity in Spain: Review of its current situation according to the opinion of specialists in the field." Journal of Renewable and Sustainable Energy **5**(1): 012801.

182. Ruiz, J. A., et al. (2013). "Biomass gasification for electricity generation: Review of current technology barriers." Renewable and Sustainable Energy Reviews **18**: 174-183.

183. Sansaniwal, S., et al. (2017). "Recent advances in the development of biomass gasification technology: A comprehensive review." Renewable and Sustainable Energy Reviews **72**: 363-384.

184. Sardon, H. and A. P. Dove (2018). "Plastics recycling with a difference." Science **360**(6387): 380-381.

185. Sarıkoç, S. (2020). Fuels of the Diesel-Gasoline Engines and Their Properties. Diesel and Gasoline Engines, IntechOpen.

186. Serrano, D., et al. (2001). "Conversion of low density polyethylene into petrochemical feedstocks using a continuous screw kiln reactor." Journal of Analytical and Applied Pyrolysis **58**: 789-801.

187. Shao, S., et al. (2018). "Controlled regeneration of ZSM-5 catalysts in the combined oxygen and steam atmosphere used for catalytic pyrolysis of biomass-derivates." Energy Conversion and Management **155**: 175-181.

188. Sharuddin, S. D. A., et al. (2016). "A review on pyrolysis of plastic wastes." Energy Conversion and Management **115**: 308-326.

189. Shazman, A., et al. (2007). "Examining for possible non-thermal effects during heating in a microwave oven." Food Chemistry **103**(2): 444-453.

190. Sheldon, R. A. (2014). "Green and sustainable manufacture of chemicals from biomass: state of the art." Green Chemistry **16**(3): 950-963.

191. Sheth, P. N. and B. Babu (2009). "Experimental studies on producer gas generation from wood waste in a downdraft biomass gasifier." Bioresource Technology **100**(12): 3127-3133.

192. Shibamoto, T., et al. (2007). Dioxin formation from waste incineration. Reviews of environmental contamination and toxicology, Springer**:** 1-41.

193. Sikarwar, V. S., et al. (2016). "An overview of advances in biomass gasification." Energy & Environmental Science **9**(10): 2939-2977.

194. Simell, P., et al. (2000). "Provisional protocol for the sampling and anlaysis of tar and particulates in the gas from large-scale biomass gasifiers. Version 1998." Biomass and bioenergy **18**(1): 19-38.

195. Situmorang, Y. A., et al. (2020). "Small-scale biomass gasification systems for power generation (< 200 kW class): A review." Renewable and Sustainable Energy Reviews **117**: 109486.

196. Song, Z., et al. (2018). "Effect of steel wires on the microwave pyrolysis of tire powders." ACS Sustainable Chemistry & Engineering **6**(10): 13443-13453.

197. Stamhuis, J. (1984). "Mechanical properties and morphology of polypropylene composites. Talc-filled, elastomer-modified polypropylene." Polymer composites **5**(3): 202-207.

198. STATISTICS, W. G. B. (2018). World Bioenergy Association: Stockholm, Sweden.

199. Stefanidis, S., et al. (2011). "In-situ upgrading of biomass pyrolysis vapors: catalyst screening on a fixed bed reactor." Bioresource technology **102**(17): 8261-8267.

200. Stefanidis, S., et al. (2016). "Natural magnesium oxide (MgO) catalysts: a cost-effective sustainable alternative to acid zeolites for the in situ upgrading of biomass fast pyrolysis oil." Applied Catalysis B: Environmental **196**: 155-173.

201. Stefanidis, S. D., et al. (2011). "In-situ upgrading of biomass pyrolysis vapors: catalyst screening on a fixed bed reactor." Bioresource Technology **102**(17): 8261-8267.

202. Stefanidis, S. D., et al. (2018). "Co-processing bio-oil in the refinery for drop-in biofuels via fluid catalytic cracking." Wiley Interdisciplinary Reviews: Energy and Environment **7**(3): e281.

203. Tanger, P., et al. (2013). "Biomass for thermochemical conversion: targets and challenges." Frontiers in plant science **4**: 218.

204. Thegarid, N., et al. (2014). "Second-generation biofuels by co-processing catalytic pyrolysis oil in FCC units." Applied Catalysis B: Environmental **145**: 161-166.

205. Torres, W., et al. (2007). "Hot gas removal of tars, ammonia, and hydrogen sulfide from biomass gasification gas." Catalysis reviews **49**(4): 407-456.

206. Twigg, M. V. and J. T. Richardson (2007). "Fundamentals and applications of structured ceramic foam catalysts." Industrial & engineering chemistry research **46**(12): 4166-4177.

207. Ueno, T., et al. (2010). "Quantitative analysis of random scission and chain-end scission in the thermal degradation of polyethylene." Polymer degradation and stability **95**(9): 1862-1869.

208. Undri, A., et al. (2014). "Reverse polymerization of waste polystyrene through microwave assisted pyrolysis." Journal of Analytical and Applied Pyrolysis **105**: 35-42.

209. Undri, A., et al. (2014). "Efficient disposal of waste polyolefins through microwave assisted pyrolysis." Fuel **116**: 662-671.

210. van der Meijden, C. M., et al. (2010). "The production of synthetic natural gas (SNG): A comparison of three wood gasification systems for energy balance and overall efficiency." Biomass and bioenergy **34**(3): 302-311.

211. Venderbosch, R. and W. Prins (2010). "Fast pyrolysis technology development." Biofuels, bioproducts and biorefining **4**(2): 178-208.

212. Vitolo, S., et al. (2001). "Catalytic upgrading of pyrolytic oils over HZSM-5 zeolite: behaviour of the catalyst when used in repeated upgrading–regenerating cycles." Fuel **80**(1): 17-26.

213. Walendziewski, J. (2005). "Continuous flow cracking of waste plastics." Fuel Processing Technology **86**(12-13): 1265-1278.

214. Wang, H., et al. (2016). "Biomass conversion to produce hydrocarbon liquid fuel via hot-vapor filtered fast pyrolysis and catalytic hydrotreating." JoVE (Journal of Visualized Experiments)(118): e54088.

215. Wang, K., et al. (2014). "Comparison of in-situ and ex-situ catalytic pyrolysis in a micro-reactor system." Bioresource technology **173**: 124-131.

216. Wang, L., et al. (2008). "Contemporary issues in thermal gasification of biomass and its application to electricity and fuel production." Biomass and bioenergy **32**(7): 573-581.

217. Wang, S., et al. (2017). "Lignocellulosic biomass pyrolysis mechanism: a state-of-the-art review." Progress in Energy and Combustion Science **62**: 33-86.

218. Wang, W., et al. (2015). "Quantitative measurement of energy utilization efficiency and study of influence factors in typical microwave heating process." Energy **87**: 678-685.

219. Wang, Y., et al. (2020). "Ex-situ catalytic fast pyrolysis of soapstock for aromatic oil over microwave-driven HZSM-5@ SiC ceramic foam." Chemical Engineering Journal **402**: 126239.

220. Widayatno, W. B., et al. (2016). "Upgrading of bio-oil from biomass pyrolysis over Cu-modified β-zeolite catalyst with high selectivity and stability." Applied Catalysis B: Environmental **186**: 166-172.

221. Williams, P. T. and E. A. Williams (1999). "Fluidised bed pyrolysis of low density polyethylene to produce petrochemical feedstock." Journal of Analytical and Applied Pyrolysis **51**(1-2): 107-126.

222. Wong, S., et al. (2015). "Current state and future prospects of plastic waste as source of fuel: A review." Renewable and Sustainable Energy Reviews **50**: 1167-1180.

223. Woolcock, P. J. and R. C. Brown (2013). "A review of cleaning technologies for biomass-derived syngas." Biomass and bioenergy **52**: 54-84.

224. Wright, M. M. and R. C. Brown (2007). "Comparative economics of biorefineries based on the biochemical and thermochemical platforms." Biofuels, Bioproducts and Biorefining: Innovation for a sustainable economy **1**(1): 49-56.

225. Wu, J., et al. (2014). "TG/FTIR analysis on co-pyrolysis behavior of PE, PVC and PS." Waste Management **34**(3): 676-682.

226. Xanthos, M. (2010). Functional fillers for plastics, John Wiley & Sons.

227. Xiao, X., et al. (2011). "Two-stage steam gasification of waste biomass in fluidized bed at low temperature: Parametric investigations and performance optimization." Bioresource Technology **102**(2): 1975-1981.

228. Xie, Q., et al. (2012). "Syngas production by two-stage method of biomass catalytic pyrolysis and gasification." Bioresource Technology **110**: 603-609.

229. Xingzhong, Y. (2006). "Converting waste plastics into liquid fuel by pyrolysis: developments in China." Feedstock Recycling and Pyrolysis of Waste Plastics: Converting Waste Plastics into Diesel and Other Fuels: 729-755.

230. Xu, C. C., et al. (2010). "Recent advances in catalysts for hot-gas removal of tar and NH3 from biomass gasification." Fuel **89**(8): 1784-1795.

231. Yang, H.-J., et al. (2013). "Silicon carbide powders: temperature-dependent dielectric properties and enhanced microwave absorption at gigahertz range." Solid state communications **163**: 1-6.

232. Yang, X., et al. (2013). "Pyrolysis and dehalogenation of plastics from waste electrical and electronic equipment (WEEE): A review." Waste Management **33**(2): 462-473.

233. Yildiz, G., et al. (2016). "Challenges in the design and operation of processes for catalytic fast pyrolysis of woody biomass." Renewable and Sustainable Energy Reviews **57**: 1596-1610.

234. Yitao, S., et al. (2009). "Optimization of gasoline hydrocarbon compositions for reducing exhaust emissions." Journal of Environmental Sciences **21**(9): 1208-1213.

235. Yu, J., et al. (2016). "Thermal degradation of PVC: A review." Waste Management **48**: 300-314.

236. Yung, M. M., et al. (2009). "Review of catalytic conditioning of biomass-derived syngas." Energy & fuels **23**(4): 1874-1887.

237. Zacher, A. H., et al. (2014). "A review and perspective of recent bio-oil hydrotreating research." Green Chemistry **16**(2): 491-515.

238. Zhang, D., et al. (2017). "Present situation and future prospect of renewable energy in China." Renewable and Sustainable Energy Reviews **76**: 865-871.

239. Zhang, H., et al. (2012). "Catalytic fast pyrolysis of wood and alcohol mixtures in a fluidized bed reactor." Green Chemistry **14**(1): 98-110.

240. Zhang, M., et al. (2006). "Trends in microwave-related drying of fruits and vegetables." Trends in Food Science & Technology **17**(10): 524-534.

241. Zhang, S.-p., et al. (2016). "The integrated process for hydrogen production from biomass: Study on the catalytic conversion behavior of pyrolytic vapor in gas–solid simultaneous gasification process." International Journal of Hydrogen Energy **41**(16): 6653-6661.

242. Zhang, S., et al. (2015). "High quality syngas production from microwave pyrolysis of rice husk with char-supported metallic catalysts." Bioresource Technology **191**: 17-23.

243. Zhang, X. and H. Lei (2016). "Synthesis of high-density jet fuel from plastics via catalytically integral processes." RSC advances **6**(8): 6154-6163.

244. Zhang, X., et al. (2015). "Gasoline-range hydrocarbons produced from microwave-induced pyrolysis of low-density polyethylene over ZSM-5." Fuel **144**: 33-42.

245. Zhang, X., et al. (2017). "An overview of a novel concept in biomass pyrolysis: microwave irradiation." Sustainable Energy & Fuels **1**(8): 1664-1699.

246. Zhang, Y., et al. (2020). "Fast microwave-assisted pyrolysis of wastes for biofuels production–A review." Bioresource Technology **297**: 122480.

247. Zhang, Y., et al. (2020). "Exergy and energy analysis of pyrolysis of plastic wastes in rotary kiln with heat carrier." Process Safety and Environmental Protection **142**: 203-211.

248. Zhao, D., et al. (2019). "The Chemistry and Kinetics of Polyethylene Pyrolysis: A Feedstock to Produce Fuels and Chemicals." ChemSusChem.

249. Zhao, X., et al. (2011). "Microwave pyrolysis of straw bale and energy balance analysis." Journal of Analytical and Applied Pyrolysis **92**(1): 43-49.

250. Zhou, C.-H., et al. (2011). "Catalytic conversion of lignocellulosic biomass to fine chemicals and fuels." Chemical Society Reviews **40**(11): 5588-5617.

251. Zhou, J., et al. (2018). "Development and application of a continuous fast microwave pyrolysis system for sewage sludge utilization." Bioresource Technology **256**: 295-301.

252. Zhou, N. and N. T. Dunford (2017). "Thermal Degradation and Microwave-Assisted Pyrolysis of Green Algae and Cyanobacteria Isolated from the Great Salt Plains." Transactions of the ASABE **60**(2): 561-569.

253. Zhou, N., et al. (2018). "Silicon carbide foam supported ZSM-5 composite catalyst for microwave-assisted pyrolysis of biomass." Bioresource Technology **267**: 257-264.

254. Zhou, N., et al. (2020). "Syngas production from biomass pyrolysis in a continuous microwave assisted pyrolysis system." Bioresource Technology **314**: 123756.

255. Zuo, W., et al. (2011). "The important role of microwave receptors in bio-fuel production by microwave-induced pyrolysis of sewage sludge." Waste Management **31**(6): 1321-1326.